PhD-Thesis

Role of lipoprotein homeostasis in tumor growth

submitted by

Jianfeng Huang

for the Academic degree of

Doctor of Philosophy

(Ph.D.)

at the

Medical University of Graz

Institute of Pathology

Under supervision of

Univ. Prof. Dr. Gerald Hoefler, M.D.

(2015)

TABLE OF CONTENTS

Zusammenfassung

[Hintergrund]

Übergewicht ist eines der häufigsten Gesundheitsprobleme weltweit. Neuere Erkenntnisse zeigen bei Fettleibigkeit ein erhöhtes Risiko für die Entwicklung einer breiten Palette von bösartigen Tumoren, einschließlich malignen Lymphomen. Insbesondere kann die Krebs-assoziierte Kachexie den Fettstoffwechsel stark beeinflussen. Eine eventuell vorhandene bidirektionale Kausalität zwischen der Tumorentstehung und dem Lipid-Stoffwechsel der Patienten ist weitgehend unerforscht.

[Methoden]

Wir verwendeten Bcr / Abl transformierte B-Zellen (TPBC), um die Auswirkungen und die zugrunde liegenden Mechanismen der Entstehung von aggressiven Lymphom auf die systemische Lipidmobilisation und den Lipid-Umsatz zu bestimmen. Zwei lipidsenkende Strategien, der Lipidsenker Fenofibrat und Mausmodelle mit defizienter VLDL Produktion - Carboxylesterase 3 / Triacylglycerol Hydrolase (Ces3 / TGH) –bzw. Phosphatidylethanolamin N-Methyltransferase (PEMT) – wurden verwendet, um zu untersuchen, ob die Einschränkung der exogenen Lipidzufuhr das Tumorwachstum beeinflussen kann.

[Ergebnisse]

Das Tumorwachstum korrelierte signifikant mit dem Verlust des weißen Fettgewebe (WAT) in Mäusen. Die Tumorentwicklung verursachte eine Lipidakkumulation in der Leber, bedingt durch eine erhöhte hepatische Fettsäure (FA) Aufnahme und eine beeinträchtigte FA Oxidation. Metabolische Untersuchungen mit radioaktiv markierten Substanzen zeigte eine beschleunigte Synthese des freien Cholesterins [^{3}H]-acetat und eine Veresterung von [^{3}H]-oleat zu Cholesterylester (CE) und Triglycerid (TG) in primären Hepatozyten von

Tumor-tragenden Mäusen (Tu), was zu einer erhöhten Sekretion von TG in das Kulturmedium führte. Die hepatische VLDL Produktionsrate in Tu-tragenden Mäusen war im Vergleich zu nicht-Tumor-tragenden (Non-Tu) Kontrollen erhöht. In Verbindung mit einer gestörten Clearance von TG Lipoproteinen aus dem Blutkreislauf, die durch Fett-Toleranz Tests und die Bestimmung der TG Hydrolase Aktivitäten untersucht wurde, führte eine verstärkte VLDL Produktion zu einer Hypertriglyceridämie in Tu-Mäusen. Darüber hinaus wurde eine verringerte Menge von hepatischen LDLR Protein und eine erhöhte Konzentrationen von Plasma PCSK9 in der Tu-Gruppe beobachtet, was zum Auftreten von Hypercholesterinämie führte.

Die Tumor-fördernde Funktion von Very low/ Low-Density Lipoprotein (VLDL/LDL) Spiegeln auf das Zellwachstum wurde *in vitro* bestätigt. Die Proliferation von transformierten B-Zellen war in Lipoprotein-Mangelserum (LPDS) stark reduziert. Es zeigte sich eine Induktion der Apoptose. Hingegen führte eine Supplementierung von VLDL/LDL-Cholesterin oder, in geringerem Maße, von HDL zu einer Unterdrückung der beschriebenen Phänomene.

Weitere Evidenz ergibt sich aus den Ergebnissen der lipidsenkenden Strategien. Beide Lipidsenker, Fenofibrat und Ces3/TGH-Mangel, verhinderten die tumorinduzierte Hyperlipidämie bei Mäusen und unterdrückten das Tumorwachstum. Fenofibrat stimulierte die FFA-Aufnahme in der Leber und stellte die FA Oxidationskapazität der Leber wieder her. Dadurch wurde die Clearance der Lipide, die aus WAT freigesetzt wurden, beschleunigt. Der Schutz vor gesteigertem Tumorwachstum in *Ces3/Tgh*$^{-/-}$ Mäusen kann durch die Inhibierung des tumorinduzierten und PCSK9-vermittelten Abbaus des Leber-LDL-Rezeptors und durch eine Abnahme des LDL-Umsatzes erklärt werden. Interessanterweise zeigte sich keine derartige Wirkung in *Pemt*$^{-/-}$ Mäusen, sodass es auch zu keiner Unterdrückung des Tumorwachstums kam.

[Fazit]

Unsere Daten zeigen, dass die TPBC tumorinduzierte Hyperlipidämie in Form einer Rückkopplungsschleife das Tumorwachstum durch Bereitstellung von pro-tumorigenem LDL-Cholesterin teilweise unterstützt. Die Auswirkungen von Fenofibrat auf den Fettstoffwechsel der Leber und die dadurch bedingte Senkung der Serumlipide, sowie der Schutz des Leber-LDLR vor PCSK9-induziertem Abbau in *Ces3/Tgh*$^{-/-}$ Mäuse, sind beide in der Lage, das Wachstum von B-Zell-Lymphomen zu unterdrücken. Dies könnte zur Entwicklung einer neuen Behandlungsstrategie gegen maligne Tumore verwendet werden.

Abstract

[Background]

Obesity is considered as one of the most common public health problems worldwide. Recent evidence strongly linked obesity to an increased risk for developing a broad range of malignant tumors including lymphoma. Notably, tumor development and especially cancer-associated cachexia could influence the host lipid metabolism. The bidirectional causality between tumor development and host lipid abnormality is, remarkably, largely unexplored.

[Methods]

We used Bcr/Abl transformed B cells (TPBC) to determine the impact and the underlying mechanisms of aggressive lymphoma formation on systemic lipid mobilization and turnover. Two lipid lowering strategies, a lipid lowering drug, fenofibrate, and two VLDL production-deficient mouse models – carboxylesterase3/triacylglycerol hydrolase (Ces3/TGH)- and phosphatidylethanolamine *N*-methyltransferase (PEMT)- knockout mice, were used to determine whether limitation of exogenous lipid supply could influence tumor growth.

[Results]

In mice, B-cell tumor size significantly correlated with depletion of white adipose tissues (WAT). Tumor development induced hepatic lipid accumulation due to enhanced hepatic fatty acid (FA) uptake and impaired FA oxidation. Metabolic labeling assays in primary hepatocytes isolated from tumor-bearing (Tu) mice showed accelerated synthesis of free cholesterol from [^{3}H]-acetate and increased esterification of [^{3}H]-oleate into cholesteryl ester (CE) and triglyceride (TG) tumor, resulting in increased secretion of TG/CE into the growth media. In line, the hepatic VLDL production rate was increased in tumor-bearing mice compared to non-tumor

bearing controls (Non-Tu). Together with perturbed clearance of TG-rich lipoproteins from the bloodstream as determined by a fat tolerant test and by TG hydrolase activities assays, enhanced VLDL production leads to hypertriglyceridemia in Tu mice. Moreover, decreased protein levels of hepatic LDLR and elevated concentrations of plasma PCSK9 were observed in the Tu group, leading to hypercholesterolemia. The tumor-supportive function of very low-/low- density lipoproteins (VLDL/LDL) on cell growth was confirmed *in vitro*. Lipoprotein-deficient serum (LPDS) media drastically reduced tumor B-cell proliferation and provoked apoptosis. Supplementation of VLDL/LDL or cholesterol, and, to a lesser extent, high density lipoproteins (HDL) could reverse effects conferred by LPDS.

Further support this hypothesis stems from the results of lipid lowering strategies. Both the lipid-lowering drug fenofibrate and Ces3/TGH deficiency in mice significantly reversed tumor-induced hyperlipidemia and suppressed tumor growth. Fenofibrate stimulated FFA uptake by the liver and restored hepatic FA oxidation capacity, thereby accelerating the clearance of lipids released from WAT. The mechanism of protection against tumor growth in *Ces3/Tgh*$^{-/-}$ mice could be attributed to the reversal of tumor-induced PCSK9-mediated degradation of hepatic LDLR and decreased LDL turnover. Interestingly, *Pemt*$^{-/-}$ mice failed to exert such an effect and, thus, tumor growth was not suppressed.

[Conclusion]

Our data demonstrate that TPBC tumor-induced hyperlipidemia encompasses a feedback loop to support tumor growth in part by providing pro-tumorigenic LDL-cholesterol. Fenofibrate-associated effects on hepatic lipid metabolism and deprivation of serum lipids, as well as protection of hepatic LDLR from PCSK9-mediated degradation in *Ces3/Tgh*$^{-/-}$ mice, are both capable to suppress B-cell lymphoma growth. These findings may lead to novel treatment strategies against tumor growth.

ABBREVIATIONS

ACC: acetyl-CoA carboxylase

ACLY: ATP-citrate lyase

ACOX: Acyl-Coenzyme A Oxidase

AMPK: 5’ AMP-activated protein kinase

Apo: Apolipoprotein

CD36: FA translocase

CE: cholesteryl ester

Ces3/TGH: carboxylesterase3/triacylglycerol hydrolase

CM: chylomicron

CPT: carnitine palmitoyltransferase

FASN: fatty acid synthase

FFA: free fatty acid

FTT: fat tolerant test

HDL: high-density lipoprotein

HMGCR: 3-hydroxy-3-methylglutary-CoA reductase

HMGCS: 3-hydroxy-3-methylglutary-CoA syntase

HNF1α: hepatic nuclear factor 1α

IL-6: interleukin 6

Insig2: insulin induced gene 2

ITT: insulin tolerant test

LCAD: long-chain acyl-coenzyme A dehydrogenase

LD: lipid droplet

LDL: low-density lipoprotein

LDLR: low-density lipoprotein receptor

LPDS: lipoprotein deficient serum

LPL: lipoprotein lipase

MCAD: medium-chain acyl-coenzyme A dehydrogenase

MCP1: monocyte chemotactic protein 1

mTORC: mammalian target of rapamycin complex 1

Mttp: microsomal triglyceride transfer protein

NEFA: non-esterified fatty acid

OGTT: oral glucose tolerant test

PCSK9: proprotein convertase subtilisin/kexin type 9

PEMT: phosphatidylethanolamine *N*-methyltransferase

PL: phospholipids

PPARα: peroxisome proliferator-activated receptor α

SCAP: SREBP cleavage-activating protein

SCD: stearoyl-CoA desaturase

SREBP: sterol-regulatory element binding protein

S1P: site 1 protease

TPBC: BCR-Abl transformed precursor B-cell

TC: total cholesterol

TG: triglyceride

TNFα: tumor necrosis factor alpha

VEGF-A: vascular epithelial growth factor A

VLDL: low-density lipoprotein

VLDLR: low-density lipoprotein receptor

WAT: white adipose tissues

WT: wild type

1. Introduction

1.1. Tumor Metabolism

Cell proliferation is a central mechanism in embryogenesis, body growth and proper function of adult tissues as well as in tumorigenesis. Since division of each cell into two daughter cells requires a doubling of the biomass, cells which respond to growth stimuli must rewire their metabolic program to meet the great demand of macromolecules(1).

1.1.1. Glucose Metabolism

1.1.1.1. Warburg Effect

The term “Warburg effect” describes the observation that in contrast to non-malignant cells, most cancer cells predominantly produce energy by a high rate of glycolysis followed by lactate fermentation in the cytosol, rather than by glycolysis followed by oxidation of pyruvate in mitochondria . Malignant, rapidly growing tumor cells typically have glycolytic rates up to 200 times higher than those of their normal tissues; even if oxygen is abundant. Otto Warburg postulated this change in metabolism to be the fundamental cause of cancer (2, 3). Today, mutations in oncogenes and tumor suppressor genes are thought to be responsible for malignant transformation, and the Warburg effect is considered to be a result of these mutations rather than the cause of malignancy(4, 5). For instance, the synthesis of the sugar transporter GLUT1 is induced to facilitate glucose uptake by the growth kinase Akt in response to insulin (6) or by hypoxia inducible factor (HIF) and H-ras (7). Moreover, the synthesis of the majority of glycolytic enzymes could be promoted by HIF-1α and oncogene c-Myc (8).

1.1.1.2. Reverse Warburg Effect

Otto Warburg speculated an impairment of mitochondrial oxidative phosphorylation (OXPHOS) in tumor cells. As a consequence, cells are forced to generate ATP through aerobic glycosis. However, this view is recently subjected to challenges based on multiple observations showing intact mitochondrial function in certain types of cancer cells (reviewed in (9)). Several reports have pointed out the role of mitochondrial FA oxidation-derived ATP in survival of tumor cells. *Plas DR*'s lab conveyed the message that the mitochondrial FA oxidation is particularly important for cell survival when glycolysis is interrupted by inactivation of mTORC1 signaling through S6K1 knockdown or rapamycin (10). In concert, *Tak Mak*'s group discovered the unexpected ectopic expression of brain specific CPT1 isoform C in other organ-originated tumor cells. CPT1C, via ATP generation, could rescue tumor cells from metabolic stress and prevent cell death against mTORC1 inhibition (11). The potential of cancer cells to grow and survive will also be reduced by the limit of cytosolic NADPH. The mitochondria organelle is the main power plant for generation of ATP and NADPH through TCA cycle and FA oxidation. NADPH not only provides reductive equivalents to protect cells against oxidative stress-induced cell death, but also contributes to anabolic reactions to support cell growth.

The concept of "Reverse Warburg Effect" was first proposed by *Lisanti MP*'s group in 2009. Principally, due to ROS-induced metabolic stress production, cancer associated fibroblasts (CAFs) rewire to catabolic status to create a nutrient-abundant microenvironment. These nutrients includes lactate, ketone bodies, fatty acids and amino acids are bona fide mitochondrial fuels, which are important for tumor cells and have tumor-supportive functions(12).

Collectively, the glycolytic phenotype in cancer cells observed by Warburg is likewise attributable to avid aerobic glycolysis-caused suppression of OXPHOS rather than defects in mitochondrial function (13).

1.1.2. Glutamine Metabolism

Although substantial efforts have been taken to therapeutically target glucose metabolism of tumor, the plasticity of tumor cells to adapt to the harsh nutrient/oxygen conditions alerts scientists the complexity of the metabolism of cancer cells because in certain occasions, tumor cells divert their demand from glucose to other nutrients especially glutamine in order to retain uncontrolled growth and survival. In fact, withdrawal of glutamine, rather than glucose, causes more severe cell death in Myc-transformed cells.

Glutamine is the most abundant amino acid in the plasma and an additional energy source in tumor cells especially when fermentation of glucose is curtailed due to glucose scarcity. Glutamine is a critical source of nitrogen, an essential chemical element required for new nucleotide and amino acid synthesis. Glutamine also acts as a source of carbon, to compensate the loss of intermediates in TCA (citric acid cycle, also called Krebs cycle) and to produce more pyruvate when TCA cycle is inefficient due to lack of glucose. In fact, some types of tumor are addicted to glutamine. Depletion of glutamine supply will stop tumor growing and turn it to cell death.

Glutamine is transported into cells by transporter ASCT2, and then hydrolyzed to glutamate by glutaminase (GLS). Glutamate can be converted into α-ketoglutarate (α-KG) and enters the TCA cycle. This step provide an alternative survival for cells to generate ATP, reducing equivalents and enriched carbon chains to cope with energy deficit, synthesis FA via breakdown of citrate and amino acids through aminotransferase. *Jorge Moscat* and his colleagues have reported that tumor cells undergo metabolic reprogramming and depend more on glutaminolysis when glucose is deprived (14). This could be of paramount importance because when GLUT1 inhibitor is thought as an advantageous cure to kill cancer, this harsh stress might initiate a potential cancerous metabolic rewiring and drive cells into a

glucose-independent stage and to escape from this therapeutic approach. We summarize the pathways how tumor utilize glucose and glutamine to synthesis biomass such as amino acids, lipids and ribose (Fig.1).

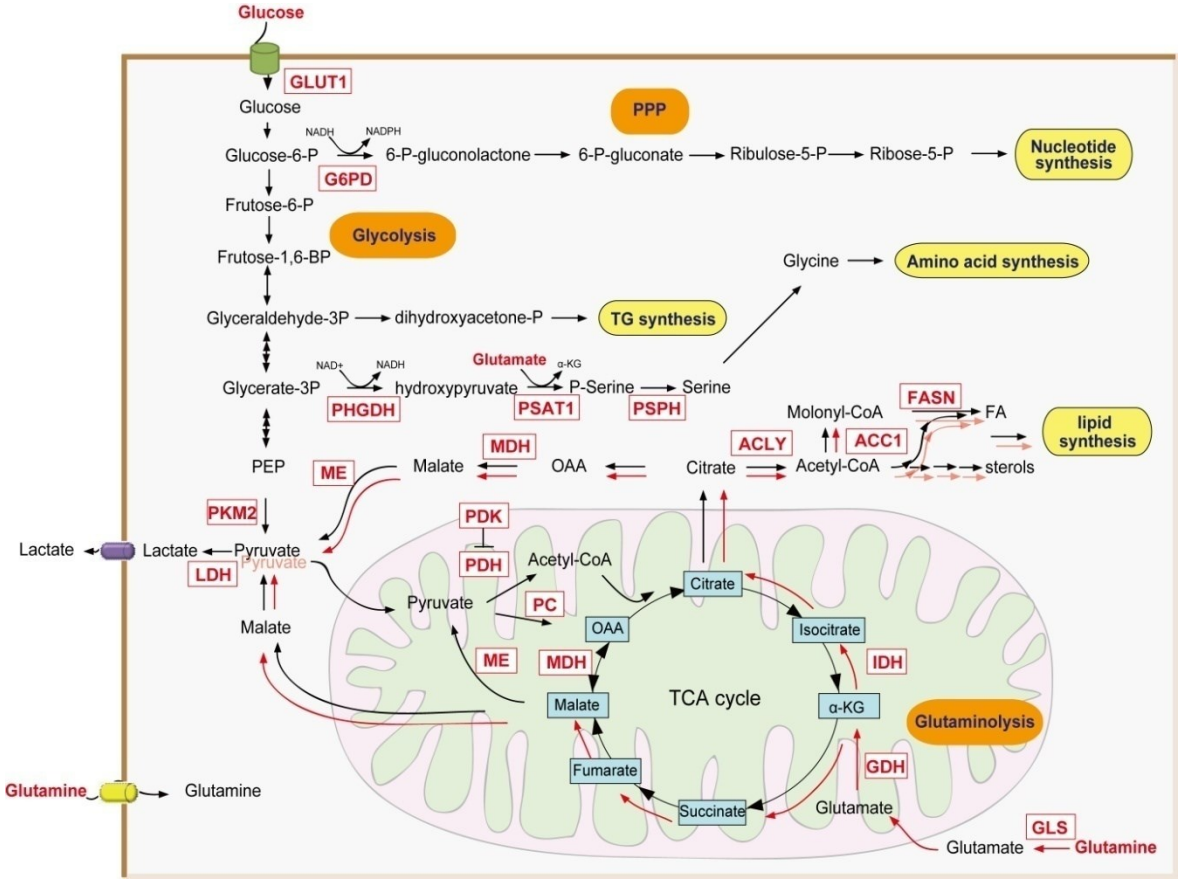

Figure 1. Glucose and glutamine metabolism in tumor at a glance. *Tumor cells generally use glucose and glutamine to generate ATP and redox, which are required for anabolic process. Carbon and nitrogen from glucose/glutamine are critical sources for synthesis of macromolecules (amino acids, lipids and nucleotide acids).* ***Abbreviation****: PDH, pyruvate dehydrogenase; PC, pyruvate carboxylase; LDH, isocitrate dehydrogenase; PEP, Phosphoenolpyruvic acid; LDH, lactate dehydrogenase; PDK, pyruvate dehydrogenase kinase; PKM2, pyruvate kinase isoform 2, mitochondrial; G6PD, glucose 6-phosphate dehydrogenase; OAA, oxaloacetate; ME, malic enzyme;GLUT1, glucose transporter 1; GLS, glutaminase; GDH, glutamate dehydrogenase; ACLY, ATP citrate lyase; ACC, acety-coA carboxylase, FASN, fatty acid synthase; PPP, pentose phosphate pathway; TCA cycle, citric acid cycle.*

1.1.3. Lipid Metabolism

Although tumor cells undergoing the Warburg effect are driven to rapid proliferation when glucose is abundant, a broad diversity of nutrient dependence would confer cells better adaptation to nutrient availability and metabolic stress. Tumor cells generally demand high amounts of fatty acids (FA) and cholesterol as they rapidly proliferate. Numerous studies in the last half century have confirmed hyperactivation of *de novo* lipogenesis in various types of neoplastic lesions. Targeting lipogenesis through various pharmacological inhibitors of rate-limiting enzymes such as fatty acid synthase (FASN), stearoyl-CoA desaturase-1 (SCD1), ATP-citrate lyase and their common upstream mediator sterol-regulatory element binding protein-1 (SREBP1) was effective in tumor suppression (15). However, cancer cells may not solely rely on *de novo* lipogenesis as source of lipids, as they are capable to rapidly convert exogenous FA into lipids required for proliferation and pro-tumorigenic lipid signaling in cancer cells (16). Several studies have also demonstrated elevated cholesterol-rich LDL uptake and LDL receptor (LDLR) expression in a wide range of tumors including glioblastoma (17), leukemia (18) and lung cancer (19). Overexpression of LDLR in human breast carcinoma cell facilitates tumor cell proliferation (20), while shRNA silencing of LDLR dramatically reduces cholesterol uptake and cell proliferation in pancreatic tumor cells, indicating that LDLR can be considered as a novel metabolic target in tumor suppression (21). Lipoprotein lipase (LPL) that hydrolyzes triglyceride-rich very low-density lipoprotein (VLDL), in concert with FA translocase (CD36) is critical for cancer cells to acquire FA from the culture medium (22).

FA can also be acquired from intracellular metabolic pathways. As aforementioned, glutamine is important carbon source for cell growth in concert with glucose. In glucose depletion condition or some tumors harboring mutations in TCA cycles, the normal oxidative mitochondrial function is defective and citrate derived from glucose is insufficient for acetyl-coA production and FA synthesis. In these cases,

tumor cells orchestrate glutamine-dependent reductive carboxylation rather than canonical oxidative metabolism to fuel the TCA cycles and form citrate by mitochondrial and cytosolic isocitrate dehydrogenase isoform 1 and 2 (IDH1/2) (23). We summarize the mechanisms whereby tumor cells obtain the FA and cholesterol both in external and internal manner (Fig. 2).

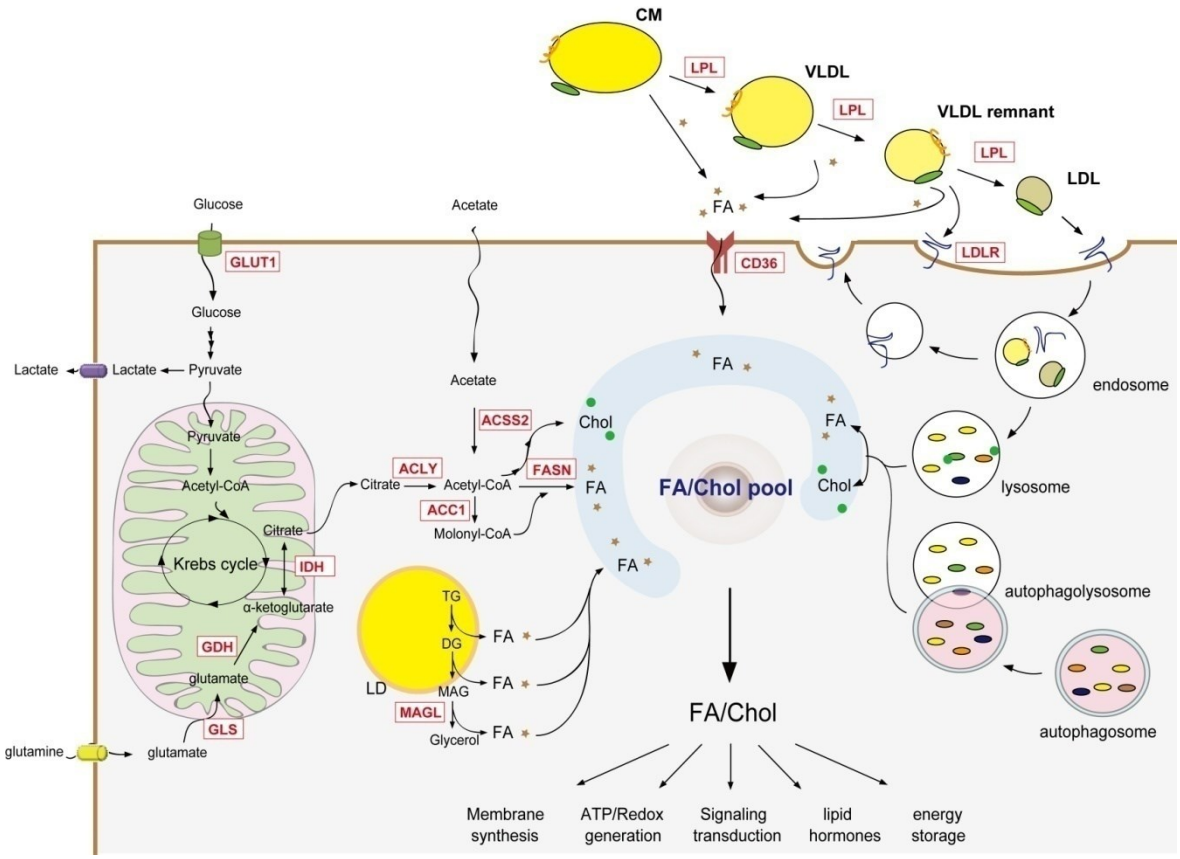

Figure 2. Lipid metabolism in tumor at a glance. *Besides glucose and glutamine, lipid (fatty acids and Cholesterol in particular) are an extremely relevant energy source. They can be derived from the circulating lipoproteins, or can be potentially obtained from hydrolysed triglycerides (intracellular lipid droplets) by neutral hydrolases in the cytoplasm or acid hydrolases in the lysosome or autophagolysosome. FA can also be synthesized by Acety-CoA. Intracellular Acety-CoA mainly comes from breakdown of citrate, which is a critical TCA intermediate and transported into cytoplasma from mitochondria when TCA cycle is overloaded. TCA flux can be replenished by glucose via glycolysis in cytoplasm or by glutamine through glutaminolysis and reductive carboxylation in mitochondria. Acety-CoA can also be directly converted by acetate, which is abundant in plasma. The FA and Cholesterol can be further utilized in membrane synthesis (phospholipids, sphingomyelin etc.), ATP/Redox production via TCA cycle, signaling transduction (lipid-derived molecules or protein modification by isoprenoid), lipid hormones (especially sterols) and energy storage as TG in lipid droplet. Genes (lipid transporters/enzymes) marked in red box are reported to be abundantly expressed in malignancies.* ***Abbreviation****: FA, fatty acid; Chol, cholesterol; LPL, lipoprotein lipase; CD36, FA translocase; VLDL/LDL/HDL, very low/low/high-density lipoprotein; LDLR, LDL receptor; GLUT1, glucose transporter 1; GLS, glutaminase; GDH, glutamate dehydrogenase; IDH, isocitrate dehydrogenase; ACLY, ATP citrate lyase; ACC, acety-coA carboxylase, FASN, fatty acid synthase; ACSS2, acety-coA synthase; MAGL, monoacylglycerol lipase.*

1.1.4. Metabolic Reprogramming in Tumor Microenvironment

1.1.4.1. Lipid and tumor stromal cells

Tumor microenvironment contains innate and adaptive immune cells that can recognize and destroy tumors. Macrophages are major players of tumor immunity. *Sag D. et. al.* reported that mice exclusively lacking macrophage-specific ATP-binding cassette transporter G1 (ABCG1), which promotes cholesterol efflux from cells and regulates intracellular cholesterol homeostasis, suppressed subcutaneousMB49-bladder carcinoma and B16-melanoma growth and promoted a phenotypic shift of the macrophages from a tumor-promoting M2 to a tumor-fighting M1within the tumor. This evidence suggests that cholesterol in tumor-associated macrophages (TAM) plays a critical role in tumor development.

Lipid-derived small molecules are also involved in signaling transduction in tumors. The role of sphingosine-1-phosphate (S1P), a bioactive lipid mediator, has been implicated in cancer progression. A specific inhibitor of sphingosine kinase, which impedes S1P production in cancer cells, led to reduced S1P levels, reduced number of metastases of breast tumors to lymph nodes and lungs. It alleviated the tumor burden in a mouse model, suggesting a role of S1P in stimulating angiogenesis and lymphangiogenesis in tumor microenvironment (24). Another bioactive lipid mediator, prostaglandin E2 (PGE2), was shown to be involved in the promotion of tumor progression, metastatic spread and, possibly, initiation (25). Sinha *et al.* reported that PGE2 is responsible for the accumulation and retention of myeloid-derived suppressor cells, which inhibit immunosurveilance and, thereby, allow the uncontrolled proliferation of (pre)malignant cells (26).

Cancer stem cells (CSC) are considered to be cells with specific ability to differentiate into all cell types found in a particular cancer type, and are thought to be responsible for cancer recurrence after therapy. *Tirinato* et al. reported high

levels of lipid droplets (LDs) as distinctive markers of CSC in colorectal cancer, and that xenotransplanted colorectal cancer CSCs with abundant LDs display the highest tumorigenic property (27).

1.1.4.2. Lipid and Hypoxia

Hypoxia is a pervasive microenvironmental factor that affects normal development and considered to be a hallmark of cancer and to be instrumental in metabolic reprogramming of tumor cells (28). Tumor hypoxia is mainly caused by defective vasculature due to the unregulated proliferation tumor. Tumor outgrowing the existing vasculature can lead to diminished O_2 and nutrient supplies, which can increase cellular reactive oxygen species (ROS) and cause endoplasmic reticulum (ER) stress and, eventually, reduces tumor growth (29). The hypoxic environment of a tumor leads to stabilization of the hypoxia-inducible factor-1a (HIF-1a), stimulating glycolytic flux in tumor cells (30). In contrast to the established role in glucose metabolism, the involvement of HIFs and the molecular mechanisms regarding the effects of hypoxia on lipid metabolism are poorly characterized. Several studies reported the accumulation of TG and LDs in tumor cells under hypoxic conditions, activating lipin 1, a phosphatidate phosphatase isoform that catalyzes the penultimate step in triglyceride biosynthesis (31). This is accompanied by upregulation of Fatty Acid Binding Protein 3 (FABP3) and FABP7 due to fatty acid uptake, and adipophilin (ADRP), which is required for the formation of LD membranes (32). The formation of LDs could protect tumor cells from increased ROS toxicity under hypoxia and resulted in decreased cell survival (32).

The transcriptional expression of SCD1, which desaturates *de novo* synthesized lipids, is increased under hypoxic conditions via SREBPs (33). However, under O_2 deprivation, cell death occurs because of the enzymatic inactivation of oxygen-consuming SCDs, rendering cells dependent on exogenous unsaturated

lipids. Hypoxic cells can also bypass the effects of the SCD inhibitor by scavenging serum fatty acids (*e.g.* fatty acid tail from lysophospholipids), diminishing the need for acetyl-CoA and the oxygen-dependent SCD1-reaction (34). Restricting the supply of exogenous lipid to hypoxic cells could lead to a critical lipid deficiency and cause cell death by eliciting ER stress and activating the unfolded protein response (UPR) (29).

1.2. Aberrant Systemic Lipid Homeostasis and Cancer

1.2.1. Obesity and Cancer

Obesity is considered as one of the most common public and worldwide health problems. Obesity is usually accompanied by metabolic syndromes such as hepatosteatosis, atherosclerosis, and diabetes. Recent evidence also strongly linked obesity to an alarming risk for developing several malignant tumors. *Calle et al.* reported that individuals with a body mass index (BMI) >40 are prone to higher rates of death due to diverse types of cancers (*e.g.* colon, esophagus, gallbladder, liver, rectum, pancreas, kidney, myeloma and lymphoma) (35). Meta-analysis unveil a strong association of BMI with the incidence and mortality for DLBCL, the most common form of aggressive B cell lymphoma and Hodgkin's lymphoma (36). Increased hormone levels including adipokines (*e.g.* leptin, adiponectin (37)) and growth factors (*e.g.* insulin-like growth factor (38, 39)) are potential mechanisms by which obesity could induce cancer. Nevertheless, direct evidence linking excess lipid supply and B-cell lymphoma growth and progression is still missing.

1.2.2. Adipose Lipolysis and Cancer

Loss of WAT and skeletal muscle are well recognized as predominant symptoms of cancer-associated cachexia and contribute markedly to cancer-associated death.

The loss of fat mass has been attributed to increased lipolysis in adipocytes. In cachexia, the expression of hormone sensitive lipase (HSL) was increased, showing a strong correlation with *in vitro* lypolytic activity (40). Ablation of another key lipase, adipose triglyceride lipase (ATGL), is shown to prevent tumor-induced WAT loss in mice (41). All these data suggest selective inhibition of lipases may prevent fat and muscle loss in cachexia.

In fact, the breakdown of lipids in the adipose tissue distal from the tumor drives the efflux of FFA and glycerol into circulation, which could serve as nutritional sources of tumor. FFA can be used directly by tumors as energy supply and for biomass synthesis. Glycerol needs to be converted to glucose via gluconeogenesis in order to be used by the tumor cells (42). In a recent study, *Nieman et al.* described an observation of lipid transfer from adipocytes to cancer cells when co-culturing them. This FA transfer could be blocked by a FABP4 inhibitor. Interestingly, co-injection of ovarian cancer cells with adipocytes in mice show promotion in growth compared to that of cancer cells alone, indicating that FA efflux from adipocyte supports tumor growth (43).

1.2.3. Lipoprotein Abnormalities and Cancer

Several groups reported decreased serum levels of total cholesterol (TC) and increased triglyceride (TG) concentrations in patients with solid tumors (44-46). Similar results were observed in hematological malignancies (45, 47), oral (48), as well as head and neck cancers (49), whereas the correlation with breast cancer remains controversial (45, 50). Unfortunately, no data are available for different types of malignant lymphoma such as diffuse large B-cell lymphoma and Burkitt's lymphoma, which are characterized by one of the fastest growth rates of human malignancies. To investigate whether low LDL-cholesterol (LDL-C) is associated with an increased risk of cancer incidence, a Mendelian randomization study has

been performed, in a population with spontaneous decrease of LDL-C as a result of one of the three polymorphisms, proprotein convertase subtilisin/kexin type 9 (PCSK9), ATP-binding cassette sub-family G member 8 (ABCG8) or apolipoprotein E (ApoE). A cancer risk that is comparable with that in normal subjects (51), suggests that low LDL-C *per se* does not cause cancer. Notably, in prostate cancer, the reduction of plasma TC levels in patients with metastatic disease compared to non-metastatic patients and healthy men, is associated with increased catabolism of LDL (39). Given that enriched circulating cholesterol provokes growth of breast and prostate tumor in mice (52, 53), presumably the reduction of plasma LDL-C in cancer patients is at least partially attributable to the intake by tumors via LDLR, probably as a fuel source. In mice, PCSK9 deficiency reduces liver metastasis in part by its ability to lower cholesterol levels, which is abolished by feeding a high cholesterol diet (54). Taken together a bidirectional causality between tumor development and lipoprotein abnormality remains to be investigated further.

1.3. Impact of Lipid Lowering Strategies on Tumor Growth

1.3.1. Lipid Lowering Drugs

The nuclear receptor peroxisome proliferator-activated receptor alpha (PPARα) transactivates gene transcription in response to specific endogenous (*e.g.* fatty acids (FA) (55)) or exogenous ligands (*e.g.* fibrates (56)). PPARα plays a central role in lipid metabolism and inflammation in various tissues (reviewed in (57)). PPARαagonists are widely prescribed for the treatment of hyperlipidemia (55). Recently, their anti-tumorigenic “side-effects” have been described in various types of tumors (58). The precise mechanism(s) by which PPARα agonists impede tumor growth is still not fully elucidated. However, it could be at least in part be attributed to the inhibition of angiogenesis (59) in mice and a pro-apoptotic activity was reported in mantle cell lymphoma *in vitro* (60). Nevertheless, whether there is a link between the lipid-lowering properties of PPARα agonists and tumor suppression is

still poorly studied.

HMGCR (3-hydroxy-3-methylglutaryl-CoA reductase) is a rate-limiting enzyme in the biosynthesis of isoprenoid compounds, including ubiquinone, dolichol and sterols (61). HMGCR inhibitors, statins, have been used to treat hypercholesterolemia by accelerating the circulating LDL clearance via hepatic LDLR. Ample clinical and experimental evidence suggests a tumor-suppresive function of statins against diverse types of tumors (62). How statins exactly exert the anti-tumor effects remain largely unexplored, but might be partially due to the following mechanisms: i) interruption of the transition of G1-S in the cell cycle; ii) interference with cell signaling (*e.g.* insufficient isoprenoids that affect membrane anchoring of GTPases, a Ras and Rho family member (63)); iii) inhibition of *de novo* synthesis of cholesterol, leading to disturbed maintenance of membrane fluidity and integrity; iv) apoptosis induction by depleting geranylgeranylated proteins (64) or by deregulating the balance of pro-apoptotic BAX and anti-apoptotic BCL-2 levels (65).

The pharmaceutical drugs fibrates and statins are widely prescribed for the treatment of hyperlipidemia and atherosclerosis. Considering the importance of exogenous lipids as an alternative lipid source supporting of tumor progression as described above, it is conceivable that the systemic lipid lowering effect could also contribute to tumor suppression. Evidence to support this hypothesis will be described in the Results Section.

1.3.2. Hypolipidemic Mouse Models

Two hypolipidemic mouse models with attenuated ApoB lipoprotein production are introduced here. The endoplasmic reticulum localized carboxylesterase 3/triacylglycerol hydrolase (Ces3/TGH) [annotated as carboxylesterase 1 (CES1) in

humans] promotes VLDL assembly (66, 67). Expression of Ces3/TGH in hepatoma cells augmented secretion of TG and ApoB100 in the VLDL density range (68) while pharmacological inhibition in primary hepatocytes showed the opposite effect (69, 70). Fasting plasma VLDL concentration was elevated in liver-specific CES1/TGH transgenic mice fed a chow diet (71). In contrast, mice lacking Ces3/TGH displayed reduced ApoB and TG in plasma upon a chow or western diet (69, 72). Similar reduction in VLDL secretion was also observed in *Ces3/TGH*$^{-/-}$ mice cross-bred with *Ldlr*$^{-/-}$ mice and fed a Western-type diet (73).

Hepatocyte-specific phosphatidylethanolamine *N*-methyltransferase (PEMT) catalyzes the methylation reactions in the conversion of phosphatidylethanolamine (PE) to phosphatidylcholine (PC) (74). Hepatocytes from *Pemt*$^{-/-}$ mice secreted significantly less VLDL-TG into the medium, while transfection with PEMT cDNA enhanced its secretion (75). *Pemt*$^{-/-}$ mice fed a high-fat diet had reduced plasma TG and ApoB compared to control (76). Mice lacking both PEMT and LDLR fed a Western-type diet displayed substantial protection against atherosclerosis compared to *Ldlr*$^{-/-}$ mice due to decreased atherogenic lipoprotein profile in plasma (77).

These two hypolipidemic mouse models are used as supporting genetic models to investigate the effect of global lipid lowering on tumor progression. Further evidence to support this hypothesis will be depicted in the Results Section.

2. AIM AND APPROACH

Our study aims to analyze the systemic effects of B-cell tumors on lipoprotein metabolism and the underlying mechanisms. In addition influences of lipid-lowering effect on B-cell tumor growth are investigated. To achieve these goals, the following approaches were taken:

- **Mechanisms of tumor-induced hyperlipidemia:**

1. Lipid storage in WAT and lipoprotein profiles in the circulation were evaluated to assess tumor-induced lipid mobilization from WAT.
2. Hepatic VLDL secretion rate was determined to study impact of tumors on VLDL production.
3. Fat tolerant test (FTT) and post-heparin-plasma TG hydrolase activities assay were applied to determine how tumors affect TG-rich lipoproteins clearance.
4. Hepatic LDLR expression and its upstream signaling were explored to study the influences of tumors on LDL turnover.

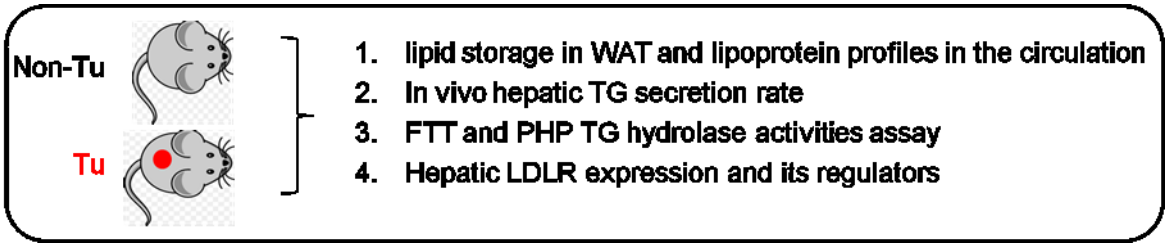

Abbreviation: Non-Tu, non-tumor bearing mice; Tu, tumor-bearing mice; PHP, post-heparin-plasma; WAT, white adipose tissue; LDLR, low-density lipoprotein receptor

5. Metabolic labeling assays to study alteration of lipogenesis in primary hepatocytes from tumor-bearing mice.

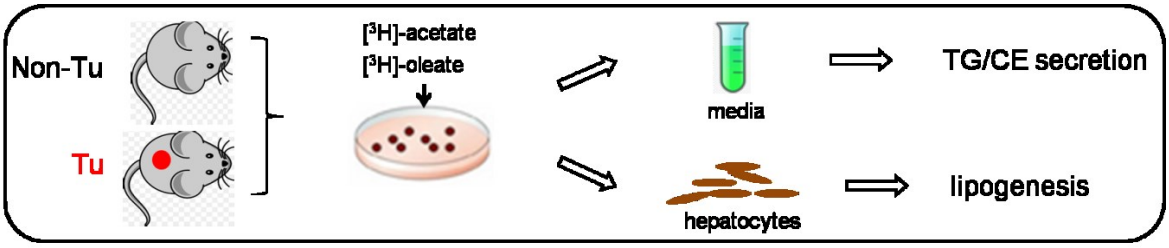

- **Lipid lowering strategies:**

1. Tumors were grown in wild type mice fed with 0.2% fenofibrate containing chow to study the influences of pharmaceutical lipid lowering on tumor growth.

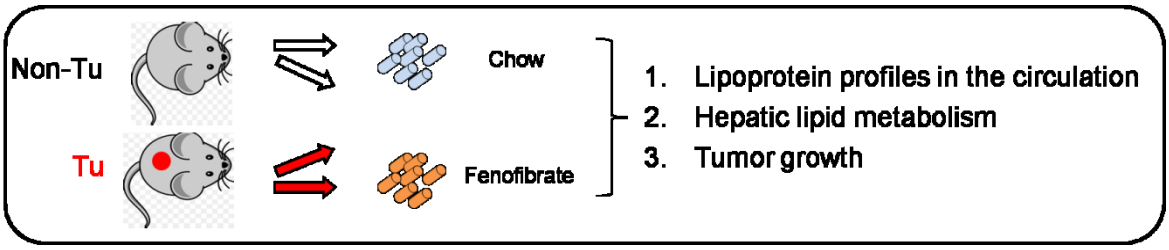

2. Tumors were grown in *Ces3/Tgh*$^{-/-}$ and *Pemt*$^{-/-}$ mice to investigate the impacts of genetic hypolipidemia on tumor growth.

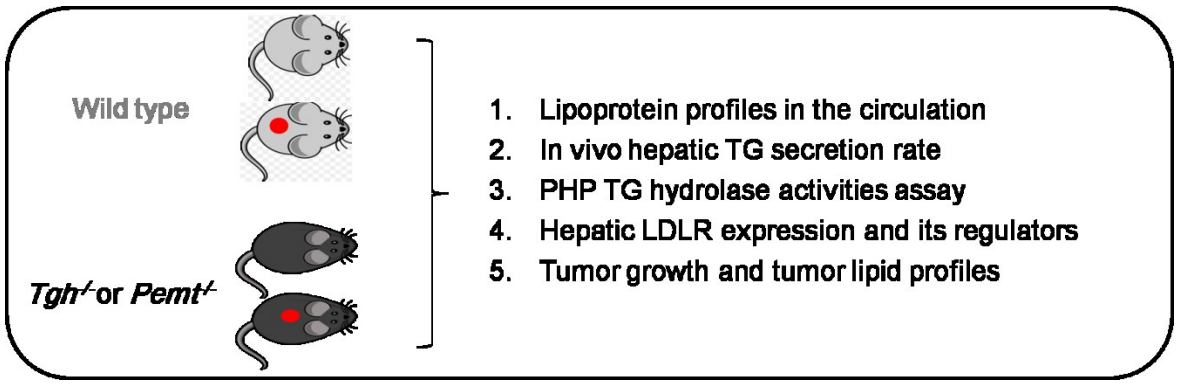

Abbreviation: Ces3/Tgh, carboxylesterase3/triacylglycerol hydrolase; Pemt, phosphatidylethanolamine *N*-methyltransferase

3. METHODS

This section is partially reused from the publication (78) with modifications and the unpublished manuscript in collaboration with Prof. Dr. Richard Lehner (University of Alberta, Edmonton, Canada). The usage of relevant contexts in this section is with the permission of Elservier and Richard Lehner & Gerald Hoefler.

3.1. Materials

Fatostatin was obtained from Cayman Chemical (MI, USA), water-soluble cholesterol, hydroxypropyl-β-cyclodextrin (HPCD), lipoprotein-deficient serum (LPDS) and mouse recombinant TNFα were purchased from Sigma-Aldrich (Germany). All human purified lipoproteins (VLDL, LDL, acLDL, HDL) were from healthy subjects and prepared according to routine protocols. The following antibodies were used: Akt (#9272), phospho-Ser473-Akt (#4060), AMPKα (#2532), phospho-Thr172-AMPKα(#2535), ACC (#3662), FASN (#3189), β-actin (#4967) all from Cell Signaling (MA, USA); SREBP2 (sc-5603) from Santa Cruz (USA); SREBP1 and HMGCR antibodies were kindly provided by Drs. Joseph Goldstein & Michael Brown and Dr. Russell Debose-Boyd (UT Southwestern), respectively; LDLR antibodies were kindly given by Dr. Da-wei Zhang (University of Alberta); appropriate secondary antibodies were used. Mttp, ApoE and ApoB antibodies were generated in-house in Dr. Richard Lehner's lab (University of Alberta).

3.2. Animals and Tumor Inoculation

Twelve to fifteen week old male C57Bl/6J mice were housed with 12 h light/dark cycle and permitted *ad libitum* consumption of water and food. During experiments, food intake and body weight were monitored. All experimental protocols using *Ldlr*$^{-/-}$ mice in Section 4.1 and *PPARα*$^{-/-}$ mice in Section 4.2 with as well as their

corresponding wild-type control were performed in the animal facility of the Medical University of Graz in accordance with animal protocol BMWF-66.010/0110-II/3b/2010, as approved by the Austrian government. Other experimental protocols using *Ces3/Tgh*$^{-/-}$ mice, *Pemt*$^{-/-}$ mice and wild-type mice with C57Bl/6N background in Section 4.3 were approved by the University of Alberta Animal Care and Use Committee and were performed in accordance with the guidelines of the Canadian Council on Animal Care.Animals were divided randomly into groups as indicated. 1.5X10^5 Bcr/Abl-transformed precursor B-cells (TPBCs) or PBS solution as negative control were injected subcutaneously over the flank. For fenofibrate treatment, mice were fed regular chow diet (4.5 % w/w fat) or chow diet mixed with 0.2% w/w fenofibrate (Sigma-Aldrich, Germany). Three dimensions of tumors were measured by digital display caliper and tumor volume was estimated based on the formula “1/2 × length × width × height”. Non-fasting, fasting and refeeding regimen were applied. “Non-fasting” indicates withdrawal of food during daytime (8 a.m. – 1 p.m.) with minimal dietary stress to mice. “Fasting” denotes 16 hr overnight removal of food (6 p. m. – 10 a.m.). “Refeeding” indicates overnight fasting plus food supply with chow diet for the following 12 hr. Mice were sacrificed under anesthesia with isoflurane and plasma was collected by retro-orbital bleeding. Thereafter, mice were sacrificed by cervical dislocation and tissues were rapidly excised, weighed, and either frozen in liquid nitrogen or stored in 4% neutral-buffered formalin for subsequent preparation of paraffin blocks.

3.3. Creation and Maintenance of Bcr/Abl-transformed Precursor B-cells

Bcr/Abl-transformed precursor B-cells (TPBCs) were created as previously reported (79). Briefly, bone marrow was isolated from C57Bl/6J mice. Cells were transduced with GFP/p185$^{bcr/abl}$ viral supernatant produced from Φ-NX (Phoenix) cells. GFP is used as a transduction marker for sorting out primary positive cells. Selected cell lineages were further sorted by fluorescence-activated cell sorting

(FACS) based on expression of the B-cell markers B220, CD43 and CD19. TPBCs were maintained in RPMI 1640 medium containing 10% FBS (PAA, Pasching, Austria) in a 37°C incubator with 5% CO_2.

3.4. Quantitative Reverse Transcription Real-time PCR

Total RNA was extracted from liver, dissected tumor tissue or cultured cells using Trizol LS. cDNA was synthesized from 2 mg of total RNA with High Capacity cDNA Reverse Transcription Kit (Applied Biosystems, Vienna, Austria) or Superscript Ⅲ Reverse Transcriptase (Invitrogen, CA). For qPCR, SYBR Green PCR Master Mix from Invitrogen and the Applied Biosystems 7900 HT Sequence Detection System were used for experiments done in the Medical University of Graz, Platinum SYBR Green qPCR SuperMix-UDG kit was used in a Rotor-Gene 3000 instrument (Montreal Biotech, Canada) for qPCR results obtained at the University of Alberta. A standard curve was used to calculate the relative mRNA levels of each gene, normalized to cyclophilin A or 18s as reference genes. All primers were synthesized at the DNA Core Facility of the University of Alberta. Primers used in this study are listed in Table 2.

3.5. Subcellular Fractionation and Protein Extraction

Total protein from liver and tumor samples (100 mg each) were homogenized in RIPA lysis buffer containing a protease inhibitor cocktail and phosphatase inhibitor (Roche Diagnostics, Québec, Canada). For liver fractionation, 100 mg liver samples were homogenized in 1mL lysis buffer containing 250 mM sucrose, 50 mM Tris, 1 mM EDTA, pH 7.4 supplemented with a protease inhibitor cocktail. Tissue lysates were centrifuged at 500×*g* for 15 min at 4°C to separate supernatant (cytoplasmic fraction) and pellet. Pellets were washed gently and resuspended in nuclear extraction buffer. After gentle shaking on ice for 30 min, samples were

centrifuged at $10^5 \times g$ for 30 min at 4°C to yield the supernatant (nuclear fraction). For nuclear fraction separation, similar steps as for nuclear preparation from tissues were performed. Aliquots were assayed or protein concentrations were determined by the Bradford Protein Assay (Bio-Rad, ON, Canada).

3.6. Immunoblotting

Western blotting was performed using total or fractionated protein extracts (30 µg protein for liver and hepatocyte samples and 50 µg protein for tumor samples) or plasma and probed with antibodies listed above. Immunoreactivity was detected by ECL (Amersham-Pharmacia, Québec, Canada) or SuperSignal West Dura (Thermo Scientific, IL, USA) to enhance the signal. Immunoblot was scanned and quantified using G-Box (SYNGENE, UK).

3.7. Apoptosis Assay

Cell apoptosis was assessed by a LSRII flow cytometry (BD Biosciences, USA). Annexin V and 7AAD were purchased from BD Biosciences and used as early and late stage apoptotic markers, respectively.

3.8. Lipid and Lipoprotein Analysis

For serum lipid profile analysis, blood was collected as described above and centrifuged for 20 min at 1800 g. Serum was stored at -80°C until analysis. Serum TG, total (TC) and free cholesterol (FC), phospholipid (PL) (DiaSys, Germany), and non-esterified fatty acids (NEFA) (Wako, Germany) were quantified spectrophotometrically. For lipoprotein analysis performed by Anton Ibovnik (Institute of Molecular Biology and Biochemistry, Medical Universitty of Graz), 200 µl plasma pools from each condition were subjected to fast protein liquid

chromatography (FPLC) (Pharmacia P-500; Pfizer Pharma, Karlsruhe, Germany) equipped with a Superose 6 column (Amersham Biosciences, Piscataway, NJ). Lipoproteins were eluted with 10 mM Tris-HCl, 1 mM EDTA, 0.9% NaCl, and 0.02% NaN_3 (pH 7.4). TC and TG concentrations in 0.5 ml fractions were measured enzymatically (TC: Greiner Diagnostics AG, Bahlingen, Germany; TG: DiaSys, Holzheim, Germany). To enhance sensitivity, sodium 3, 5-dichloro-2-hydroxy-benzenesulfonate was added to the reaction buffer. For FPLC analysis performed in the Lipid core facility of the University of Alberta, plasma from 5 non-fasted mice was pooled in each group and applied onto size-exclusion fast-protein liquid chromatography (FPLC) (71).

Quantitative immunoturbidimetric assays for apolipoprotein (Apo) B was obtained from Rolf Greiner Biochemica (Flacht, Germany). Assays were performed using a Hitachi 917 automated analyzer (Boehringer Mannheim, Germany). For determination of isotope-labeled lipids from plasma and hepatocytes were descried previously (80). Briefly, lipids were extracted with chloroform/methanol (2:1), resolved by thin-layer chromatography (TLC) in chloroform/methanol/acetic acid/water (25:15:2.5:1) for separation of phospholipids or in hexane/isopropyl ether/acetic acid (15:10:1) for separation of neutral lipids. Lipids were visualized by exposure of the TLC plates to iodine vapor. Radioactivity in various lipid species was determined by liquid scintillation counting. For determination of tissue lipids, liver and tumor sample were washed with phosphate-buffered saline (PBS) and frozen. Approximately100 mg tissue samples were homogenized in 1 mL methanol and total lipids were isolated from homogenates by Folch extraction (81). Protein concentration in homogenates was used as reference. The mass of tissue TG, TC, CE and NEFA were determined as described above.

3.9. Tissue FA Uptake

Liver and tumor tissue were excised freshly from mice, and 30-50mg pieces were used for the assay. Tissues were washed with PBS containing 5 mM EDTA and 0.1% (w/v) BSA. Tissue samples were cut into 3mm^2 size pieces and washed with PBS containing 5 mM EDTA. The substrate containing 2.5mM oleate:BSA complex and 2µCi/ml [^{14}C]-oleate as tracer was incubated with the samples in a 24-well plate for 1h at 37°C under regular shaking. [^{14}C]-oleate uptake and remaining radioactivity in the medium was determined by liquid scintillation counting. The amount of absorbed FA was calculated by reduction of radioactivity in the media (initial - final) and normalized by protein concentrations, which were quantified by the DC^{TM} Protein Assay (Bio-Rad, Austria) based on the manufacturer protocol.

3.10. Metabolic Labeling Studies

Primary hepatocytes, freshly isolated from non-fasted mice by perfusion of 0.8mg/mL Collagenase Type I (Worthington Biochemical Group, NJ) through the portal vein, were incubated with DMEM containing 15% FBS for 4 hr for cell attachment as described previously (69). For incorporation of exogenous substrates into lipids, hepatocytes were washed twice, then incubated for 4 hr in 2 mL serum-free DMEM containing either 5 µCi [^{3}H]-oleate (combined with 400 µM oleate conjugated with 0.5% fatty acid-free BSA) or 5 µCi [^{3}H]-acetate (combined with 50 µM sodium acetate). After incubations, cells and media from some of the dishes were collected for analysis (pulse). Remaining cells were washed with PBS to remove unabsorbed substrate and incubated with DMEM for further 12 hr. Cells and media were collected for analysis (chase). [^{3}H]-labeled lipid classes were determined following lipid extraction and TLC by liquid scintillation counting as described above.

3.11. Histology and Immunohistochemistry

Tumors of sacrificed mice were carefully isolated, fixed in 4% neutral buffered formaldehyde solution for 24 h and embedded in paraffin while livers were frozen in liquid nitrogen. 2 µm thick sections were cut and stained with haematoxylin and eosin (H&E). Caspase-3, CD31, Ki67 and F4/80 IHC were performed using specific antibodies against active caspase-3 (R&D, USA), CD31 (Thermo scientific, USA), Ki67 (Novocastra, UK) and F4/80 (Serotec, USA) respectively and appropriate secondary antibodies as previously described (82). For determination of vessel density, the slides were scanned and CD31-positive cells were quantified and normalized to total analyzed area using ScanScope software (Aperio technologies, USA). For quantification of caspase-3 positive cells, the slides were scanned at 40x magnification and manually quantified in 60 power fields.

3.12. ELISA

TNFα and IL-6 quantitative ELISA kits were purchased from eBioscience (Vienna, Austria). Mouse PCSK9 ELISA Kit was purchased from R&D Systems (MN, USA). For serum samples, diluted serum (1:2) was loaded. For tumor lysates, 40-60 mg frozen samples were homogenized by MagNa Lyzer (Roche, Germany) for 3x15 s at 6500g in RIPA lysis buffer with proteinase inhibitor cocktail (Pierce, Germany), then kept on ice for 20 min. After centrifugation for 10 min at 4000g, protein concentrations in lysates were determined as described above. 50µg proteins were loaded in each 96-well plate. ELISA was performed according to the manufacturer protocol.

3.13. Post-heparin Plasma TG Hydrolase Activity Assay

Post-heparin plasma (PHP) was drawn 20 min after subcutaneous injection of

sodium heparin (500U/kg body weight). Enzyme activities of lipoprotein lipase (LPL) and hepatic lipase (HL) in PHP were assayed as previously described (83).

3.14. Hepatic VLDL Secretion

To measure the rate of VLDL-TG secretion, mice were fasted overnight followed by subcutaneous injection with P-407 (1 mg/g body weight) to inhibit HL and LPL activity. Plasma samples were drawn right before P-407 injection as initial time point and 1, 2, and 3 hr after injection. Plasma TG from each time point was measured as described above.

3.15. Fat tolerant test

Overnight fasted mice were gavaged with 150 μL olive oil containing 10 μCi [^{3}H]-triolein. Blood was drawn immediately before the gavage as initial time point and at 1, 2, 3, 4, and 5 hr post-gavage. Lipids were extracted and separated by TLC. Radioactivity in TG-corresponding bands was determined by liquid scintillation counting.

3.16. *In Vivo* Insulin Signaling

Overnight fasted mice were anesthetized and body temperature was maintained using a lamp. A minimal midline laparotomy was performed, and sterile saline or bovine insulin (0.75 units/kg body weight) was administrated into the portal vein. After 5 min mice were sacrificed, liver and muscle were excised and immediately snap frozen in liquid nitrogen. Protein was extracted from tissues by RIPA lysis buffer and insulin signaling was assessed by immunoblotting with anti-Akt and anti-phospho-Akt (ser473) antibodies.

3.17. OGTT and ITT

Oral Glucose Tolerance Test (OGTT) was performed with overnight fasted mice. Glucose solution (2 g/kg body weight) was administered by oral gavage. Glucose levels were monitored before and 15, 30, 60, and 120 min post-gavage using blood glucose strips (Roche Diagnostics, Québec, Canada). For Insulin Tolerance Test (ITT), mice were fasted during daytime (8 a.m. - 1 p.m.) and injected intraperitoneally with bovine insulin (1 U/kg body weight). Similarly, glucose levels were determined before and 15, 30, 60, 90, 120, and 180 min after injection.

3.18. Statistics

Data are presented as mean ± SEM. Statistical analysis was performed using GraphPad Prism 5. Statistical significance was determined by the Student´s unpaired two-tailed *t* test or ANOVA followed by Bonferroni posttest. Correlation was studied by Pearson's correlation test. Values of $P < 0.05$ were considered as significantly different.

4. RESULTS

4.1. B-cell Tumor Induced Hyperlipidemia in Support of Tumor Growth

This result section is partially reused from the publication (78) with modifications and unpublished data. The relevant materials are reproduced with the permission of Elservier.

4.1.1. Tumors Induce WAT Loss and Hyperlipidemia

We selected Bcr/Abl transformed B-cell (TPBC) tumors as our experimental tumor model because of its high proliferation rate *in vitro* and rapid growth in mice. Thus we speculated that there might be an increased demand for nutrients such as FFA that *in vivo* might be supplied by systemic lipid mobilization. Indeed, loss of WAT was observed in tumor-bearing (hereafter referred to “Tu”) wild type (WT) mice with a significant inverse correlation between WAT weight and tumor weight (R^2=0.43, *P<0.01*) (Fig. 3A). Consistently, adipocytes size was reduced in animals of the tumor group (Fig. 3B). To account for the possible influences of tumor burden on metabolic changes and energy expenditure we monitored food intake and checked the physiological state of the animals from the time tumors became visible until the end of the experiment. Food intake did not differ significantly (Fig. 3C). We also did not detect abnormal behavior or overt signs of discomfort or sickness.

Next we explore if accelerated FA efflux from WAT could result in an increase of lipids in the circulation. Expectedly, plasma apolipoprotein (ApoB) 100 (a marker of VLDL and LDL) and 48 (present in VLDL and chyromicrons (CMs)) were increased in Tu WT mice compared to non-tumor bearing (hereafter referred to “Non-Tu”) controls (Fig. 3D). Tumor-associated increase of VLDL/LDL levels was not

perturbed in *Ldlr*$^{-/-}$ mice (Fig. 3E), a hyperlipidemic mouse model deficient in LDL clearance, suggesting a potential involvements of VLDL production and/or turnover in Tu mice.

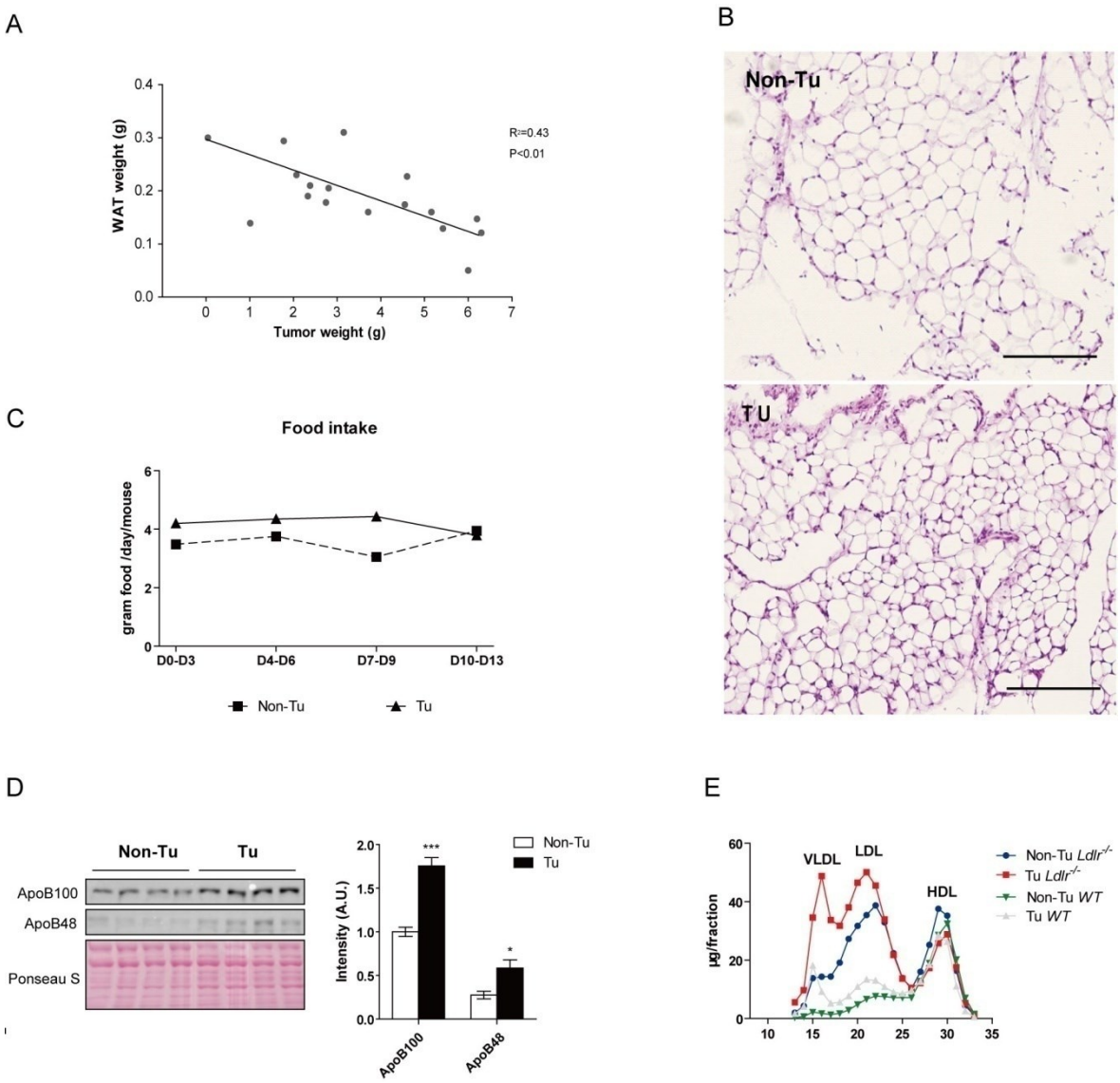

Figure 3. Tumors induce WAT loss and hyperlipidemia. *(A) Inverse correlation between tumor weight and gonadal WAT weight (n=17) determined 13-15 days post-injection of tumor cells. Significance was studied by Pearson's correlation test. (B) H&E staining of gonadal WAT of mice. Scale bar: 50µm. H&E staining was done by Silvia Schauer (Medical University of Graz). (C)Food intake during the experiment was measured. (D) Immunoblot of plasma ApoB100 (509 kDa) and ApoB48 (250 kDa) in Tu/Non-Tu-bearing WT mice. Ponceau S staining served as loading control. (E) Total cholesterol concentrations in plasma (day 14, pooled from 5 mice each) after separation of lipoproteins by FPLC.FPLC was performed by Elke Stadelmeyer and Anton Ibovnik (Medical University of Graz). Error bars represent SEM. Unpaired t-test. *, p<0.05; ***, p<0.001.* ***Abbreviation****: WAT, white adipose tissue; Tu, tumor-bearing; Non-Tu, non-tumor control; VL/L/H-DL, very low/low/high-density lipoprotein; ApoB, apolipoprotein B.*

4.1.2. Tumors Increase VLDL Production and Decrease CM/VLDL Turnover

Next we explored whether the observed tumor-induced increase of plasma VLDL/LDL is due to enhanced hepatic VLDL secretion. Fasting plasma NEFA concentrations were similar between Tu and Non-Tu groups (Fig. 4A). In the Tu group, however, hepatic TG and free cholesterol (FC) content were decreased by 49.5% ($p = 0.035$, Fig. 4B) and 34.3% ($p = 0.018$, Fig. 4C), respectively. Correspondingly, the number of cytosolic lipid droplets in hepatocytes was also reduced in the Tu group (Fig. 4D). These results suggest that tumor growth stimulates VLDL secretion although hepatic protein levels of microsomal triglyceride transfer protein (Mttp), ApoB and ApoE (Fig. 4E) were unaltered.

In addition, we determined hepatic *de novo* lipogenesis in the Tu and Non-Tu groups. Primary hepatocytes isolated from Tu-bearing mice incorporated 2.4-fold more [^{3}H]-acetate into FC and 1.8-fold more into CE (Fig. 4F). The increased amount of available intracellular cholesterol resulted in 3.0- and 1.3-fold more esterification of [^{3}H]-oleate into CE and TG in Tu-bearing mice, respectively (Fig. 4G). Moreover, reduced intracellular labeled FAs suggest enhanced FA channeling into cholesterol and TG in livers of Tu-bearing mice (Fig. 4F, G). The increased intracellular TG and cholesterol pool may support increased secretion of lipids in the form of ApoB-containing lipoproteins. However, this enhanced secretion of TG was normalized after withdrawal of exogenous FA (Fig. 4H), suggesting that the tumor enhances secretion of newly synthesized TG rather than preformed TG. In agreement with our previous report that tumors suppress mRNA expression of PPARα and its target genes in liver (78), acid soluble metabolites (ASM) derived from [^{3}H]-oleate via FA oxidation were decreased in the Tu group (Fig. 4I), which could provide an alternative FA source for TG and CE synthesis.

Fat tolerant tests (FTT) revealed that CMs of Tu-bearing mice accumulated 1.9-fold more TG compared to Non-Tu-bearing mice ($p = 0.001$) (Fig. 4J). The slope after 3

hours is similar in the two groups, whereas it is steeper in the Tu group in the first 3 hr, suggesting that increased CM secretion also contributes to tumor-induced hyperlipidemia. Interestingly, comparable amounts of radioactivity were found in tumor and white adipose tissue (WAT) (Fig. 4K), suggesting rapid lipoprotein lipase (LPL)-mediated uptake of CM-derived lipids by the tumor.

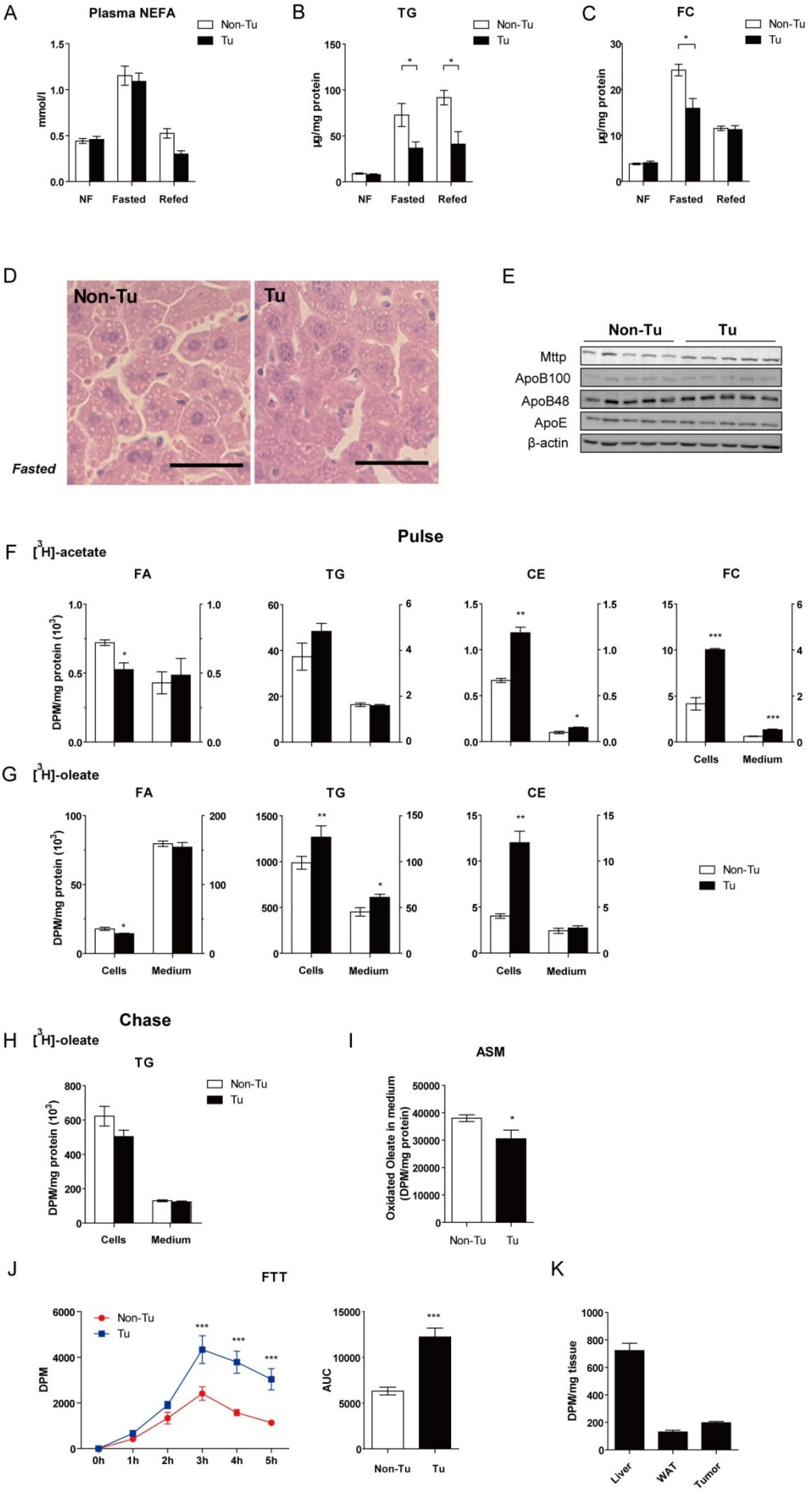
A
Plasma NEFA
Non-Tu
Tu
mmol/l
NF
Fasted
Refed
B
TG
µg/mg protein
C
FC
D
Non-Tu
Tu
Fasted
E
Mttp
ApoB100
ApoB48
ApoE
β-actin
Pulse
F [3H]-acetate
FA
TG
CE
FC
DPM/mg protein (10³)
Cells
Medium
G [3H]-oleate
Chase
H [3H]-oleate
I
ASM
Oxidated Oleate in medium (DPM/mg protein)
J
FTT
DPM
AUC
0h
1h
2h
3h
4h
5h
K
DPM/mg tissue
Liver
WAT
Tumor

Figure 4. Tumors increase VLDL production and decrease CM/VLDL turnover. *(A – C) Plasma NEFA concentrations and liver (B) FC and (C) TG levels from non-fasted (NF), o/n fasted and refed (10 hrs) mice with/without tumors (day 14, n = 4 – 5). (D) Immunoblot of VLDL assembly-related proteins (Mttp, ApoB100/48 and ApoE) and loading controls (β-actin) in liver tissues (n = 5) from non-tumor (Non-Tu) and tumor (Tu) bearing mice. (E) Microscopic images of histological specimen of liver from o/n fasted WT mice stained with H&E (n = 3). Scale bar, 10 μm.H&E was performed by facility service in the Department of Pathology(University Alberta). (F – H) De novo lipogenesis in primary hepatocytes. Cells were incubated with (F) [^{3}H]-acetate or (G) [^{3}H]-oleate as substrates for "Pulse". (H) Cells were incubated with [^{3}H]-oleate, washed and then chased with serum-free DMEM. (I) ASM-derived from incomplete oxidation of oleate in primary hepatocytes were determined. Medium after chase ([^{3}H]-oleate as substrate before chase) was collected and ASM were extracted. Data in (F – I) (n = 3) are representative for two independent experiments with similar results. Radioactivity was determined by liquid scintillation counting and normalized to protein content. (J) FTT in Tu/Non-Tu bearing WT mice (day 14). Radioactivity in TG fraction was measured (n = 7). Statistic differences at different time points were determined by two-way ANOVA. ***, p<0.001. (K) Radioactivity distribution after fat tolerant test (n = 7). Liver, gonadal WAT and tumor were dissected from mice sacrificed 6 hr after oral gavage of [^{3}H]-triolein-containing olive oil. Tissues were minced and dissolved in lysis buffer (1% SDS, 0.1N NaOH) at 60℃overnight. Radioactivity was determined by liquid scintillation counting and normalized to protein content. Error bars represent SEM. If not stated otherwise, statistic differences were analyzed by unpaired t-test. *, p<0.05; **, p<0.01; ***, p<0.001.* ***Abbreviation****: Mttp, microsomal triglyceride transfer protein; ApoE, apolipoprotein E; ASM, acid soluble metabolites; WAT, white adipose tissue; FTT, Fat tolerant test;*

.

4.1.3. Tumors Decrease Hepatic LDLR Protein Expression but not its Transcription

Liver accounts for approximately 70% of LDL turnover in the circulation mainly via LDLR. Hepatic LDLR levels inversely correlate with plasma LDL concentrations. Here we show that the amount of hepatic LDLR was profoundly reduced in Tu-bearing mice (Fig. 5A). The expression of *Ldlr* mRNA is known to be under the control of SREBPs, SREBP2 in particular. Hepatic expression levels of SREBP1 and 2 precursors and their processing into transcriptionally active forms were distinct between Non-Tu- and Tu-bearing mice. In non-fasted mice, along with decreased LDLR protein expression (-64.7%, $p = 0.001$), the precursor and mature form of SREBP1 were reduced by 49.1% ($p = 0.031$) and 53.8% ($p = 0.023$), respectively, whereas no change in SREBP2 precursor but a declining trend of its mature form (44.9%, $p = 0.14$) were observed (Fig. 5A). *Fbxw7*, which catalyzes the ubiquitination of ER-located mature SREBPs and subsequent degradation, was up-regulated in Tu-bearing mice, whereas mRNA expression levels of genes involved in SREBP processing (*Insig2*, *Scap*, *S1p*) were unchanged (Fig. 5B). Unexpectedly, except *Pcsk9*, other SREBP target genes including *Ldlr* were all transcriptionally unchanged in Tu-bearing mice (Fig. 5C). In concert, protein levels of FASN, acetyl-CoA carboxylase (ACC)1/2 and 3-hydroxy-3-methylglutary-CoA reductase (HMGCR) were also unaltered (Fig. 5D). The comparably low levels of LDLR in Tu-bearing mice persisted even during overnight (o/n) fasting (-59.1%, $p = 7 \times 10^{-4}$, Fig. 5E) and refeeding (-41.5%, $p = 0.07$, Fig. 5F) regardless of the reported absence of mature SREBPs in fasting and the complete restore of mature SREBP1 and 2 after refeeding (Fig. 5F). These results indicate that the down-regulation of LDLR protein levels is independent of SREBPs activities.

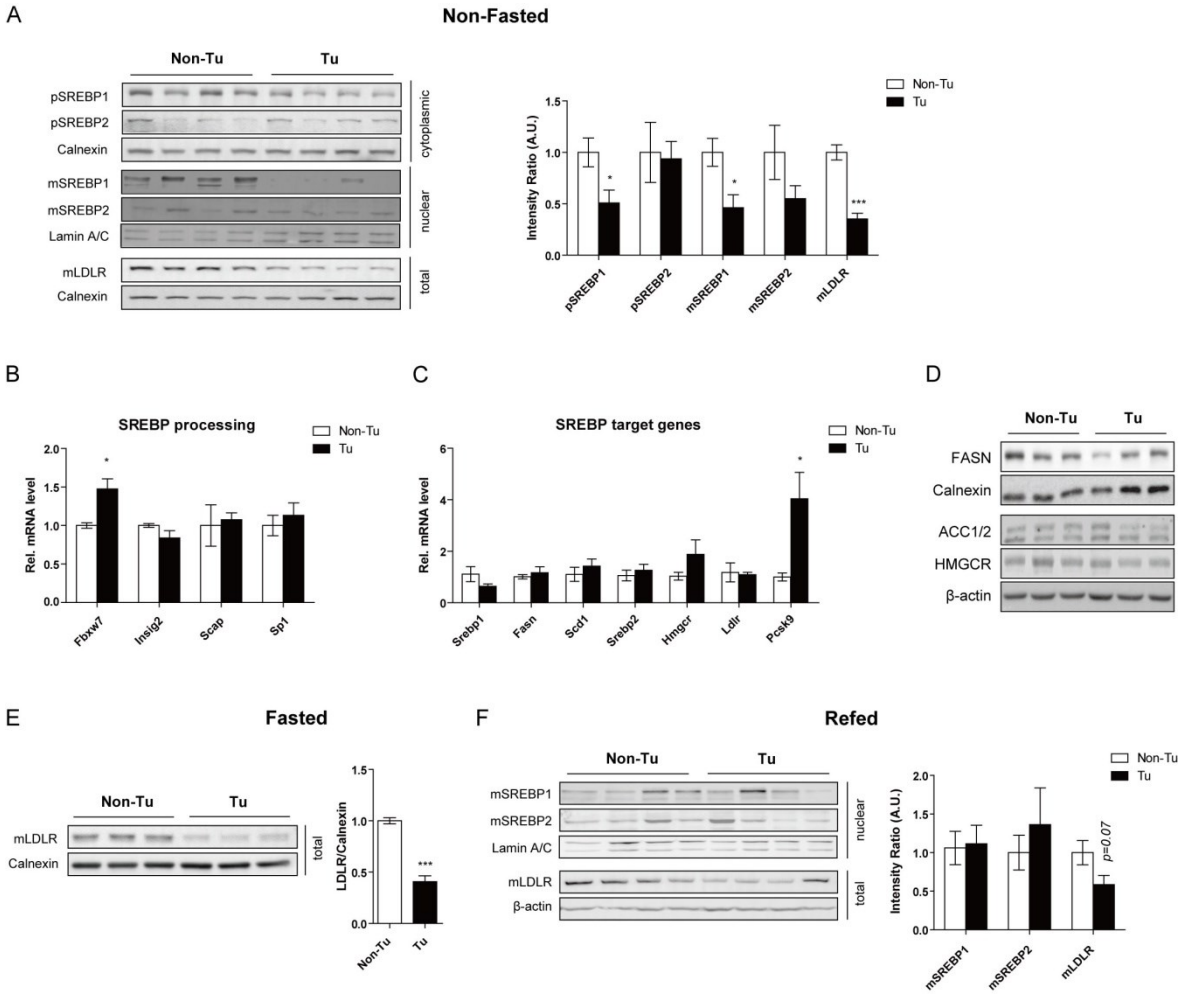

Figure 5. Tumors decrease hepatic LDLR protein expression but not its transcription. *(A) Immunoblot of hepatic SREBP1/2 precursor (pSREBP1/2; 125 kDa), mature SREBP1/2 (mSREBP1, 68 kDa; mSREBP2, 62 kDa) and mature LDLR (mLDLR, 130 kDa) in non-fasted mice. Loading control: Lamin A/C (70 kDa, nuclear fraction); Calnexin (90 kDa, cytosolic fraction and total) (n = 4). (B and C) Hepatic transcriptional levels of (B) genes involved in SREBP processing and (C) Srebp1/2 and their target genes (n = 5), relative to cyclophilin A mRNA expression.(D) Immunoblot of FASN (273 kDa), ACC1/2 (265/280 kDa) and HMGCR (95 kDa), Calnexin and β-actin (45 kDa) in liver tissues (n = 3) were used as loading controls.(E and F) Immunoblot of hepatic mSREBP1/2 and mLDLR in (E) fasted (n = 3) and (F) refed (n = 4) mice. Error bars represent SEM. Unpaired t-test. *, p<0.05; ***, p<0.001.* ***Abbreviation****: SREBP, sterol regulatory element-binding proteins; ACC, acetyl-CoA carboxylase; Hmgcr, 3-hydroxy-3-methylglutary-CoA reductase; Fasn, fatty acid synthase; Pcsk9, proprotein convertase subtilisin/kexin type 9; SCAP: SREBP cleavage-activating protein; S1p, site 1 protease; Insig2, insulin induced gene 2.*

4.1.4. Glucose Homeostasis is Unaffected by Tumor Growth

It is widely accepted that glucose serves as the primary source for tumor growth. The induction of hyperlipidemia conferred by tumors via distinct mechanisms prompted us to investigate whether tumor growth could also induce hyperglycemia and in turn support its growth. Interestingly, blood glucose levels after o/n fasting and in non-fasted condition were both significantly lower in Tu-bearing mice (Fig. 6A). Next, we determined insulin sensitivity in liver and muscle. Basal phosphorylation of AKT in livers of Tu-bearing mice was higher, whereas insulin-stimulated activation of AKT was comparable between both groups (Fig. 6B). Both basal and stimulated phosphorylation of AKT was unchanged in skeletal muscle in the Tu group (Fig. 6B). Consistently, oral glucose tolerant test (OGTT) and insulin tolerant test (ITT) showed no changes between Tu- and Non-Tu-bearing mice (Fig. 6C, D). These data suggest that unlike lipoproteins, global glucose homeostasis remains unaltered in Tu-bearing mice.

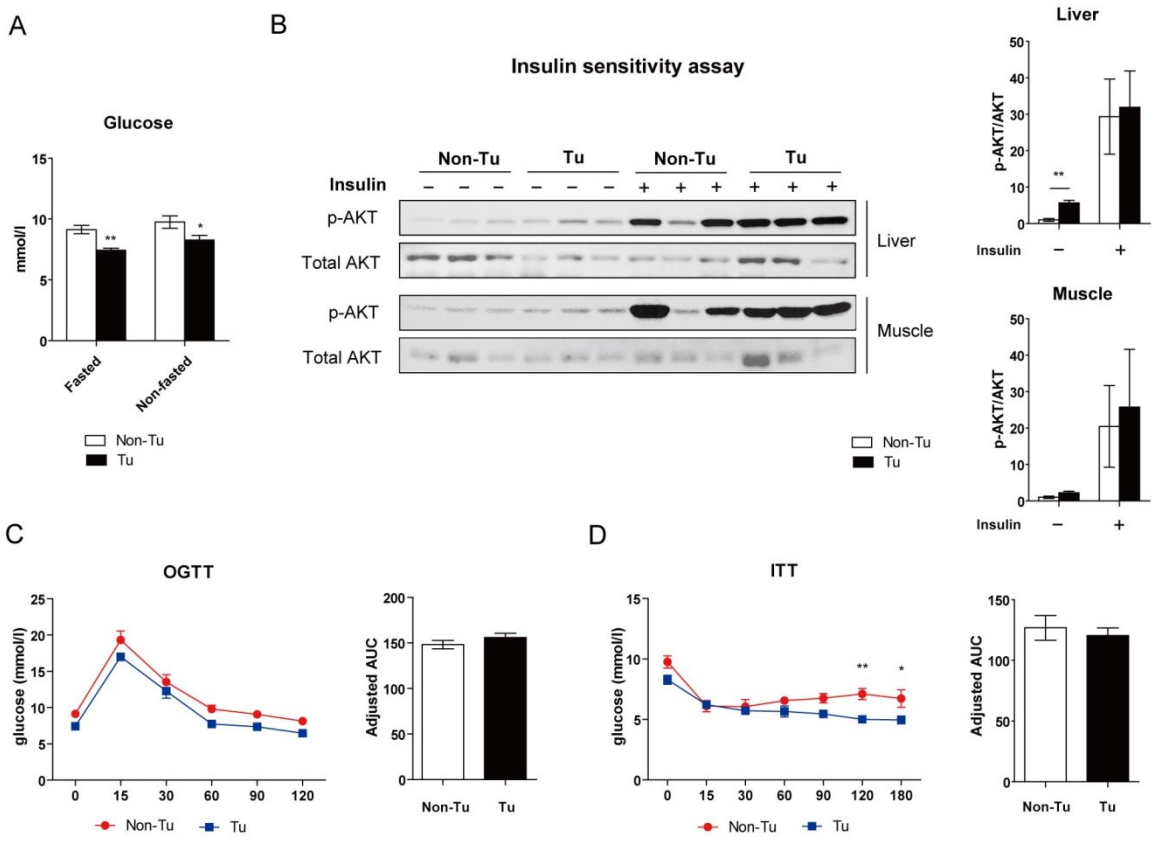

Figure 6. Glucose homeostasis is unaffected by tumor growth. *(A) Blood glucose concentrations from o/n fasted and non-fasted mice (n = 6 - 7). (B) Insulin sensitivity was assessed in livers and muscles of o/n fasted Tu-/Non-Tu-bearing mice on day 13 (n = 3 /group). Total Akt and Ser473 phosphorylated (p-) Akt were probed by immunoblotting and quantified. (C) OGTT was performed in o/n fasted mice on day 12 (n = 7). Statistic differences at different time points were determined by two-way ANOVO. (D) ITT was conducted in mice fasted for five hours during day-time (8 a.m. – 1 p.m.) on day 12 (n = 6). Area under curve (AUC) of each was adjusted by normalizing the curve to its corresponding value at initial time point. Statistic differences at different time points were determined by two-way ANOVO. *, p<0.05; **, p<0.01. Error bars represent SEM. Unpaired t-test except indicated otherwise. *, p<0.05; **, p<0.01.* ***Abbreviation****: OGTT, oral glucose tolerance test; ITT, insulin tolerance test.*

4.1.5. The Influences of Lipoprotein Supply on Tumor Growth

To investigate whether growth of tumor cells is dependent on exogenous lipid supply we used transformed B-cells with rapid growth properties. Incubation of cells in medium containing lipoprotein deficient serum (LPDS) resulted insignificant growth inhibition compared to standard FBS medium. Supplementation of VLDL, LDL or HDL significantly enhanced the growth rate of the tumor cells and prevented cell death caused by lipoprotein depletion in a dose dependent manner (Fig. 7A, B). Importantly, cholesterol addition alone was also able to alleviate cell death (Fig. 7A, B). Increased apoptosis rates confirmed that severe cell death occurred upon lipid withdrawal and that it can be reversed by re-supplying lipoproteins or cholesterol (Fig. 8A, B).

A

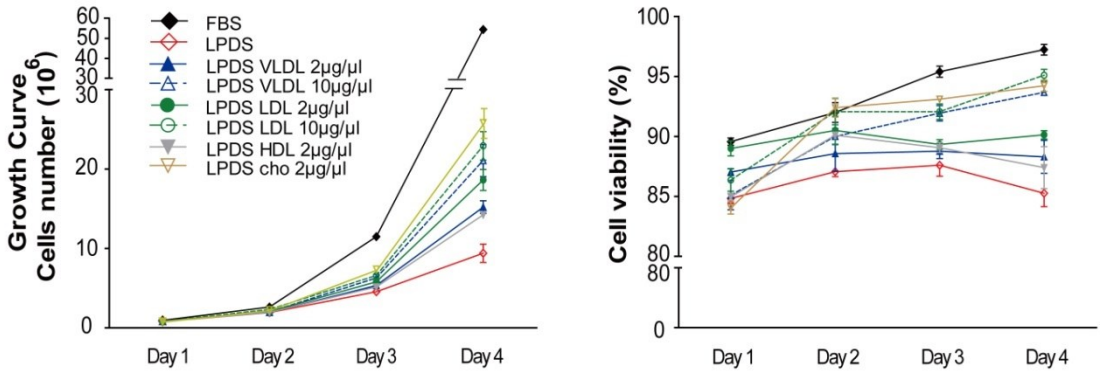

B

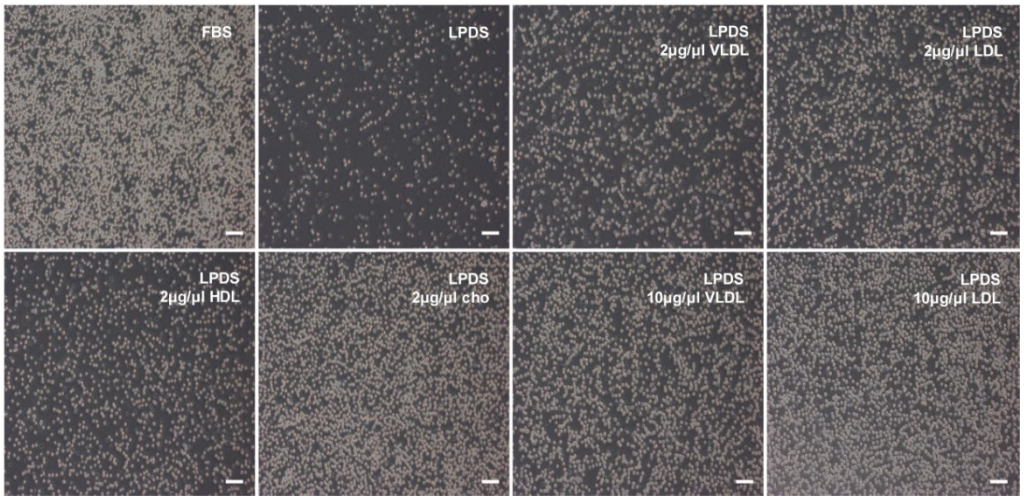

Figure 7. The influences of lipoprotein supply on tumor growth. *(A) Growth curve of TPBCs treated with 10% FBS or LPDS medium supplemented with/without 2 or 10 µg/mL cholesterol in the forms of VLDL, LDL, HDL or cholesterol (chol). Viable cell number and viability was determined by a CASY cell counter (n = 3). Data are presented as mean ± SEM. Differences between groups were analyzed by Two-way ANOVA. (B) Morphological images of transformed B-cells on day 4 (n = 3). Scale bar: 200 µm. Data are representative of two separate experiments with similar results.* ***Abbreviation****: TPBCs, transformed precursor B-cells; FBS, Fetal bovine serum; LPDS, lipoprotein-depleted serum.*

Three independent approaches to prevent tumor cells from utilizing cholesterol were employed: 1) depletion of cell membrane cholesterol by cyclodextrin; 2) inhibition of cholesterol synthesis and intake by blockage of the SREBP pathway; 3) inhibition of lysosomal hydrolysis of endocytosed VLDL remnant/LDL cholesteryl esters by NH_4Cl (Fig. 8C). All the three approaches significantly suppressed transformed B-cell growth. (Fig. 8D - F), suggesting a central role of cholesterol in tumor growth.

To investigate the mechanism by which tumor cells take up lipids from lipoproteins, mRNA expression of genes involved in TG hydrolysis and lipid transport were determined. Interestingly, levels of Ldlr, Lpl and CD36, were abundant in tumors, whereas levels of *VLDL receptor* (*Vldlr*) were28-fold lower than *Ldlr* (Fig. 8G). The tremendous difference in the expression levels of two lipoprotein receptors suggests LDLR might play a major role in catalyzing lipoprotein uptake by tumors (schematic depiction in Fig. 8C). *Ldlr* mRNA expression is under the control of SREBPs. However, little is known about *Ldlr* expression profiles in cancer. Here we analyzed expression correlation based on the mRNA profiles obtained from the Cancer Genome Atlas Project (TCGA) and found that *Ldlr* mRNA levels are highly and significantly correlated to Srebp1 and 2 and their target genes in a wide range of human cancer types (Table 1), implying that *Ldlr* is transcriptionally regulated by

both SREBPs and might share similar expression patterns with other SREBPs target genes in cancers.

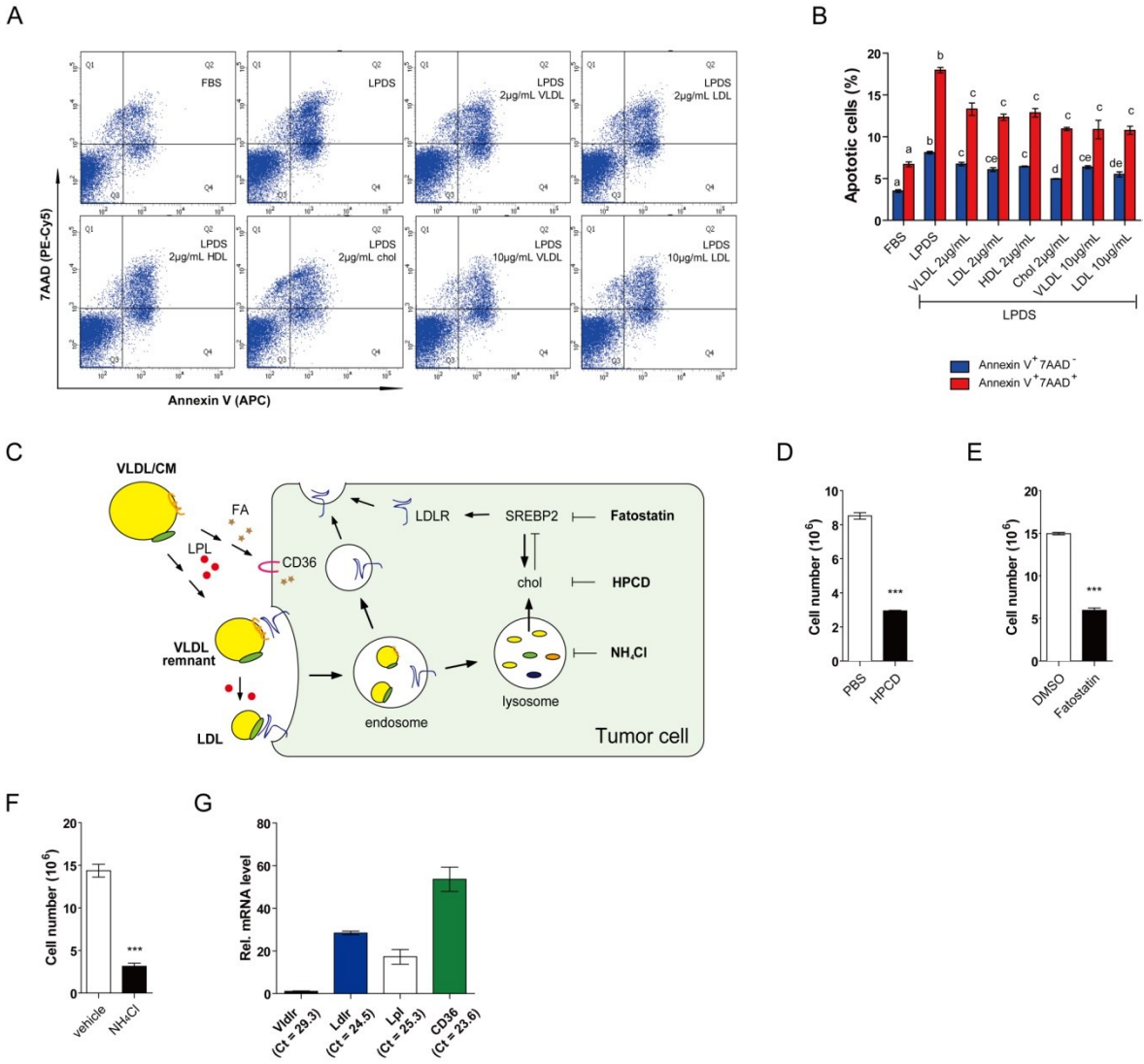

Figure 8. The influences of lipoprotein supply on tumor growth. *(A) Analysis of apoptosis by flow cytometry (day 2, n=3). (B) Quantification is presented as mean ± SEM. Differences between treatments were analyzed by one-way ANOVA. Same letters indicate no significant difference. (C) The scheme depicts cellular targets on which the following reagents (D - F) act. (D) Cholesterol depletion on growth of TPBCs. Cells were incubated with 1% HPCD (dissolved in PBS) or PBS at 37°C for 20 min followed by washing with PBS twice. Cholesterol-depleted cells were further cultured in 10% LPDS medium for 40 hr (n = 3). (E) Fatostatin (5 μM in 5% FBS medium) on growth of TPBCs (36 hr, n = 3). (F) Lysosomal inhibitor NH_4Cl (20 mM in 10% FBS medium) on growth of TPBCs (36 hr, n = 3). (G) mRNA expressions of tumor lipid transporters and hydrolase (n = 3). Ct (circle threshold) values are also indicated. Unpaired t-test, ***, p<0.001.* ***Abbreviation****: HPCD, hydroxypropyl-β-cyclodextrin; LPL, lipoprotein lipase, CD36, fatty acid translocase.*

Table 1.mRNA expression correlation between *Ldlr* and SREBPs target genes in human cancers

Cancer	SREBP1 target gene	SREBP2 target gene
Diffuse Large B-cell Lymphoma (n = 25)	Scd (r = .425), Fasn (r = .396)	
Acute Myeloid Leukemia (n = 173)	Scd (r = .398), Srebp1 (r = .33)	Hmgcr (r = .315), Hmgcs1 (r = .364), Srebp2 (r = .7)
Prostate Adenocarcinoma (n = 216)	Scd (r = .541), Fasn (r = .371), Acly (r = .46), Srebp1 (r = .351)	Hmgcr (r = .621), Hmgcs1 (r = .604), Srebp2 (r = .658)
Glioblastoma (n = 151)	Scd (r = .39), Fasn (r = .495), Acly (r = .436), Acc (r = .391), Srebp1 (r = .41)	Hmgcr (r = .44), Hmgcs1 (r = .488), Srebp2 (r = .558)
Brain Low Degrade Glioma (n = 376)	Scd (r = .332), Fasn (r = .384), Acc (r = .344)	Hmgcr (r = .621), Hmgcs1 (r = .643), Srebp2 (r = .513)
Pheochromocytoma & Paraganglioma (n = 97)	Scd (r = .613), Fasn (r = .438), Srebp1 (r = .468)	Hmgcr (r = .633), Hmgcs1 (r = .718), Srebp2 (r = .533)
Head & Neck Squamous Cell Carcinoma (n = 279)	Scd (r = .383), Fasn (r = .407), Acly (r = .308)	Hmgcr (r = .441), Hmgcs1 (r = .486)
Adrenocortical Carcinoma (n = 54)	Scd (r = .652), Fasn (r = .666), Acly (r = .633), Acc (r = .543)	Hmgcr (r = .87), Hmgcs1 (r = .87), Srebp2 (r = .63)
Kidney Chromophobe (n = 66)	Scd (r = .673), Fasn (r = .465), Srebp1 (r = .396)	Hmgcr (r = .467), Hmgcs1 (r = .354), Srebp2 (r = .676)
Breast Invasive Carcinoma (n = 992)	Scd (r = .539), Fasn (r = .329), Acly (r = .342)	Hmgcr (r = .412), Hmgcs1 (r = .435), Srebp2 (r = .547)
Ovarian Serous Cystadenocarcinoma (n = 265)	Scd (r = .421), Srebp1 (r = .408)	Hmgcs1 (r = .311), Srebp2 (r = .588)
Uterine Corpus Endometrial Carcinoma (n = 124)	Scd (r = .537), Fasn (r = .338), Acc (r = .376)	Hmgcr (r = .302), Hmgcs1 (r = .454), Srebp2 (r = .53)
Thyroid Carcinoma (n = 496)	Scd (r = .631), Srebp1 (r = .465)	Srebp2 (r = .419)

Correlation was studied by Spearman's correlation. The coefficient value r is shown in brackets. Genes were shown only when $p<0.05$and r > 0.3.

Scd: stearoyl-CoA desaturase; Acly: ATP-citrate lyase; Srebp: sterol-regulatory element binding protein; Acc: acetyl-CoA carboxylase; Hmgcr: 3-hydroxy-3-methylglutary-CoA reductase; Hmgcs: 3-hydroxy-3-methylglutary-CoA syntase; Ldlr: low density lipoprotein receptor.

4.2. Fenofibrate Suppresses B-cell Tumor by Modulating Lipid Metabolism

This result section is partially reused from the publication (78) with modifications. The materials are reproduced with the permission of Elservier.

4.2.1. Fenofibrate Suppresses B-cell Tumor Growth Independent of Angiogenesis, Apoptosis and Inflammation

In Section 4.1 we confirmed the high proliferation rate of TPBC tumor cells. Our aim in Section 4.2 was to investigate whether rapid proliferation of tumor B-cell can be reversed by a pharmaceutical approach lowering serum lipids. Fenofibrate is a serum lipid lowering drug that functions as a PPARα ligand and activator(56) and exerts anti-tumorigenic activity in several types of tumors (58). In line with this report fenofibrate administration for 13 days significantly suppressed TPBC tumor growth in WT mice but not in *PPARα*$^{-/-}$ mice (Fig.9A). To determine whether PPARα activation directly inhibits tumor cell proliferation, we investigated the impact of the PPARα agonist Wy14643on B-cell proliferation *in vitro*. Surprisingly, Wy14643 failed to alter growth of transformed B-cells *in vitro* (Fig. 9B).

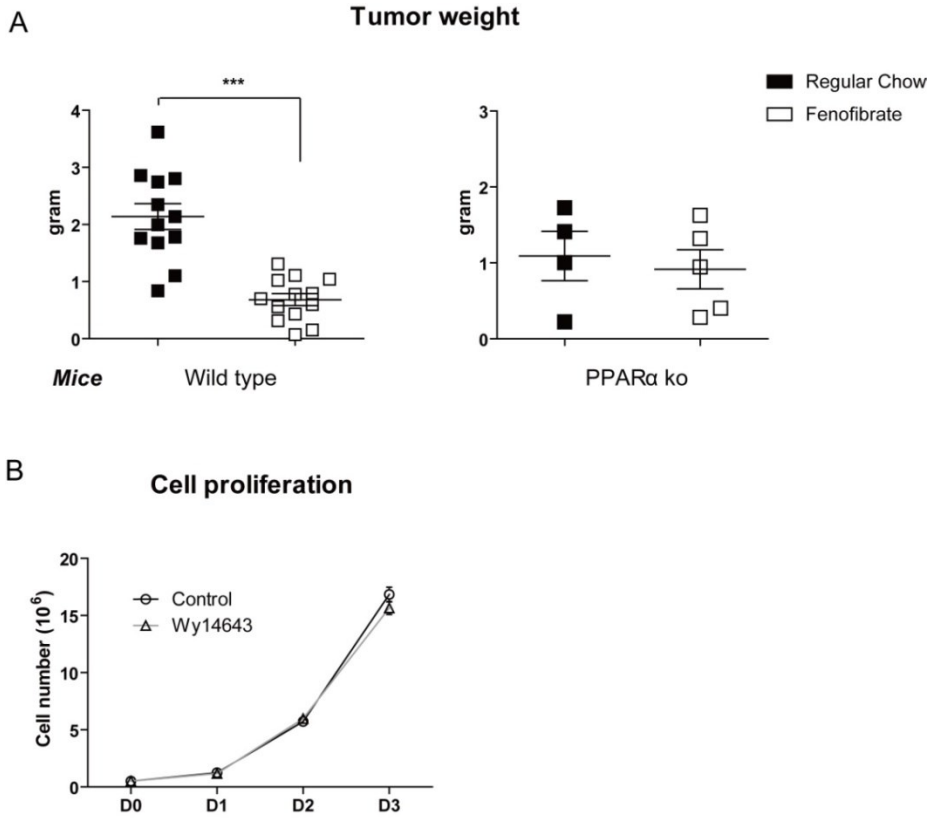

Figure9. Fenofibrate suppresses TPBC tumor growth in vivo. *(a) Tumor weights in wild type (WT) mice (n=13 for each group) and PPARα knock-out (ko) mice (n=4-5 per group) fed with regular chow or chow supplemented with 0.2% (w/w) fenofibrate were determined 13 days post-injection of Bcr/Abl-transformed B-cells (TPBC) subcutaneously. (b) The effect of Wy14643 (50μM) on TPBC proliferation in 10% FBS media was determined by cell counting (n=3). Data are presented as mean ± SEM. Unpaired t-test, ***, p<0.001.* ***Abbreviation****: PPARα, peroxisome proliferator-activated receptor α.*

One study has attributed the tumor-suppressive effects of PPARα agonists to angiogenesis inhibition based on evidence from B16-F10 melanoma models (59). However, we found no significant differences with respect to tumor vessel density in TPBC tumors treated with fenofibrate (Fig. 10A, B). In addition, there was no change in protein expression of vascular endothelial growth factor A (VEGF-A) from tumor lysates upon fenofibrate treatment (Fig. 10C).

Next, we investigated the potential involvement of apoptosis in tumors. While a pro-apoptotic activity of fenofibrate was reported in mantle cell lymphoma *in vitro* (60), a similar effect was not observed in our tumor model. Apoptotic cells (determined by cleaved caspase-3 IHC) were only rarely observed in fenofibrate treated and untreated tumors (Fig. 10D). Albeit we did find a small but not significant increase of apoptotic cells upon fenofibrate treatment (Fig. 10E), we believe that the negligible number of apoptotic cells in both conditions does not explain the observed anti-tumor effect of fenofibrate.

The anti-inflammatory effect of fenofibrate (57, 84) has also been suggested to influence tumor growth. PPARα positive stromal cells might regulate tumor growth in an inflammation reaction dependent manner. It is known that inflammatory mediators (*e.g.* IL-6) are integral to BCR/Abl-driven tumorigenesis (85, 86) and that inflammatory mediators are clinically associated with poor outcome in B-cell lymphoma (87).These hints prompted us to measure TNFα and IL-6 concentrations in the bloodstream and in tumors. While both were undetectable in the control group, they were abundant in Tu mice (Fig. 10F). Notably, fenofibrate treatment did not reduce their levels in Tu mice (Fig. 10G, H), which might result from macrophage infiltration into the tumor microenvironment (Fig. 10F).

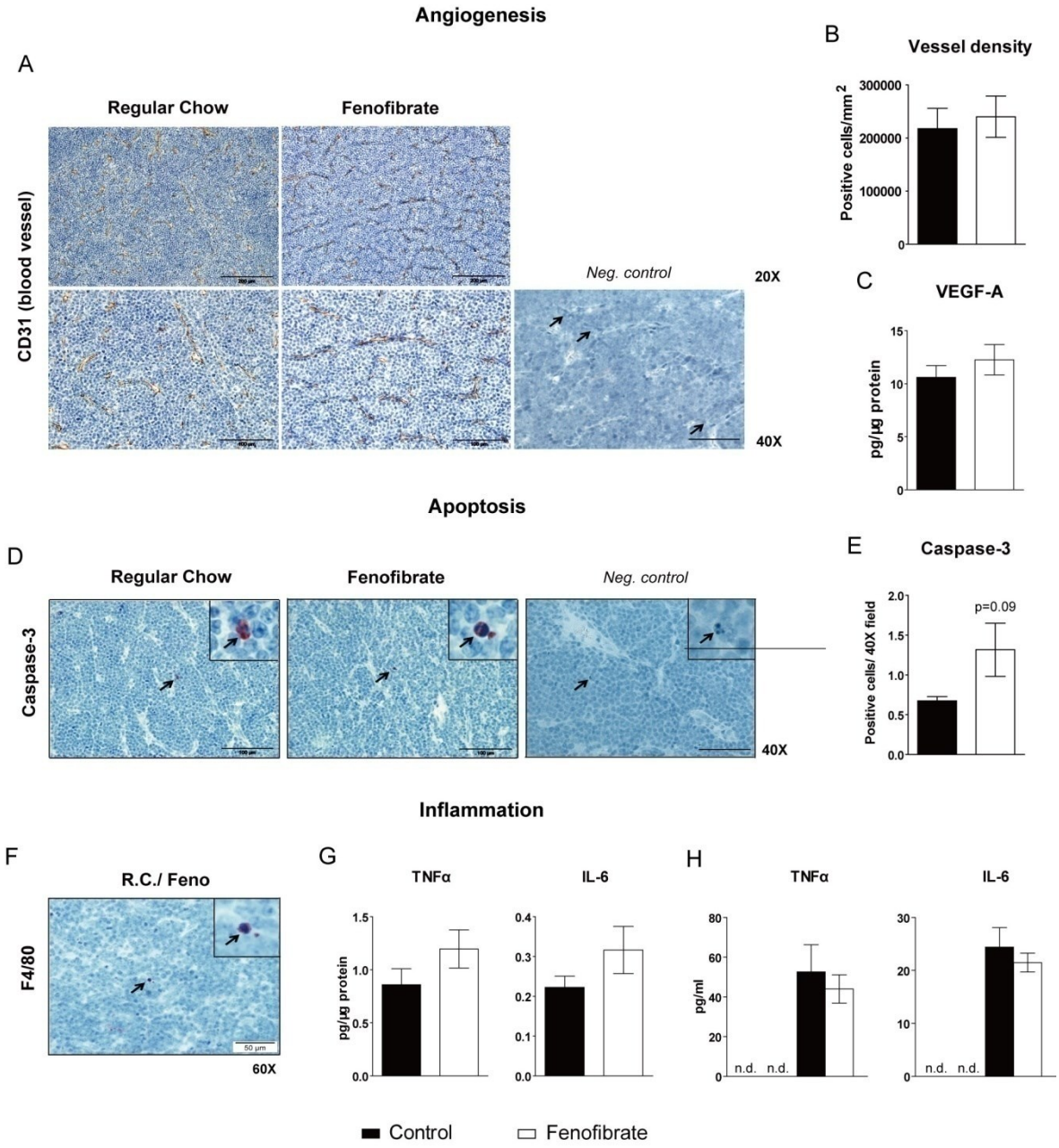
Angiogenesis
A
Regular Chow
Fenofibrate
CD31 (blood vessel)
Neg. control
20X
40X
B
Vessel density
Positive cells/mm2
300000
200000
100000
0
C
VEGF-A
pg/µg protein
15
10
5
0
Apoptosis
D
Regular Chow
Fenofibrate
Neg. control
Caspase-3
40X
E
Caspase-3
Positive cells/ 40X field
p=0.09
2.0
1.5
1.0
0.5
0.0
Inflammation
F
R.C./ Feno
F4/80
50 µm
60X
G
TNFα
IL-6
pg/µg protein
1.5
1.0
0.5
0.0
0.4
0.3
0.2
0.1
0.0
H
TNFα
IL-6
pg/ml
80
60
40
20
0
30
20
10
0
n.d.
n.d.
Control
Fenofibrate

Figure 10. Fenofibrate treatment does not influence tumor angiogenesis and apoptosis. *(A) IHC of CD31on sections of paraffin-embedded tumor specimen from WT mice. (B) Number of CD31 positive cells / mm^{2}tumor area (n=5). (C) VEGF-A protein levels in tumor lysates determined by ELISA. IHC of (D) cleaved (active) caspase-3 and (F) F4/80 on tumor specimen. Negative staining of caspase-3 is also shown. IHC was performed by Silvia Schauer (Medical University of Graz). (E) Number of cleaved caspase-3 positive cells quantifiedat 40x magnification in 60 high power fields (n= 5).TNFα and IL-6 in (G) tumor lysates or (H) serum were determined by ELISA (n = 7). Data are presented as mean ± SEM. Unpaired t-test.* ***Abbreviation****: TNFα, tumor necrosis factor alpha; IL-6, interleukin 6; VEGF-A, vascular epithelial growth factor A; R.C./Feno, Regular chow or chow containing fenofibrate*.

4.2.2. Fenofibrate Increases WAT Loss, Hepatic FA Uptake and Oxidation

In agreement with results in Section (4.1.1.), a significant reduction of WAT weight was detected in visceral and gonadal WAT in Tu mice fed with chow diet, while it was not significantly altered inperirenal WAT (Fig. 11A – C). Fenofibrate treatment induced gonadal WAT loss in Non-Tu mice and further in Tu mice (Fig. 11A – C). The loss of WAT caused by fenofibrate is very likely due to accelerated FA turnover.

As the liver is the main organ for uptake of FFA released from WAT and subsequent esterification into TG for storage or export into the circulation (88), hepatic lipid turnover might be an important factor modulating the cachexia-associated effects conferred by TPBC tumor growth. Strikingly, increased total liver TG content was found in Tu mice fed with regular chow with additional increments of liver TG storage upon fenofibrate treatment (Fig. 11D). Consistently, isotope labeled oleate uptake was enhanced by fenofibrate both in Non-Tu and Tu groups (Fig. 11E). However, only Non-Tu fenofibrate-treated mice showed a significantly increased FFA content (Fig. 11F). This might be due to enhanced FA esterification in Tu mice.

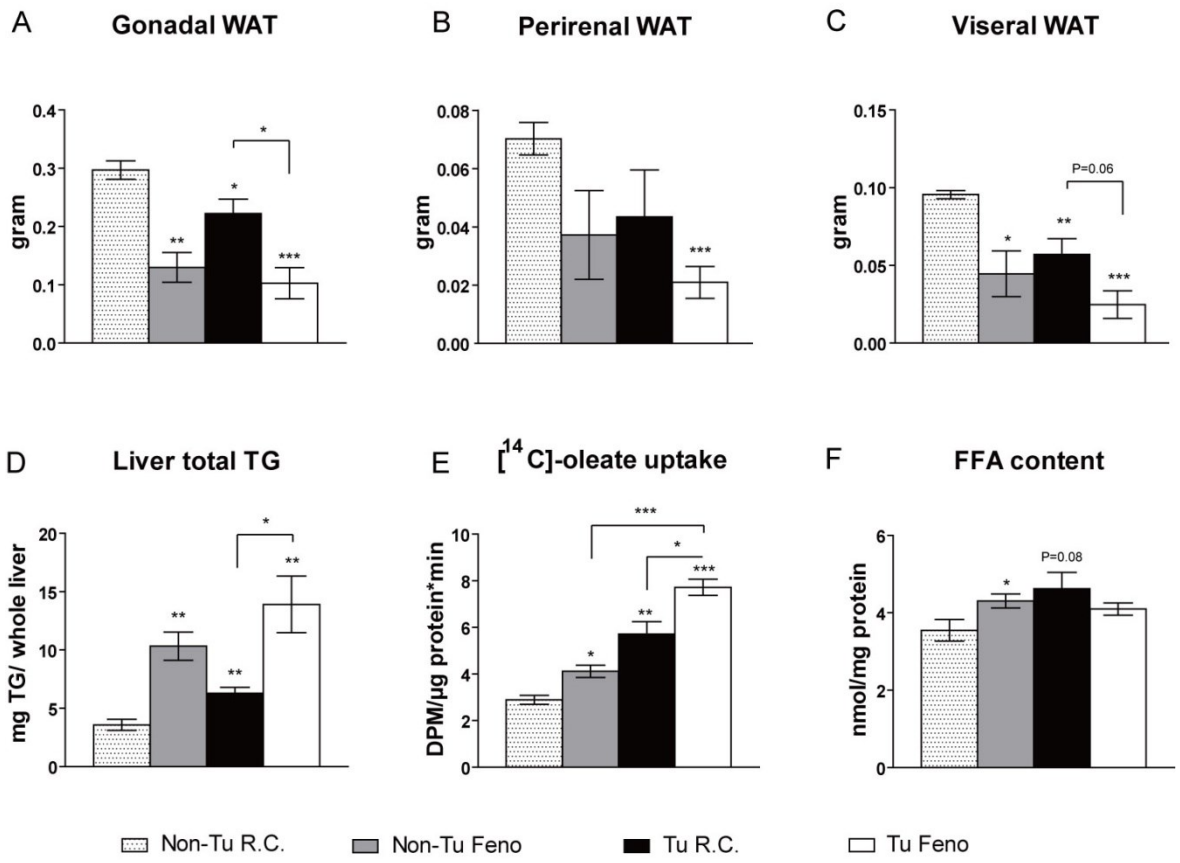

Figure 11. Fenofibrate increases loss of WAT and hepatic FA uptake. *(A) Gonadal, (B) perirenal and (C) visceral WAT weight of mice, fed with regular chow (R.C.) or fenofibrate-supplemented chow (Feno) after 13 days of treatment. (D) Total liver TG content was calculated as (mg TG/mg liver sample × liver weight (mg)). (E) Ex vivo [^{14}C]-oleate uptake and (F) hepatic FFA concentrations were quantified. Data are presented as mean ± SEM (n=4-5). Unpaired t-test, *, p<0.05; **, p<0.01; ***, p<0.001 indicate significant different when compared to Non-Tu R.C. or between two indicated groups.* ***Abbreviation****: WAT, white adipose tissue*

PPARα-mediated hepatic FA oxidation is central to intracellular lipid clearance(89). Interestingly, transcripts of PPARα and its target genes were reduced in Tu mice compared with control mice fed regular chow, which were restored by fenofibrate treatment (Fig. 12A). The inflammatory reaction that was detected in livers of Tu mice, was ameliorated by fenofibrate (Fig. 12B). In line with *in vivo* results, mRNA profiles of PPARα and its targets were also down-regulated in immortalized AML-12hepatocytes treated either with recombinant TNFα or co-cultured with macrophages(Fig. 12C – D). Consistently, transcriptional activity of the PPRE containing promoter was also decreased in AML-12when co-cultured with macrophages (Fig. 12E). All these data suggest a critical role of hepatic inflammation in tumor bearing mice in the impairment of PPARα mediated FAβ-oxidation. This effect might also provide excess FA for hepatic VLDL secretion.

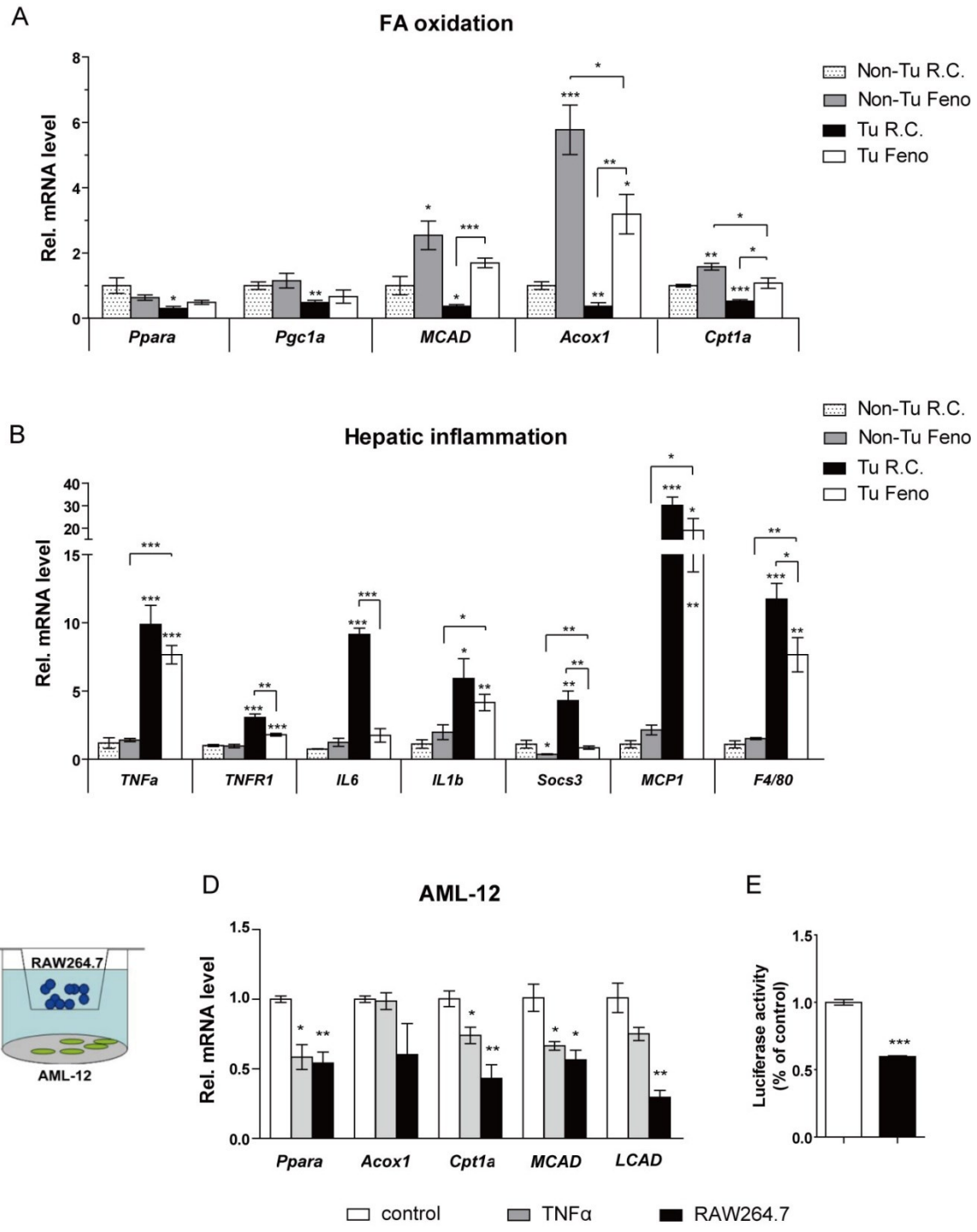
A
FA oxidation
Rel. mRNA level
Non-Tu R.C.
Non-Tu Feno
Tu R.C.
Tu Feno
Ppara
Pgc1a
MCAD
Acox1
Cpt1a
B
Hepatic inflammation
Rel. mRNA level
TNFa
TNFR1
IL6
IL1b
Socs3
MCP1
F4/80
C
RAW264.7
AML-12
D
AML-12
Rel. mRNA level
Ppara
Acox1
Cpt1a
MCAD
LCAD
control
TNFα
RAW264.7
E
Luciferase activity (% of control)

Figure 12. Fenofibrate increases hepatic FA oxidation. *Expression profiles of (A) PPARα target genes involved in FA oxidation and (B) inflammatory markers in the liver (n=4–5). (C) Scheme of Transwell system where AML-12 immortalized hepatocytes and RAW264.7 macrophage cells were co-cultured. (D) mRNA levels of PPARα and its targets in AML-12 were determined. AML-12 cells were either stimulated with 30 ng/ml mouse recombinant TNFα or co-cultured with RAW264.7 in the transwell system for 48 hours (n = 3). (F) Using a luciferase reporter system, PPRE promoter activity was assessed in AML-12 cells co-cultured with RAW264.7 cells in the transwell system for 36 hours (n = 3). Data are presented as mean ± SEM (n=4–5). Unpaired t-test, *, p<0.05; **, p<0.01; ***, p<0.001 indicate significant different when compared to Non-Tu R.C. (A and B), to control (C) or between two indicated groups.* ***Abbreviation****: Ppara, proxisome proliferator-activated receptoralpha; Pgc1a, proxisome proliferator-activated receptor gamma coactivator 1 alpha; MCAD, medium-chain acyl-CoA dehydrogenase; LCAD, long-chain acyl-CoA dehydrogenase; Cpt1a, carnitine palmitoyltransferase 1; Acox1, Acyl-CoA oxidase 1; TNFa, tumor necrosis factor alpha; TNFR1, tumor necrosis factor receptor 1; MCP1, monocyte chemoattractant protein 1;IL-6, interleukin 6; IL1b, interleukin 1 beta; Socs3, suppressor of cytokine signaling 3.*

4.2.3. Fenofibrate Suppress Tumor-induced Hyperlipidemia

Serum levels of triglyceride (TG), total cholesterol (TC), free cholesterol (FC) and phospholipids (PL) were increased in Tu mice compared with Non-Tu control mice. Interestingly, fenofibrate treatment completely normalized these increments to the levels of Non-Tu fenofibrate-treated mice (Fig. 13A - D).

Increased cholesterol in Tu mice corresponds to VLDL/LDL-C (Fig. 13E). Consistently, plasma levels of ApoB were increased 3-fold in Tu mice (Fig. 13F). As expected, fenofibrate significantly reduced plasma VLDL/LDL-C and ApoB to levels similar as in Non-Tu fenofibrate-treated mice (Fig.13E, F). Further FLPC analysis confirmed the drastic increase in VLDL and LDL in Tu mice fed with regular chow compared to control mice (Fig. 13G). Fenofibrate dramatically reduced VLDL levels in Non-Tu mice, and VLDL and LDL in Tu mice (Fig. 13G). The protein components of VLDL, ApoCII and CIII, are key regulators of LPL activity in capillaries. Upon fenofibrate, hepatic ApoCII increased but ApoCIII deceased in Tu mice (Fig. 13H, I). The resulting increased ApoCII/III ratio upon fenofibrate might accelerate hydrolysis of lipoprotein-TG in peripheral organs, which might explain the observed reduction of lipid levels in circulation.

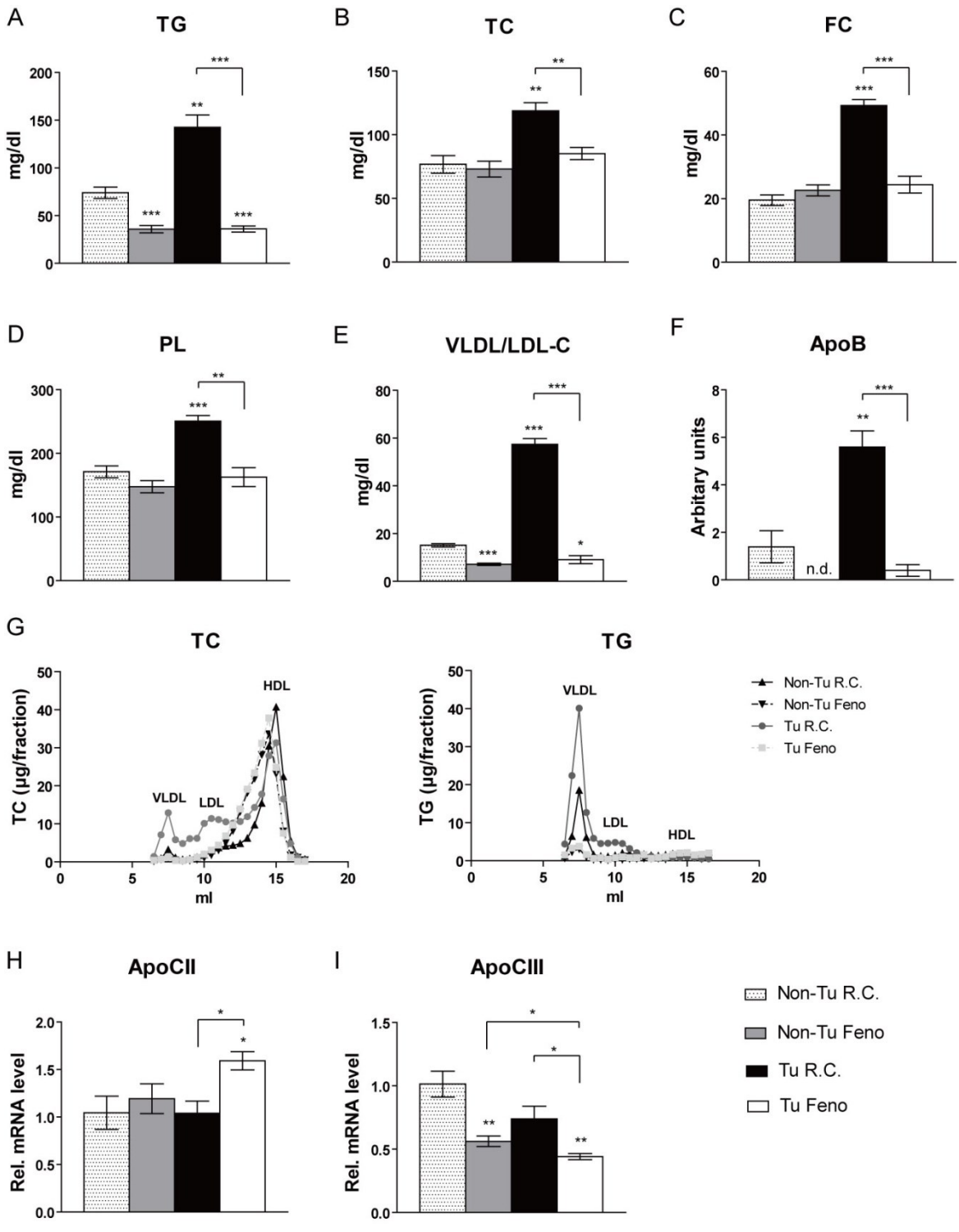
A
TG
mg/dl
B
TC
mg/dl
C
FC
mg/dl
D
PL
mg/dl
E
VLDL/LDL-C
mg/dl
F
ApoB
Arbitary units
n.d.
G
TC
TC (µg/fraction)
VLDL
LDL
HDL
ml
TG
TG (µg/fraction)
VLDL
LDL
HDL
ml
Non-Tu R.C.
Non-Tu Feno
Tu R.C.
Tu Feno
H
ApoCII
Rel. mRNA level
I
ApoCIII
Rel. mRNA level
Non-Tu R.C.
Non-Tu Feno
Tu R.C.
Tu Feno

Figure 13. Fenofibrate suppress tumor-induced hyperlipidemia. *Serum (A - D) TG, TC, FC, PL and (E) VLDL/LDL-cholesterol levels. (F) Serum ApoB was determined by immunoturbidimetric assays. (G) Lipoprotein analyses by FPLC (plasma pooled from 4-5mice). FPLC was done by Anton Ibovnik (Medical University of Graz). (H, I) mRNA levels of ApoCII and CIII. Mean ± SEM (n=4-5). Unpaired t-test, *, p<0.05; **, p<0.01; ***, p<0.001 indicate significant different when compared to Non-Tu R.C. or between two indicated groups.* ***Abbreviation****: TC, total cholesterol; FC, free cholesterol; PL, phospholipid; TG, triglyceride; ApoB, apolipoprotein B; ApoC II/III, Apolipoprotein C 2/3; VLDL/LDL-C, very low/low-density lipoprotein cholesterol.*

4.2.4. Unaltered Tumor Lipid Metabolism in Fenofibrate-treated Mice

As described above, tumor-induced WAT loss resulted in increased hepatic FA uptake and subsequently increased liver mass in fenofibrate-fed mice. In contrast the FA uptake by the tumor remained unaltered upon fenofibrate treatment (Fig.14A). In line, intracellular FFA and TG contents were also unchanged (Fig. 14B, C). Similarly, the expression of genes involved in lipid uptake (*VLDLR*, *LDLR*, *CD36*) and FA synthesis (*ACC1*, *FASN*, *SREBP1*) remained similar both *in vivo* and *in vitro* (Fig. 14D, E). Undetectable mRNA of PPARαconfirmed by comparison of CT value between WT and *PPARα*$^{-/-}$ TPBC (Fig. 14F) likely accounts for the lack of response of tumor to fenofibrate *in vivo* or to Wy14643 *in vitro*. This assumption is further supported by the fact that the PPARα targets (*CD36*, *MCAD*, and *ACOX1*) generally showed no significant responses to PPARα agonist *in vivo* and *in vitro* (Fig. 14D, E). These data together with the unaltered tumor growth in fenofibrate-treated *PPARα*$^{-/-}$ mice (Fig. 9A) strongly suggest that fenofibrate suppresses B-cells tumor growth independent of PPARα activation in the tumor but dependent of PPARα function in global lipid lowering.

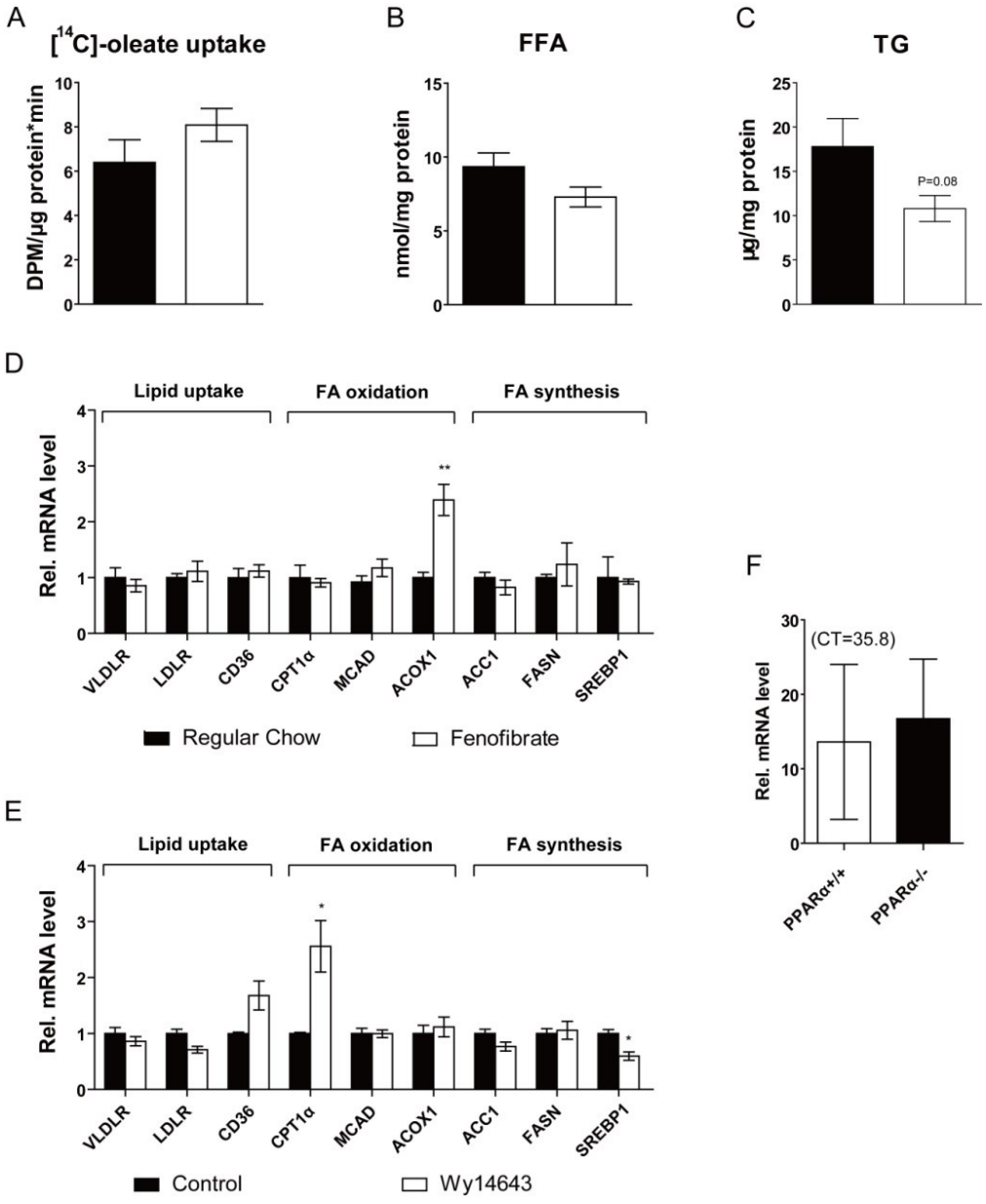

Figure 14. Impact of fenofibrate on tumor lipid metabolism. *(A) Oleate uptake, (B) intracellular FFA, and (C) TG concentrations in tumors after fenofibrate treatment. The impact of (D) fenofibrate in vivo and (E) Wy14643 in vitro on the expression of genes involved in lipid metabolism. (F) PPARα mRNA expression in TPBCs generated from wild-type mice (PPARα$^{+/+}$) or PPARα knockout mice (PPARα$^{-/-}$). CT value is shown. Unpaired t-test; *, p<0.05; **, p<0.01.* ***Abbreviation****: CT, cycle threshold; VLDLR, VLDL receptor; LDLR, LDL receptor.*

4.3. Tumor Growth in Hypolipidemic Mouse Models

The results in this section are in collaboration with Prof. Dr. Richard Lehner (University of Alberta, Edmonton, Canada) and are currently unpublished. Relevant results are reported with permission of Richard Lehner & Gerald Hoefler.

4.3.1. TGH but not PEMT Deficient Mice Partially Reverse Tumor-induced Hyperlipidemia and Suppress Tumor Growth

Two genetic hypolipidemic mouse models – Ces3/TGH knockout mice (*Ces3/Tgh*$^{-/-}$) and PEMT knockout mice (*Pemt*$^{-/-}$) were used to determine whether attenuation of VLDL secretion could reverse tumor-induced hyperlipidemia and subsequently could suppress tumor growth. Plasma TG was decreased in *Ces3/Tgh*$^{-/-}$ mice and in *Pemt*$^{-/-}$ mice (Fig. 15C, Non-Tu) concomitantly with substantially reduced plasma ApoB100, a marker of VLDL and LDL, compared to wild-type mice upon chow diet (Fig. 15G, Non-Tu). Tumor growth in all genotypes was studied. Tumor volume and weight were reduced in *Ces3/Tgh*$^{-/-}$ mice (Fig.15A, B). However, a similar reduction was not observed in *Pemt*$^{-/-}$ mice.

The opposite phenotypes in tumor growth in *Ces3/Tgh*$^{-/-}$ mice and *Pemt*$^{-/-}$ mice correlated with distinct efficacies in alleviation of tumor-induced hyperlipidemia in these two mouse models. Among all tumor groups (Tu), plasma TG levels were reduced in *Ces3/Tgh*$^{-/-}$ mice whereas no change in plasma TG concentrations was observed in *Pemt*$^{-/-}$ mice when compared to *WT* mice (Fig. 15C). In agreement VLDL was reduced in *Ces3/Tgh*$^{-/-}$ but not *Pemt*$^{-/-}$ mice (Fig. 15F, upper panel). Plasma TC was lowered in *Ces3/Tgh*$^{-/-}$ mice and in *Pemt*$^{-/-}$ mice (Fig. 15D). However, the reduced TC in *Ces3/Tgh*$^{-/-}$ mice was in VLDL and LDL fractions while that in *Pemt*$^{-/-}$ mice reduction of cholesterol was observed in HDL and LDL fractions (Fig. 15F, lower panel). Plasma NEFA was reduced in *Ces3/Tgh*$^{-/-}$ mice but

increased in *Pemt*$^{-/-}$ mice (Fig. 15E). In concert with the change in plasma lipid profiles, the abundance of ApoB100 was profoundly lower in Tu-*Ces3/Tgh*$^{-/-}$ mice compared to Tu-*WT* mice, while no change was observed in *Pemt*$^{-/-}$ mice (Fig. 15G). The alleviation of tumor-induced hyperlipidemia consequently led to significant reduction of tumor TG, FC, CE and a decrease tendency in NEFA in *Ces3/Tgh*$^{-/-}$ mice (Fig. 15H - J). In tumors, expression of fatty acid synthase (FASN) and 3-hydroxy-3-methylglutary-CoA reductase (HMGCR), key lipogenic enzymes in FA synthesis and cholesterol synthesis, respectively, were not changed upon hypolipidemic stress. However, reduction of intracellular cholesterol triggered activation of LDLR expression, which might partially compensate the loss of TG and cholesterol in tumor in *Ces3/Tgh*$^{-/-}$ mice (Fig. 15K).

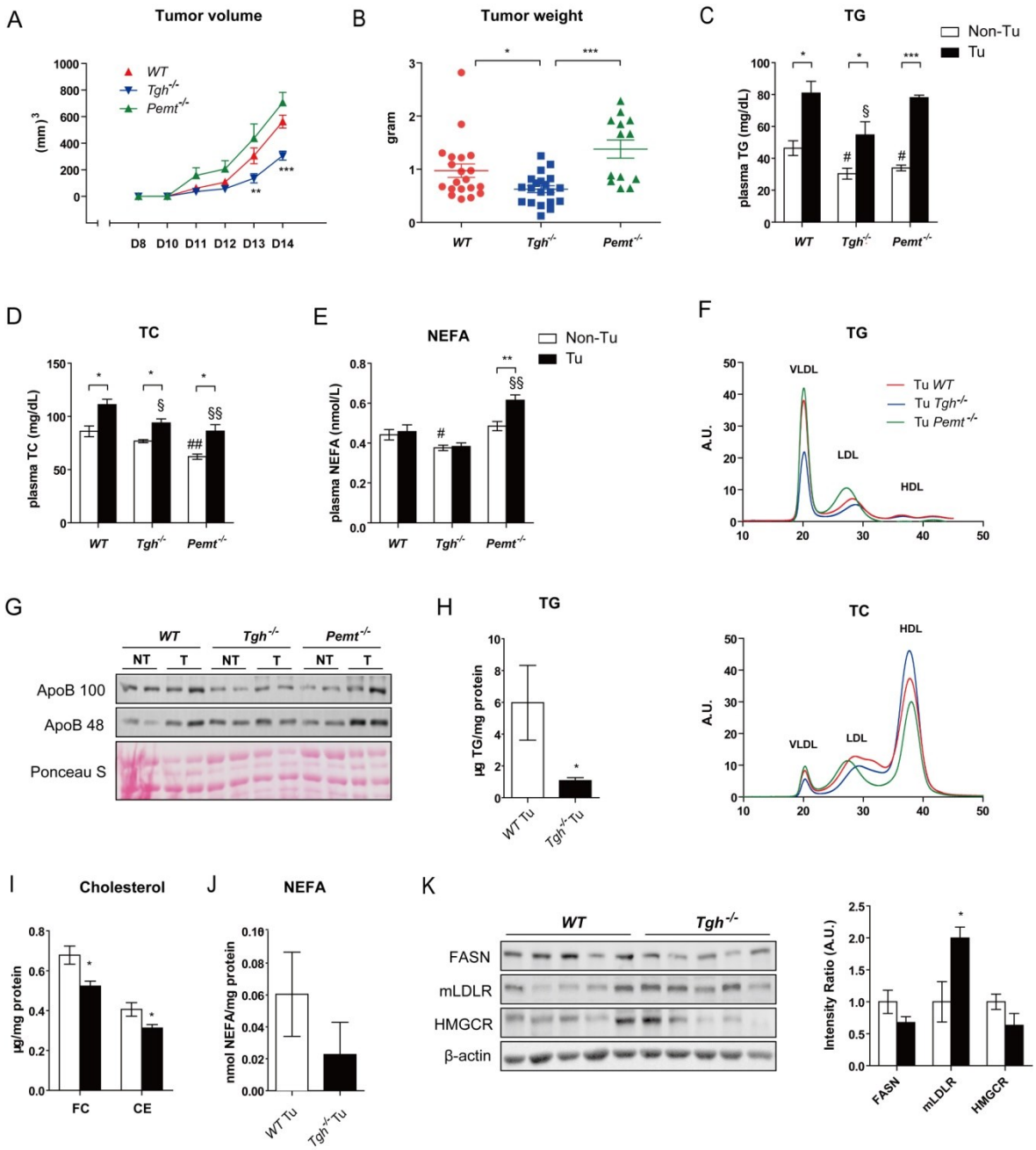
A
Tumor volume
WT
Tgh-/-
Pemt-/-
(mm)3
D8 D10 D11 D12 D13 D14
B
Tumor weight
gram
C
TG
Non-Tu
Tu
plasma TG (mg/dL)
D
TC
plasma TC (mg/dL)
E
NEFA
plasma NEFA (nmol/L)
F
TG
VLDL
LDL
HDL
A.U.
Tu WT
Tu Tgh-/-
Tu Pemt-/-
G
NT
T
ApoB 100
ApoB 48
Ponceau S
H
TG
µg TG/mg protein
WT Tu
Tgh-/- Tu
TC
I
Cholesterol
µg/mg protein
FC
CE
J
NEFA
nmol NEFA/mg protein
K
FASN
mLDLR
HMGCR
β-actin
Intensity Ratio (A.U.)

Figure 15. TGH but not PEMT deficient mice partially reverse tumor-induced hyperlipidemia and suppress tumor growth. *Wild-type (WT), Ces3/Tgh$^{-/-}$ and Pemt$^{-/-}$ mice were subcutaneously inoculated with 200,000 TPBCs, respectively. (A) Tumor volume was estimated by caliper through the entire experiment according to the formula (1/2 × length × width × height) (n = 8 - 12). Differences between each two groups were analyzed by two-way ANOVA. (*) indicate significant difference between WT mice and Ces3/Tgh$^{-/-}$ mice. (B) Tumor weight was determined after harvest on day 14. (C) Plasma TG, (D) TC and (E) NEFA levels from daytime fasted mice (08:00 – 12:00) were determined (n = 8 - 12). *, p<0.05; ***, p<0.01; ***, p<0.001 indicate a significant difference between Tu- and Non-Tu-bearing mice of respective genotypes. #, p<0.05; ##, p<0.01 indicate comparison of mice to Non-Tu WT mice. §, p<0.05; §§, p<0.01 indicate comparison to Tu WT mice. (F) Plasma (pooled from 5 mice) lipoproteins from Tu-bearing WT, Ces3/Tgh$^{-/-}$ and Pemt$^{-/-}$ mice were fractionated by FPLC. (G) Immunoblot of plasma ApoB100 (509 KDa) and B48 (250 KDa). Ponceau S staining served as loading control. Lipids were extracted from tumors excised from WT and Ces3/Tgh$^{-/-}$ mice (n = 6). (H) TG, (I) FC and CE and (J) NEFA were respectively quantified by colorimetric assay kits. (K) Immunoblot of FASN (273 KDa), mature LDLR (mLDLR, 130 KDa) and HMGCR (95 KDa) in tumor lysates from WT and Ces3/Tgh$^{-/-}$ mice (n = 6). Error bars represent SEM. Unpaired t-test except mentioned otherwise, *, p<0.05; ***, p<0.001.* ***Abbreviation****: Non-Tu, non-tumor bearing mice; Tu, tumor-bearing mice; NEFA, non-esterified fatty acid.*

4.3.2. Ces3/TGH Deficiency could neither reverse Tumor-stimulated Secretion nor decreased VLDL Turnover

Consistent with enhanced TG secretion in primary hepatocytes from Tu-bearing mice (Fig. 4F, G), VLDL secretion (determined at day 14 after injection of P-407 to inhibit peripheral lipolysis) was significantly increased in Tu- compared to Non-Tu-bearing *WT* mice (Fig. 16A). Interestingly, Ces3/TGH deficiency could attenuate VLDL production only in Non-Tu- but not in Tu-bearing mice (at least in the late stage of experimental period when tumor weight reached approximate 1 gram) (Fig. 16A). Similar to *WT*, protein levels of Mttp were also unchanged in *Ces3/Tgh*$^{-/-}$ and *Pemt*$^{-/-}$ mice (Fig. 16B). TG hydrolase (LPL plus hepatic lipase) activities were examined in post-heparin plasma (PHP) to assess the impact of tumors on peripheral VLDL clearance. In agreement with FTT result (Fig. 4J), PHP TG hydrolase activities were significantly reduced in Tu-bearing *WT* mice (Fig. 16C). A similar reduction conferred by tumor was also observed in *Ces3/Tgh*$^{-/-}$ mice (Fig. 16C), whereas hydrolase activities in *Pemt*$^{-/-}$ mice were lower than *WT* mice in both Tu- and Non-Tu-bearing situations (Fig. 16D).

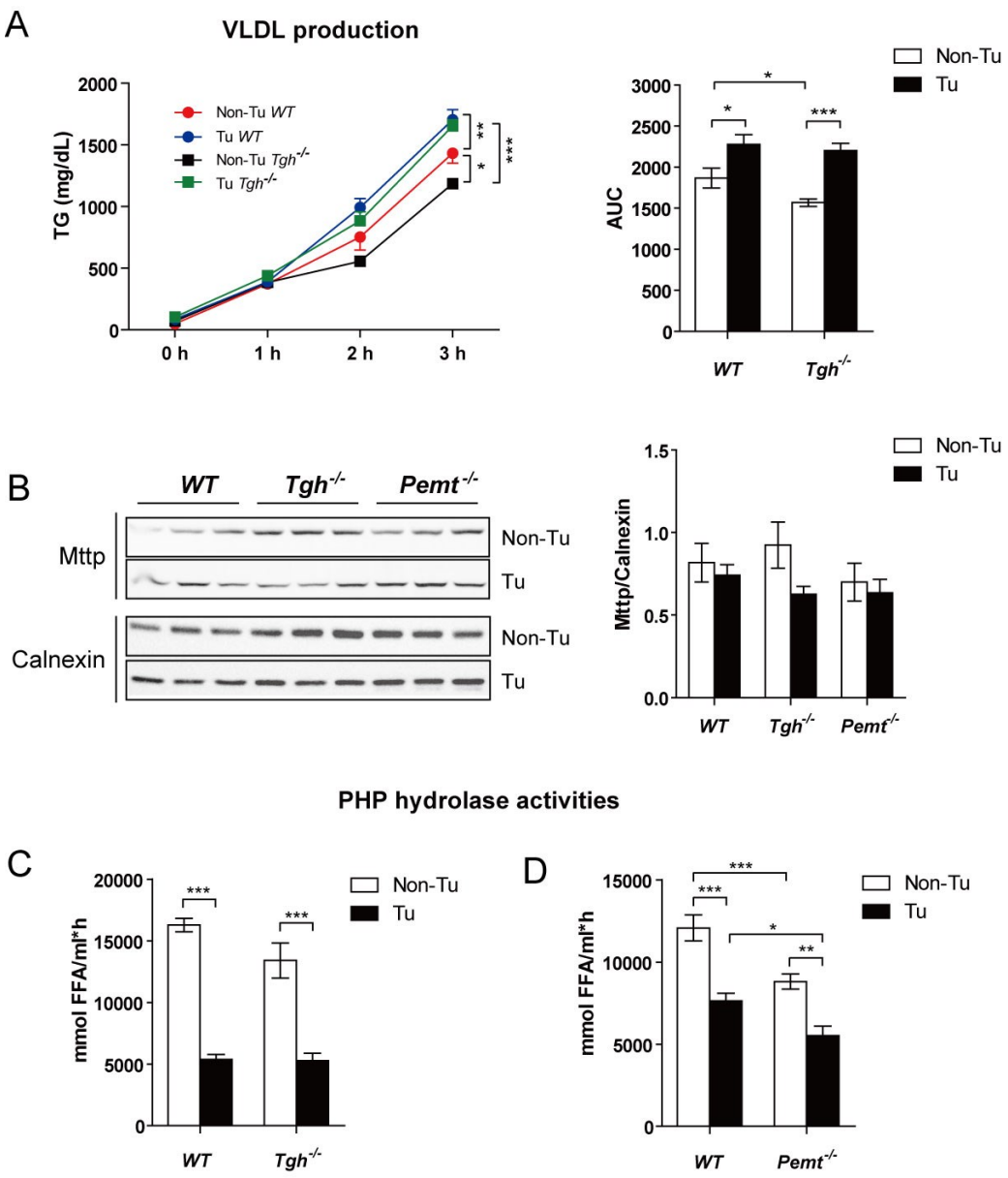

Figure 16. No change in VLDL secretion and turnover in Tu-bearing Ces3/Tgh$^{-/-}$ mice. *(A) VLDL production in Non-Tu/Tu WT and Ces3/Tgh$^{-/-}$ mice (day 13, n=5-6). TG was determined before P-407 injection as 0 and 1, 2 and 3 hr after injection. Statistic differences at different time points were determined by two-way ANOVA. (B) Immunoblot of Mttp in liver lysates (n=5/group). Calnexin serves as loading control. (C and D) TG hydrolase activities in PHP from Tu/Non-Tu-bearing WT, (C) Ces3/Tgh$^{-/-}$ and (D) Pemt$^{-/-}$ mice (day 14, n=7). Error bars represent SEM. Unpaired t-test except stated elsewhere. *, p<0.05.* ***Abbreviation****: Mttp, microsomal triglyceride transfer protein; PHP, post-heparin plasma.*

4.3.3. *Ces3/Tgh*$^{-/-}$ Mice partially restore Hepatic LDLR via Attenuation of PCSK9 Activation

We have shown that the protein levels of LDLR in liver were reduced in Tu-bearing *WT* mice. Notably, the amount of hepatic LDLR was preserved in *Ces3/Tgh*$^{-/-}$ but not *Pemt*$^{-/-}$ mice (Fig. 17A). Strikingly, increased plasma concentrations of PCSK9, which induces degradation of hepatic LDLR protein, were observed in all tumor groups regardless of the genotype (Fig. 17B). However, plasma PCSK9 levels in *Ces3/Tgh*$^{-/-}$ mice were significantly lower compared to *WT* and *Pemt*$^{-/-}$ mice in both Tu- and Non-Tu-bearing groups (Fig. 17B). Concomitantly, we observed a positive correlation between tumor weight and plasma PCSK9 levels in *WT* but not in *Ces3/Tgh*$^{-/-}$ mice (Fig.17C). In line with plasma concentrations, *Pcsk9* mRNA expression was increased in Tu-bearing *WT* and *Pemt*$^{-/-}$ mice but unaltered in *Ces3/Tgh*$^{-/-}$ mice (Fig. 17D). mRNA expression of *hepatic nuclear factor 1α* (*Hnf1a*), responsible for mammalian target of rapamycin complex 1 (mTORC1)-mediated transcriptional activation of the *Pcsk9* promoter (90), was concomitantly increased in Tu-bearing *WT* but not *Ces3/Tgh*$^{-/-}$ mice (Fig. 17E). The activity of mTORC1 can be suppressed by cellular stress such as energy deprivation and inflammation (91). Correspondingly, phosphorylation of the energy sensor 5' AMP-activated protein kinase α (AMPKα) in liver was increased in Tu-bearing *WT* mice, whereas AMPK phosphorylation was unaltered in livers from *Ces3/Tgh*$^{-/-}$ mice (Fig. 17F). These data suggest an involvement of the AMPK-mTORC1-HNF1α-PCSK9 pathway in the regulation of LDLR expression.

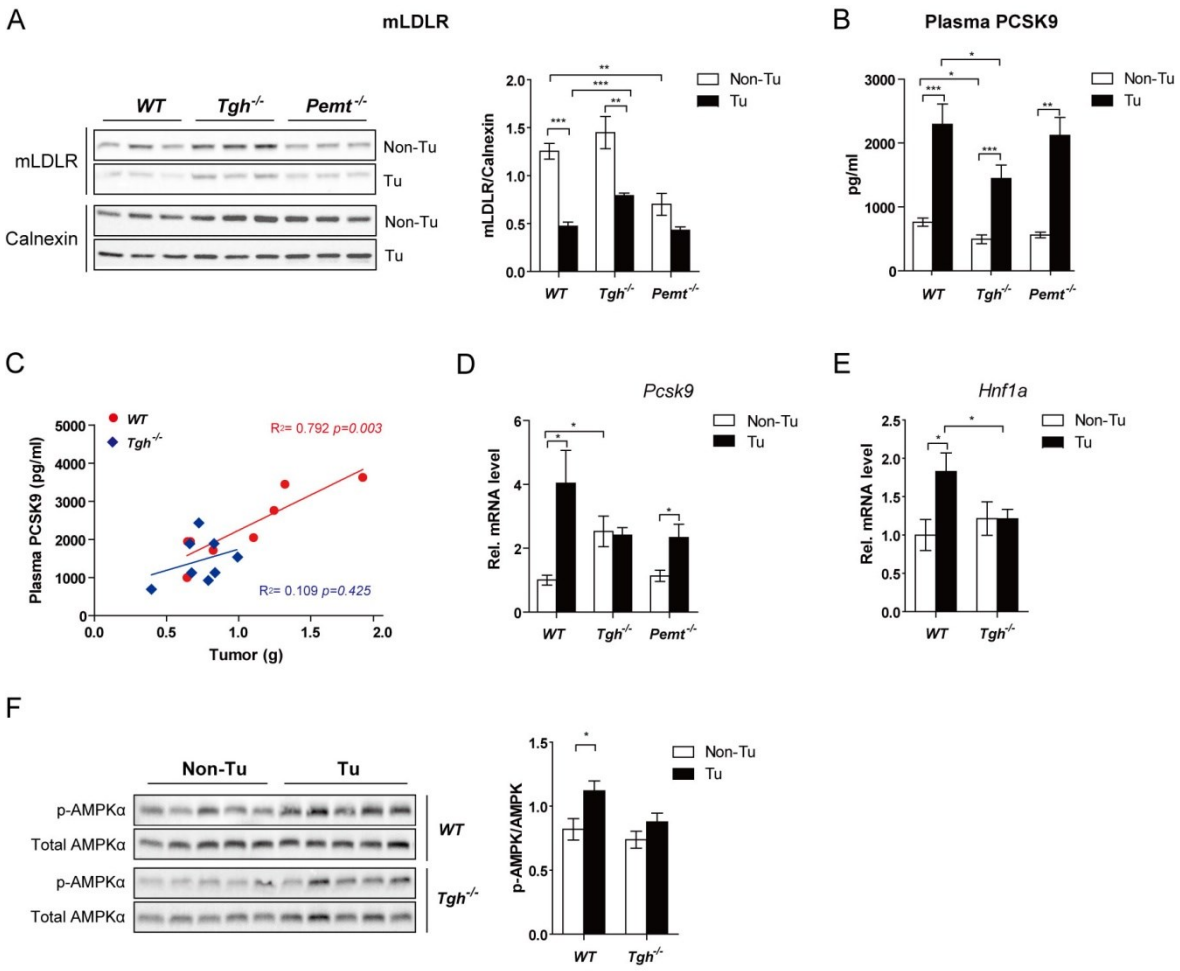

Figure 17. Ces3/Tgh$^{-/-}$ mice restore hepatic LDLR via PCSK9 inhibition. *(A) LDLR protein levels in liver from non-fasted Non-Tu/Tu bearing WT, Ces3/Tgh$^{-/-}$ and Pemt$^{-/-}$ mice determined by Immunoblot (day 14, n = 5). Calnexin (as in Fig. 16B) was used as internal reference. (B) PCSK9 plasma levels in non-fasted Non-Tu/Tu bearing WT, Ces3/Tgh$^{-/-}$ and Pemt$^{-/-}$ mice (n = 8). (C) Correlation between plasma PCSK9 concentration and tumor size in WT and Ces3/Tgh$^{-/-}$ mice (n = 8) using Pearson Correlation Coefficient test. Hepatic (D) Pcsk9 and (E) Hnf1a mRNA (n = 5 - 7). Pcsk9 levels in WT mice are same as in Fig. 3C.(F) Immunoblot of Thr172 phosphorylated (p-)/ total AMPKα (62 kDa; n = 5 - 7) from livers of WT and Ces3/Tgh$^{-/-}$ mice. Error bars represent SEM. Unpaired t-test unless indicated otherwise. *, p<0.05; **, p<0.01;***, p<0.001.* ***Abbreviation****: Hnf1a, hepatic nuclear factor 1α (Hnf1a); AMPKα, 5' AMP-activated protein kinase α; Pcsk9, proprotein convertase subtilisin/kexin type 9.*

4.3.4. *Ces3/Tgh*$^{-/-}$ Mice Protect Liver from Tumor-induced Enlargement

Increased abundance of F4/80-positive liver macrophages (Kupffer cells) was accompanied by increased proliferation rates of hepatocytes in livers of Tu-bearing mice, as determined by Ki67 staining (Fig. 18A). Tumor-associated liver enlargement was attenuated in *Ces3/Tgh*$^{-/-}$ mice (Fig. 18B). This was also reflected by loss of the positive correlation between tumor and liver weight, which was present in *WT* mice (Fig. 18C). Liver weight was also increased in Tu-bearing *Pemt*$^{-/-}$ mice (Fig. 18B) but not correlated to tumor weight (Fig. 18C). mRNA expression of pro-inflammatory markers in liver was increased in Tu-bearing mice of all genotypes, whereas no improvement was shown in *Ces3/Tgh*$^{-/-}$ compared to *WT* mice (Fig. 18D). Collectively, Ces3/TGH deficiency could alleviate tumor-induced liver enlargement, which might be associated to Pcsk9-mediated degradation of LDLR.

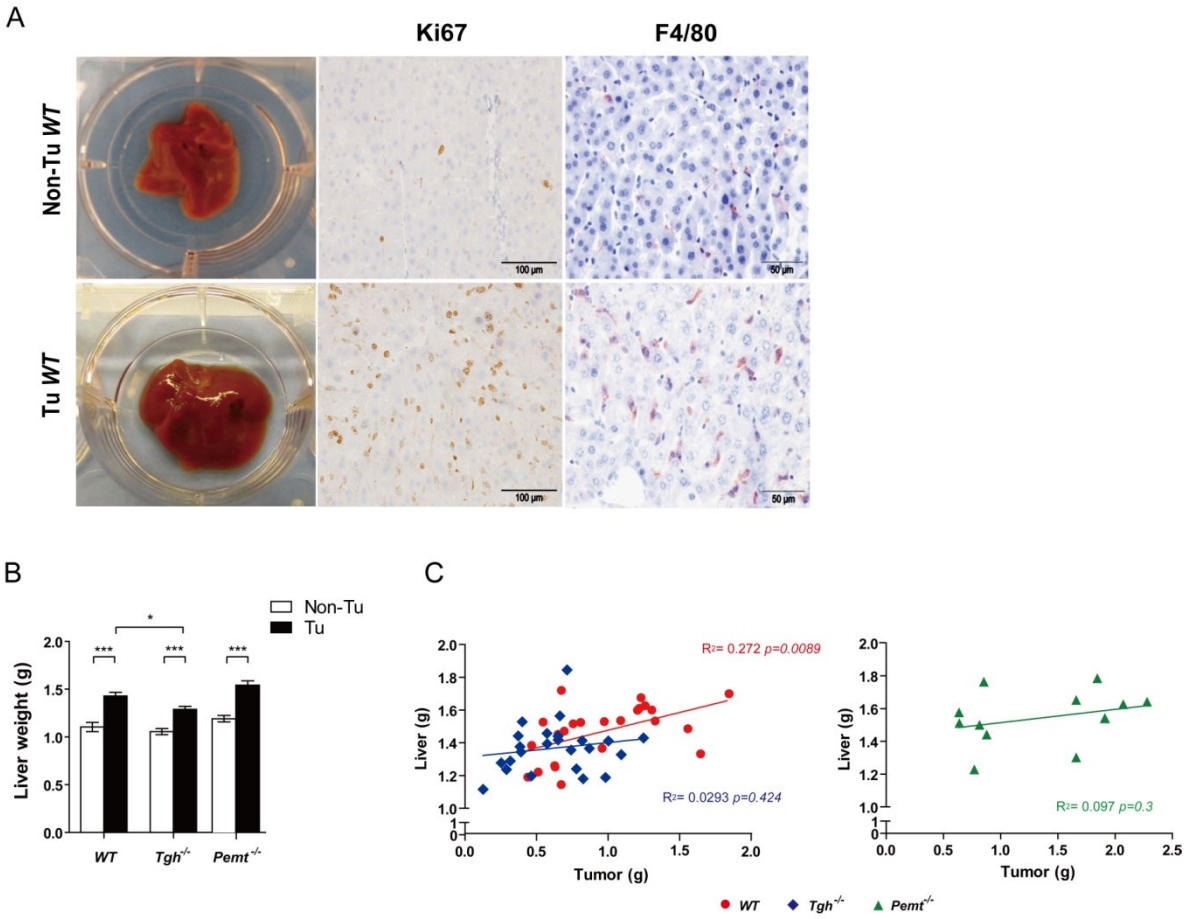
A
Ki67
F4/80
Non-Tu WT
Tu WT
100 μm
50 μm
B
Non-Tu
Tu
Liver weight (g)
WT
Tgh-/-
Pemt-/-
C
R2= 0.272 p=0.0089
R2= 0.0293 p=0.424
R2= 0.097 p=0.3
Liver (g)
Tumor (g)
WT
Tgh-/-
Pemt-/-
D
TNFa
MCP1
F4/80
Socs3
Rel. mRNA level
Non-Tu
Tu

Figure 18. Alleviation of tumor-induced liver enlargement in Ces3/Tgh$^{-/-}$ mice. *(A) Macroscopic views of livers from Non-Tu/Tu-bearing WT mice. IHC staining for Ki67 (proliferation marker) and F4/80 (macrophage marker) in liver. Scale bars: 100 μm (Ki67); 50 μm (F4/80). IHC was performed by Silvia Schauer (Medical University of Graz). (B) Liver weight (n =10-13/group). (C) Correlation between tumor weight and liver weight in WT (n = 24), Ces3/Tgh$^{-/-}$ mice (n = 24) and Pemt$^{-/-}$ mice (n = 13) with Pearson Correlation Coefficient test. (D) Transcript levels of hepatic inflammatory markers (n=5-7). Error bars represent SEM. Unpaired t-test except indicated otherwise. *, p<0.05; **, p<0.01; ***, p<0.001*. ***Abbreviation****: MCP1, monocyte chemoattractant protein 1; Socs3, suppressor of cytokine signaling 3.*

5. DISSCUSSION

This discussion is partially reused from the publication (78)with modifications and the unpublished manuscript in collaboration with Prof. Dr. Richard Lehner (University of Alberta, Edmonton, Canada). The use of relevant contents in this section is with the permission of Elservier and Richard Lehner & Gerald Hoefler.

Metabolic reprogramming of lipid metabolism is frequently reported in a wide range of tumor types. The role of lipid metabolism in the development of human malignancies and cancer-associated cachexia remains elusive but may lead to the discovery of new targets against tumors and tumor-associated diseases. In this study we utilized murine Bcr/Abl transformed primary B-cells (TPBCs) (92) as an experimental model for highly proliferating B-cell tumors such as DLBCL and acute lymphoblastic leukemia/lymphoma (ALL) to explore the regulations of tumor on systemic lipid mobilization and distribution. The rapidly growing TPBC tumors induced significant loss of WAT in at umor-mass dependent pattern, suggesting an accelerated lipid flux mobilized from WAT. Lipids, especially TG and cholesterol, are hydrophobic and must be transported in the circulation via lipoproteins. Aberrant lipoprotein profiles are often observed in cancer patients, but the mechanisms involved and the effects of dyslipidemia on tumor development and progression are still elusive. Our findings demonstrate that the highly proliferating TPBC tumors induce hyperlipidemia via elevation of VLDL and LDL levels in mice.

The liver is the main organ controlling systemic lipid mobilization; however, effects on liver metabolism in the context of tumor-associated cachexia are still poorly understood. In liver, FAs are rapidly esterified into TG, which are either stored within lipid droplets or exported as VLDL. In our study, we observed that primary hepatocytes isolated from Tu-bearing mice rapidly convert exogenous acetate into cholesterol and oleate into TG and cholesterol, which might support VLDL

production from hepatocytes. Despite unchanged gene expression involved in FA lipogenesis, the suppression of hepatic FA oxidation and the substantial flow of FA from WAT during fasting might still provide adequate amounts of FA as a source for VLDL production.

Although tumors attenuated the activity of LPL which converts VLDL into LDL, plasma LDL levels were still increased due to reduced hepatic LDLR levels. In liver, *Ldlr* expression is primarily regulated by SREBP2in cholesterol-dependent manner (93) and by SREBP1 in certain circumstances (94, 95). In our model, hepatic SREBP1 but not 2 was inactivated in Tu-bearing *WT* mice. However, in fasting and refeeding conditions when SREBP1 is absent or fully activated in an insulin-dependent manner, respectively, differences in LDLR protein expression between Tu and Non-Tu groups remained almost consistent. Importantly, inactivation of SREBP1 failed to down-regulate *Ldlr* transcriptions in mice. These data suggest a potential post-translational regulation of LDLR independent of SREBPs activities.

Our study for the first time reports tumor-induced expression of hepatic and plasma PCSK9 concentrations, leading to reduced LDLR protein levels. Notably, the positive correlation between tumor weight and plasma PCSK9 concentration was observed in *WT* mice. The tissue specificity of LDLR protein regulation by PCSK9 renders the liver the most responsive organ (96), eliminating adverse effects on tumor LDLR-mediated VLDL remnant/LDL uptake and thus suppressing tumor growth. mTORC1 is the central cellular sensor responsive to nutrients and stress and mediates the regulation of cellular homeostasis and growth by various mechanisms. mTORC1-mediated activation of PCSK9 via repression of HNF1α is involved in the maintenance of LDLR levels in liver (90). In agreement, in our model, *Hnf1a* expression was increased in *WT* mice. mTORC1 activity is negatively regulated by TSC1/2. Stress such as hypoxia, energy deprivation, DNA damage and inflammation activate TSC1/2 and thus repress mTORC1 signaling (91). Thus,

the severe inflammation in liver observed in Tu-bearing mice suggests a mechanism for potential inactivation of mTORC1, which supports our finding on *Hnf1a* expression.

Cytokines (*e.g.* TNFα and IL-6) released from activated Kupffer cells are reported to induce hepatocyte proliferation after partial hepatectomy (97). In analogy, TPBC tumor-derived cytokines are likely to be responsible for hepatic inflammation, proliferating hepatocytes and liver enlargement observed in Tu-bearing mice in our study. Proliferation of hepatocytes together with suppression of PPARα-mediated FA oxidation in the liver might result in an increased AMP/ATP ratio and activation of AMPK. As expected, activation of AMPK was observed in Tu-bearing *WT* mice, supporting the involvement of tumor-mediated mTORC1-HNF1α-PCSK9-LDLR signaling axis. In addition, PPARα has a direct influence on the level of PCSK9 due to its repression of *Pcsk9* promoter activity concomitantly with its promotion of protein degradation (98). Moreover, inflammatory stimuli (*e.g.* LPS) have been shown to stimulate *Pcsk9* expression leading to increased LDLR degradation in mouse liver (99), supporting our finding that PCSK9 might play a critical role in tumor-induced hypercholesterolemia via LDLR inactivation.

Elevated plasma levels of TG are a hallmark of the metabolic syndrome and a risk factor for atherosclerosis (100). In addition, VLDL-C and LDL-Care considered as “bad cholesterol” by distributing cholesterol to peripheral organs and hence being associated with the pathogenesis of atherosclerosis. In fact, changes in systemic lipid mobilization may also promote tumor development and progression. The importance of lipids in proliferation of malignant tumors is thought to be attributable to the provision of essential constituents as building blocks to maintain membrane integrity, to the activation of signaling pathways and to energy metabolism. Recent evidence provided first insights into the role of cholesterol for tumor development. Experimental models revealed that elevated plasma cholesterol levels due to dietary effects accelerate the development and aggressiveness of breast tumors

(101). In addition, statins, which have been introduced for the treatment of hypercholesterolemia, display anti-tumor effects against various forms of cancers including lymphoma in animal tumor models (61). In our study we found out that depletion of lipoproteins in culture medium (LPDS) induced apoptosis and suppressed growth of TPBCs. Supplementation with VLDL, LDL and, to a lesser extent, HDL, could reverse the effects mediated by LPDS. Importantly, supply of cholesterol and depletion of cellular cholesterol oppositely affect the growth rate of tumor cells, indicating that cholesterol serves as one of the pro-tumorigenic factors of VLDL/LDL which stimulated tumor cells growth. In addition to maintaining the fluidity and permeability of the plasma membrane, cholesterol together with sphingolipids forms lipid rafts to recruit signaling components and initiates distinct downstream signaling in response to intra- and extracellular stimuli (102). In B-cells, lipid rafts-mediated spatial organization of signaling cascades with clathrin regulates the internalization of antigen through the Bcr (B-cell receptor) for processing and presentation to T cells (103). In Bcr-dependent diffuse large B-cell lymphoma (DLBCL), cholesterol biosynthesis is activated to maintain the integrity of Bcr in lipid rafts and the survival pathways (104). These results argue for an important role of cholesterol in B-cell lymphoma development and progression, in which elevated serum cholesterol (mainly VLDL/LDL-C) concentration and LDL levels were observed. Unlike lipoproteins, global glucose turnover remains unaltered in the presence of our tumors in our model. However, one cannot exclude the importance of glucose as the primary source for tumor growth.

The clear link between of obesity and increased probability to develop cancer fuels the interest that lipid lowering approaches (*e.g.* pharmaceutical and genetic) may provide novel therapeutic options to treat patients suffering from various types of tumors. First we explore whether fenofibrate, a commonly used lipid-lowering agent and PPARα agonist, could improve tumor-induced lipid alterations and tumor growth. Remarkably, TPBC tumor-induced hyperlipidemia and tumor weight were diminished by fenofibrate treatment. The mechanism(s) by which fenofibrate

protects mice from tumor-triggered hyperlipidemia might be one or more of the following aspects: 1) Increased hepatic FA uptake from bloodstream presumably via fibrate upregulated expression of hepatic FATPs (105). 2) Accelerated FA oxidation in peripheral oxidative organs (skeletal muscle, heart and liver) (89) leading to a reduction of plasma FA levels that consequently starves the tumor. 3) Reduced “bad” cholesterol levels. Elevated VLDL/LDL-C:HDL-C ratio and LDL levels in tumor-bearing mice were completely normalized by fenofibrate, indicating that serum cholesterol starvation of the tumor occurs upon fenofibrate treatment. 4) Lowering serum TG concentrations via reducing hepatic VLDL-TG export and by enhancing peripheral lipolysis of VLDL via activating LPL (106, 107). As an output, fenofibrate deprives tumors of available serum TG by reducing TG export and/or increasing the capacity of peripheral organs to utilize TG. The TPBC tumor itself is not affected due to the absence of tumor PPARα. In summary, our results propose that fenofibrate suppresses B-cells tumor growth via extrinsic pathways independent of PPARα activation in the tumor.

Next, to further explore the efficacies of another lipid lowering approach on systemic lipid homeostasis and tumor progression, we introduced two genetic hypolipidemic mouse models with attenuated VLDL secretion, *Ces3/Tgh*$^{-/-}$ and *Pemt*$^{-/-}$ mice. Interestingly, while tumor-mediated augmentation of circulating VLDL/LDL was partially reversed in *Ces3/Tgh*$^{-/-}$ mice, this was not observed in *Pemt*$^{-/-}$ mice. In concert with the resistance to changes in plasma lipid profiles, *Ces3/Tgh*$^{-/-}$ but not *Pemt*$^{-/-}$ mice suppressed tumor growth. Surprisingly, no attenuation of tumor-induced VLDL secretion was observed in day 14 post tumor inoculation, leading to the assumption that the reversal of hyperlipidemia observed in Tu-bearing *Ces3/Tgh*$^{-/-}$ mice might be due to multiply aspects but not solely to VLDL production. Nevertheless, it is conceivable that the reduced VLDL secretion persists in the first 8 days (before solid tumors become systemically influential) and maintains low TG levels in *Ces3/Tgh*$^{-/-}$ mice, presumably as in *Pemt*$^{-/-}$ mice. Given the lower plasma TG concentrations in *Ces3/Tgh*$^{-/-}$ Non-Tu-bearing mice compared

to *Pemt*$^{-/-}$ mice, *Ces3/Tgh*$^{-/-}$ mice might pose a stronger suppression on growth and survival of TPBCs.

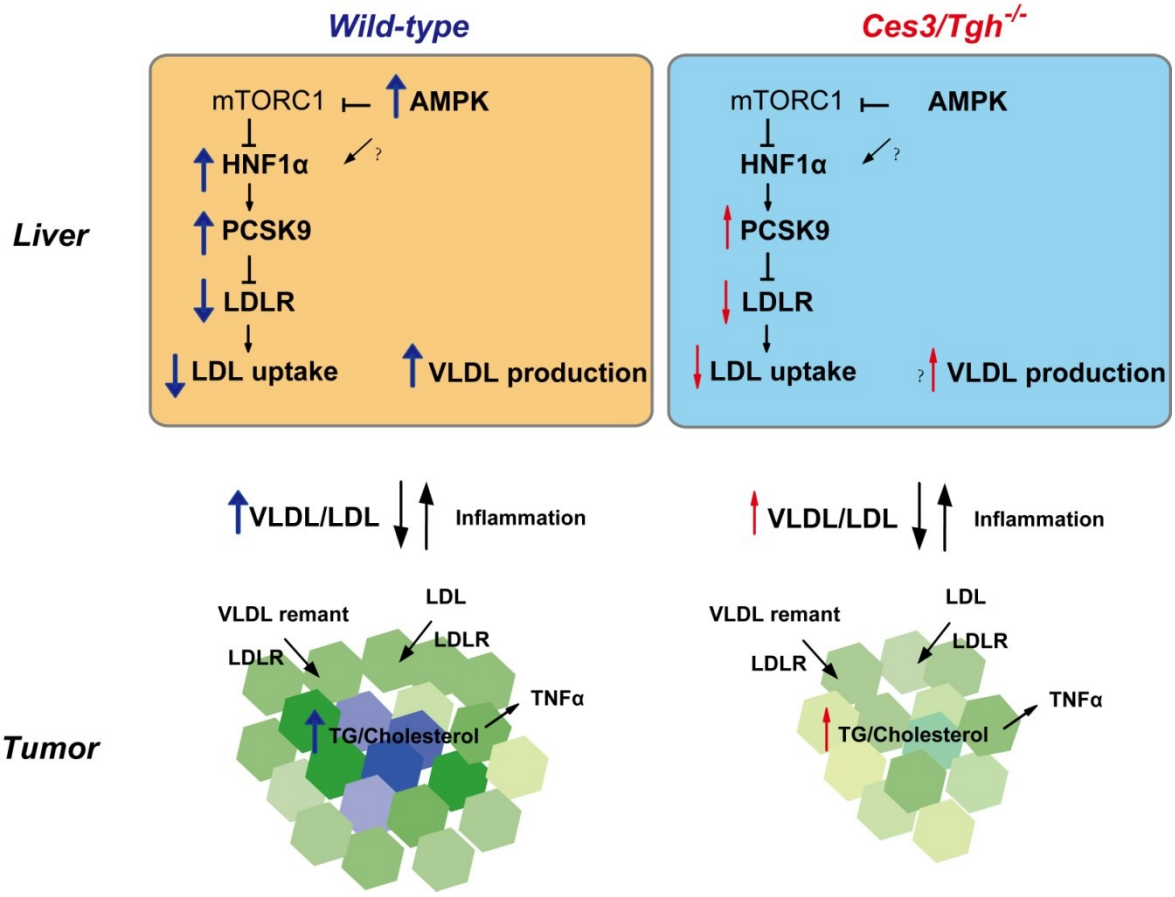

Figure 19. Schematic model of Ces3/TGH regulation of hepatic lipoprotein homeostasis in tumor-bearing mice. *In wild-type mice, stimulation of VLDL secretion from liver contributes to TPBC tumor-increased plasma VLDL. Moreover, the enhanced PCSK9-mediated LDLR degradation in liver causes insufficient LDL turnover and results in the elevation of plasma LDL. The hyperlipidemia thereby provides adequate amount of tumorigenic lipids especially cholesterol for tumor progression. In Ces3/Tgh*$^{-/-}$ *mice, despite no prevention against tumor-enhanced VLDL secretion, the hypotriglyceridemia incurred by Ces3/TGH deficiency-reduced VLDL production at the initial time, together with improvement of LDL uptake due to down-regulation of hepatic Pcsk9 expression, lead to reduced lipoprotein supply and suppression of tumor growth. Blue arrows indicate*

increase (↑) and decrease (↓) in WT mice, red arrows in Ces3/Tgh$^{-/-}$ mice; Black arrows indicate activation, "T" means inhibition.

In addition to enhanced VLDL production, VLDL/CM clearance was blunted in tumor bearing mice, which partially explains the increased plasma TG concentrations. Unlike in *Ces3/Tgh*$^{-/-}$ mice, PHP TG hydrolase activities with and without tumor in *Pemt*$^{-/-}$ mice were both lower compared to *WT* mice, suggesting that an additional defect in hydrolyzing TG from VLDL/CM occurs in *Pemt*$^{-/-}$ mice. The distinct behaviors also reflect on their different influences in LDL turnover. *Ces3/Tgh*$^{-/-}$ mice show reduced plasma PCSK9 concentrations both in Non-Tu- and Tu-bearing conditions compared to *WT* mice, whereas neither of these reduction were observed in *Pemt*$^{-/-}$ mice. The preservation of hepatic LDLR protein amount in *Ces3/Tgh*$^{-/-}$ mice is likely due to the prevention of tumor-activated AMPK-HNF1α-PCSK9 signal pathway. Consequently, hepatic LDLR is preserved in Tu-bearing *Ces3/Tgh*$^{-/-}$ mice but not *Pemt*$^{-/-}$ mice, suggesting an improvement of LDL turnover in *Ces3/Tgh*$^{-/-}$ mice. Notably, the protection against tumor-induced liver enlargement in *Ces3/Tgh*$^{-/-}$ Tu-bearing mice but not *Pemt*$^{-/-}$ mice offers a clue that Ces3/Tgh deficiency might exert an anti-inflammatory activity which might maintain physiological functions of the liver in global lipid homeostasis (Fig. 19).

In summary, as a model of rapid growth tumor, BCR-Abl dependent transformed precursor B-cell (TPBC) tumors may influence systemic lipid metabolism through production of pro-inflammatory cytokines (*e.g*. TNFα, IL-6). Elevated plasma TNFα is thought to drive FA efflux from WAT through enhanced lipolysis (108). We report that the decreased LPL-mediated hydrolysis of TG-rich lipoproteins together with enhanced VLDL production results in hypertriglyceridemia in Tu-bearing mice. Cytokines derived from tumors potentially cause liver inflammation. In livers of Tu-bearing *WT* mice, PCSK9-mediated degradation of LDLR protein is augmented by activation of AMPK and HNF1α, resulting in hypercholesterolemia. Hypertriglyceridemia and -cholesterolemia in *WT* mice presumably provide tumors

with essential exogenous lipids to support proliferation. We conclude that resistance against hyperlipidemia in *Ces3/Tgh*$^{-/-}$ mice consequently dampens tumor growth (Fig. 20). Our experimental data confirm the existence of a tumor-associated positive feedback loop linking tumor progression and aberrant lipoprotein homeostasis in mice, offer supporting evidence for the importance of the "tumor macroenvironment" in the pathogenesis of cancer and cancer-associated cachexia.

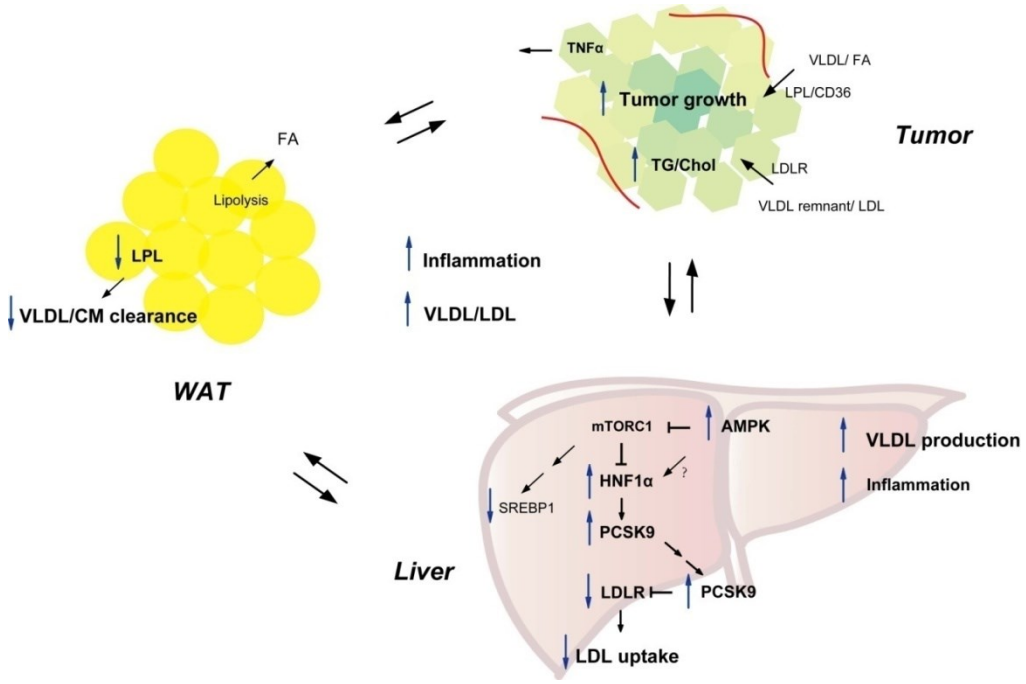

Figure 20. Schematic model of tumor impact on global lipoprotein homeostasis.

In wild-type mice, inhibition of TG-rich lipoprotein turnover in peripheral organs (e.g. WAT) together with stimulation of VLDL secretion from liver contributes to TPBC tumor-increased plasma VLDL. Moreover, the enhanced PCSK9-mediated LDLR degradation in liver causes insufficient LDL turnover and results in the elevation of plasma LDL. Hyperlipidemia thereby provides adequate amount of tumorigenic lipids especially cholesterol for tumor progression. Blue arrows indicate increase (↑) and decrease (↓); Black arrows indicate activation, "T" means inhibition.

6. REFERENCES

1. DeBerardinis RJ, Lum JJ, Hatzivassiliou G, Thompson CB. The biology of cancer: metabolic reprogramming fuels cell growth and proliferation. Cell metabolism. 2008 Jan;7(1):11-20.
2. Warburg O, Wind F, Negelein E. The Metabolism of Tumors in the Body. J Gen Physiol. 1927 Mar 7;8(6):519-30.
3. Warburg O. On the origin of cancer cells. Science (New York, NY. 1956 Feb 24;123(3191):309-14.
4. Vander Heiden MG, Cantley LC, Thompson CB. Understanding the Warburg effect: the metabolic requirements of cell proliferation. Science (New York, NY. 2009 May 22;324(5930):1029-33.
5. Chen JQ, Russo J. Dysregulation of glucose transport, glycolysis, TCA cycle and glutaminolysis by oncogenes and tumor suppressors in cancer cells. Biochimica et biophysica acta. 2012 Dec;1826(2):370-84.
6. Barthel A, Okino ST, Liao J, Nakatani K, Li J, Whitlock JP, Jr., et al. Regulation of GLUT1 gene transcription by the serine/threonine kinase Akt1. The Journal of biological chemistry. 1999 Jul 16;274(29):20281-6.
7. Chen C, Pore N, Behrooz A, Ismail-Beigi F, Maity A. Regulation of glut1 mRNA by hypoxia-inducible factor-1. Interaction between H-ras and hypoxia. The Journal of biological chemistry. 2001 Mar 23;276(12):9519-25.
8. Kim JW, Gao P, Liu YC, Semenza GL, Dang CV. Hypoxia-inducible factor 1 and dysregulated c-Myc cooperatively induce vascular endothelial growth factor and metabolic switches hexokinase 2 and pyruvate dehydrogenase kinase 1. Molecular and cellular biology. 2007 Nov;27(21):7381-93.
9. Zheng J. Energy metabolism of cancer: Glycolysis versus oxidative phosphorylation (Review). Oncol Lett. 2012 Dec;4(6):1151-7.
10. Barger JF, Gallo CA, Tandon P, Liu H, Sullivan A, Grimes HL, et al. S6K1 determines the metabolic requirements for BCR-ABL survival. Oncogene. 2013 Jan 24;32(4):453-61.
11. Zaugg K, Yao Y, Reilly PT, Kannan K, Kiarash R, Mason J, et al. Carnitine palmitoyltransferase 1C promotes cell survival and tumor growth under conditions of metabolic stress. Genes Dev. 2011 May 15;25(10):1041-51.
12. Martinez-Outschoorn UE, Lisanti MP, Sotgia F. Catabolic cancer-associated fibroblasts transfer energy and biomass to anabolic cancer cells, fueling tumor growth. Seminars in cancer biology. 2014 Apr;25:47-60.
13. Carracedo A, Cantley LC, Pandolfi PP. Cancer metabolism: fatty acid oxidation in the limelight. Nat Rev Cancer. 2013 Apr;13(4):227-32.
14. Ma L, Tao Y, Duran A, Llado V, Galvez A, Barger JF, et al. Control of nutrient stress-induced metabolic reprogramming by PKCzeta in tumorigenesis. Cell. 2013 Jan 31;152(3):599-611.
15. Al-Zoughbi W, Huang J, Paramasivan GS, Till H, Pichler M, Guertl-Lackner B, et al. Tumor macroenvironment and metabolism. Seminars in oncology. 2013 Apr;41(2):281-95.
16. Louie SM, Roberts LS, Mulvihill MM, Luo K, Nomura DK. Cancer cells incorporate and remodel exogenous palmitate into structural and oncogenic signaling lipids. Biochimica et biophysica acta. 2013 Oct;1831(10):1566-72.
17. Guo D, Reinitz F, Youssef M, Hong C, Nathanson D, Akhavan D, et al. An LXR agonist promotes glioblastoma cell death through inhibition of an EGFR/AKT/SREBP-1/LDLR-dependent pathway. Cancer discovery. 2011 Oct;1(5):442-56.
18. Vitols S, Angelin B, Ericsson S, Gahrton G, Juliusson G, Masquelier M, et al. Uptake of low density

lipoproteins by human leukemic cells in vivo: relation to plasma lipoprotein levels and possible relevance for selective chemotherapy. Proceedings of the National Academy of Sciences of the United States of America. 1990 Apr;87(7):2598-602.

19. Vitols S, Peterson C, Larsson O, Holm P, Aberg B. Elevated uptake of low density lipoproteins by human lung cancer tissue in vivo. Cancer research. 1992 Nov 15;52(22):6244-7.

20. Liu J, Xu A, Lam KS, Wong NS, Chen J, Shepherd PR, et al. Cholesterol-induced mammary tumorigenesis is enhanced by adiponectin deficiency: role of LDL receptor upregulation. Oncotarget. 2013 Oct;4(10):1804-18.

21. Crowe FL, Allen NE, Appleby PN, Overvad K, Aardestrup IV, Johnsen NF, et al. Fatty acid composition of plasma phospholipids and risk of prostate cancer in a case-control analysis nested within the European Prospective Investigation into Cancer and Nutrition. The American journal of clinical nutrition. 2008 Nov;88(5):1353-63.

22. Kuemmerle NB, Rysman E, Lombardo PS, Flanagan AJ, Lipe BC, Wells WA, et al. Lipoprotein lipase links dietary fat to solid tumor cell proliferation. Molecular cancer therapeutics. 2011 Mar;10(3):427-36.

23. Mullen AR, Wheaton WW, Jin ES, Chen PH, Sullivan LB, Cheng T, et al. Reductive carboxylation supports growth in tumour cells with defective mitochondria. Nature. 2012 Jan 19;481(7381):385-8.

24. Nagahashi M, Ramachandran S, Kim EY, Allegood JC, Rashid OM, Yamada A, et al. Sphingosine-1-phosphate produced by sphingosine kinase 1 promotes breast cancer progression by stimulating angiogenesis and lymphangiogenesis. Cancer research. 2012 Feb 1;72(3):726-35.

25. Greenhough A, Smartt HJ, Moore AE, Roberts HR, Williams AC, Paraskeva C, et al. The COX-2/PGE2 pathway: key roles in the hallmarks of cancer and adaptation to the tumour microenvironment. Carcinogenesis. 2009 Mar;30(3):377-86.

26. Sinha P, Clements VK, Fulton AM, Ostrand-Rosenberg S. Prostaglandin E2 promotes tumor progression by inducing myeloid-derived suppressor cells. Cancer research. 2007 May 1;67(9):4507-13.

27. Tirinato L, Liberale C, Di Franco S, Candeloro P, Benfante A, La Rocca R, et al. Lipid droplets: a new player in colorectal cancer stem cells unveiled by spectroscopic imaging. Stem Cells. 2015 Jan;33(1):35-44.

28. Dang CV. Links between metabolism and cancer. Genes Dev. 2012 May 1;26(9):877-90.

29. Ackerman D, Simon MC. Hypoxia, lipids, and cancer: surviving the harsh tumor microenvironment. Trends Cell Biol. 2014 Aug;24(8):472-8.

30. Semenza GL. Defining the role of hypoxia-inducible factor 1 in cancer biology and therapeutics. Oncogene. 2010 Feb 4;29(5):625-34.

31. Mylonis I, Sembongi H, Befani C, Liakos P, Siniossoglou S, Simos G. Hypoxia causes triglyceride accumulation by HIF-1-mediated stimulation of lipin 1 expression. J Cell Sci. 2012 Jul 15;125(Pt 14):3485-93.

32. Bensaad K, Favaro E, Lewis CA, Peck B, Lord S, Collins JM, et al. Fatty acid uptake and lipid storage induced by HIF-1alpha contribute to cell growth and survival after hypoxia-reoxygenation. Cell Rep. 2014 Oct 9;9(1):349-65.

33. Lewis CA, Brault C, Peck B, Bensaad K, Griffiths B, Mitter R, et al. SREBP maintains lipid biosynthesis and viability of cancer cells under lipid- and oxygen-deprived conditions and defines a gene signature associated with poor survival in glioblastoma multiforme. Oncogene. 2015 Jan 26.

34. Kamphorst JJ, Cross JR, Fan J, de Stanchina E, Mathew R, White EP, et al. Hypoxic and Ras-transformed cells support growth by scavenging unsaturated fatty acids from lysophospholipids. Proceedings of the National Academy of Sciences of the United States of America. 2013 May 28;110(22):8882-7.

35. Calle EE, Rodriguez C, Walker-Thurmond K, Thun MJ. Overweight, obesity, and mortality from cancer in a prospectively studied cohort of U.S. adults. The New England journal of medicine. 2003 Apr 24;348(17):1625-38.

36. Larsson SC, Wolk A. Body mass index and risk of non-Hodgkin's and Hodgkin's lymphoma: a meta-analysis of prospective studies. Eur J Cancer. Nov;47(16):2422-30.

37. Skibola CF, Holly EA, Forrest MS, Hubbard A, Bracci PM, Skibola DR, et al. Body mass index, leptin and leptin receptor polymorphisms, and non-hodgkin lymphoma. Cancer Epidemiol Biomarkers Prev. 2004 May;13(5):779-86.

38. Whelan JT, Ludwig DL, Bertrand FE. HoxA9 induces insulin-like growth factor-1 receptor expression in B-lineage acute lymphoblastic leukemia. Leukemia. 2008 Jun;22(6):1161-9.

39. Taslipinar A, Bolu E, Kebapcilar L, Sahin M, Uckaya G, Kutlu M. Insulin-like growth factor-1 is essential to the increased mortality caused by excess growth hormone: a case of thyroid cancer and non-Hodgkin's lymphoma in a patient with pituitary acromegaly. Medical oncology (Northwood, London, England). 2009;26(1):62-6.

40. Agustsson T, Ryden M, Hoffstedt J, van Harmelen V, Dicker A, Laurencikiene J, et al. Mechanism of increased lipolysis in cancer cachexia. Cancer research. 2007 Jun 1;67(11):5531-7.

41. Das SK, Eder S, Schauer S, Diwoky C, Temmel H, Guertl B, et al. Adipose triglyceride lipase contributes to cancer-associated cachexia. Science (New York, NY. 2011 Jul 8;333(6039):233-8.

42. Santos CR, Schulze A. Lipid metabolism in cancer. The FEBS journal. 2012 Aug;279(15):2610-23.

43. Nieman KM, Kenny HA, Penicka CV, Ladanyi A, Buell-Gutbrod R, Zillhardt MR, et al. Adipocytes promote ovarian cancer metastasis and provide energy for rapid tumor growth. Nature medicine. 2011;17(11):1498-503.

44. Muntoni S, Atzori L, Mereu R, Satta G, Macis MD, Congia M, et al. Serum lipoproteins and cancer. Nutr Metab Cardiovasc Dis. 2009 Mar;19(3):218-25.

45. Fiorenza AM, Branchi A, Sommariva D. Serum lipoprotein profile in patients with cancer. A comparison with non-cancer subjects. International journal of clinical & laboratory research. 2000;30(3):141-5.

46. Kokoglu E, Karaarslan I, Karaarslan HM, Baloglu H. Alterations of serum lipids and lipoproteins in breast cancer. Cancer letters. 1994 Jul 29;82(2):175-8.

47. Kuliszkiewicz-Janus M, Malecki R, Mohamed AS. Lipid changes occuring in the course of hematological cancers. Cellular & molecular biology letters. 2008;13(3):465-74.

48. Singh S, Ramesh V, Premalatha B, Prashad KV, Ramadoss K. Alterations in serum lipid profile patterns in oral cancer. Journal of natural science, biology, and medicine. 2013 Jul;4(2):374-8.

49. Patel PS, Shah MH, Jha FP, Raval GN, Rawal RM, Patel MM, et al. Alterations in plasma lipid profile patterns in head and neck cancer and oral precancerous conditions. Indian journal of cancer. 2004 Jan-Mar;41(1):25-31.

50. Ray G, Husain SA. Role of lipids, lipoproteins and vitamins in women with breast cancer. Clinical biochemistry. 2001 Feb;34(1):71-6.

51. Benn M, Tybjaerg-Hansen A, Stender S, Frikke-Schmidt R, Nordestgaard BG. Low-density lipoprotein cholesterol and the risk of cancer: a mendelian randomization study. Journal of the National Cancer Institute. 2011 Mar 16;103(6):508-19.

52. Alikhani N, Ferguson RD, Novosyadlyy R, Gallagher EJ, Scheinman EJ, Yakar S, et al. Mammary tumor growth and pulmonary metastasis are enhanced in a hyperlipidemic mouse model. Oncogene. 2013 Feb 21;32(8):961-7.

53. Zhuang L, Kim J, Adam RM, Solomon KR, Freeman MR. Cholesterol targeting alters lipid raft composition and cell survival in prostate cancer cells and xenografts. The Journal of clinical investigation. 2005 Apr;115(4):959-68.

54. Sun X, Essalmani R, Day R, Khatib AM, Seidah NG, Prat A. Proprotein convertase subtilisin/kexin type 9 deficiency reduces melanoma metastasis in liver. Neoplasia. 2012 Dec;14(12):1122-31.

55. Forman BM, Chen J, Evans RM. Hypolipidemic drugs, polyunsaturated fatty acids, and eicosanoids are ligands for peroxisome proliferator-activated receptors alpha and delta. Proceedings of the National Academy of Sciences of the United States of America. 1997 Apr 29;94(9):4312-7.

56. Willson TM, Brown PJ, Sternbach DD, Henke BR. The PPARs: from orphan receptors to drug discovery. Journal of medicinal chemistry. 2000 Feb 24;43(4):527-50.

57. Chinetti G, Fruchart JC, Staels B. Peroxisome proliferator-activated receptors (PPARs): nuclear receptors at the crossroads between lipid metabolism and inflammation. Inflamm Res. 2000 Oct;49(10):497-505.

58. Peters JM, Shah YM, Gonzalez FJ. The role of peroxisome proliferator-activated receptors in carcinogenesis and chemoprevention. Nat Rev Cancer. Mar;12(3):181-95.

59. Panigrahy D, Kaipainen A, Huang S, Butterfield CE, Barnes CM, Fannon M, et al. PPARalpha agonist fenofibrate suppresses tumor growth through direct and indirect angiogenesis inhibition. Proceedings of the National Academy of Sciences of the United States of America. 2008 Jan 22;105(3):985-90.

60. Zak Z, Gelebart P, Lai R. Fenofibrate induces effective apoptosis in mantle cell lymphoma by inhibiting the TNFalpha/NF-kappaB signaling axis. Leukemia. Aug;24(8):1476-86.

61. Jakobisiak M, Golab J. Potential antitumor effects of statins (Review). International journal of oncology. 2003 Oct;23(4):1055-69.

62. Chan KK, Oza AM, Siu LL. The statins as anticancer agents. Clin Cancer Res. 2003 Jan;9(1):10-9.

63. Campia I, Lussiana C, Pescarmona G, Ghigo D, Bosia A, Riganti C. Geranylgeraniol prevents the cytotoxic effects of mevastatin in THP-1 cells, without decreasing the beneficial effects on cholesterol synthesis. British journal of pharmacology. 2009 Dec;158(7):1777-86.

64. Xia Z, Tan MM, Wong WW, Dimitroulakos J, Minden MD, Penn LZ. Blocking protein geranylgeranylation is essential for lovastatin-induced apoptosis of human acute myeloid leukemia cells. Leukemia. 2001 Sep;15(9):1398-407.

65. Spampanato C, De Maria S, Sarnataro M, Giordano E, Zanfardino M, Baiano S, et al. Simvastatin inhibits cancer cell growth by inducing apoptosis correlated to activation of Bax and down-regulation of BCL-2 gene expression. International journal of oncology. Apr;40(4):935-41.

66. Dolinsky VW, Gilham D, Alam M, Vance DE, Lehner R. Triacylglycerol hydrolase: role in intracellular lipid metabolism. Cell Mol Life Sci. 2004 Jul;61(13):1633-51.

67. Dolinsky VW, Douglas DN, Lehner R, Vance DE. Regulation of the enzymes of hepatic microsomal triacylglycerol lipolysis and re-esterification by the glucocorticoid dexamethasone. The Biochemical journal. 2004 Mar 15;378(Pt 3):967-74.

68. Gilham D, Alam M, Gao W, Vance DE, Lehner R. Triacylglycerol hydrolase is localized to the endoplasmic reticulum by an unusual retrieval sequence where it participates in VLDL assembly without utilizing VLDL lipids as substrates. Molecular biology of the cell. 2005 Feb;16(2):984-96.

69. Wei E, Ben Ali Y, Lyon J, Wang H, Nelson R, Dolinsky VW, et al. Loss of TGH/Ces3 in mice decreases blood lipids, improves glucose tolerance, and increases energy expenditure. Cell metabolism. 2010 Mar 3;11(3):183-93.

70. Gilham D, Ho S, Rasouli M, Martres P, Vance DE, Lehner R. Inhibitors of hepatic microsomal

triacylglycerol hydrolase decrease very low density lipoprotein secretion. Faseb J. 2003 Sep;17(12):1685-7.

71. Wei E, Alam M, Sun F, Agellon LB, Vance DE, Lehner R. Apolipoprotein B and triacylglycerol secretion in human triacylglycerol hydrolase transgenic mice. Journal of lipid research. 2007 Dec;48(12):2597-606.

72. Lian J, Wei E, Wang SP, Quiroga AD, Li L, Di Pardo A, et al. Liver specific inactivation of carboxylesterase 3/triacylglycerol hydrolase decreases blood lipids without causing severe steatosis in mice. Hepatology (Baltimore, Md. 2012 Dec;56(6):2154-62.

73. Lian J, Quiroga AD, Li L, Lehner R. Ces3/TGH deficiency improves dyslipidemia and reduces atherosclerosis in Ldlr(-/-) mice. Circulation research. 2012 Sep 28;111(8):982-90.

74. Vance DE, Ridgway ND. The methylation of phosphatidylethanolamine. Progress in lipid research. 1988;27(1):61-79.

75. Noga AA, Zhao Y, Vance DE. An unexpected requirement for phosphatidylethanolamine N-methyltransferase in the secretion of very low density lipoproteins. The Journal of biological chemistry. 2002 Nov 1;277(44):42358-65.

76. Noga AA, Vance DE. A gender-specific role for phosphatidylethanolamine N-methyltransferase-derived phosphatidylcholine in the regulation of plasma high density and very low density lipoproteins in mice. The Journal of biological chemistry. 2003 Jun 13;278(24):21851-9.

77. Zhao Y, Su B, Jacobs RL, Kennedy B, Francis GA, Waddington E, et al. Lack of phosphatidylethanolamine N-methyltransferase alters plasma VLDL phospholipids and attenuates atherosclerosis in mice. Arteriosclerosis, thrombosis, and vascular biology. 2009 Sep;29(9):1349-55.

78. Huang J, Das SK, Jha P, Al Zoughbi W, Schauer S, Claudel T, et al. The PPARalpha agonist fenofibrate suppresses B-cell lymphoma in mice by modulating lipid metabolism. Biochimica et biophysica acta. 2013 Oct;1831(10):1555-65.

79. Hoelbl A, Schuster C, Kovacic B, Zhu B, Wickre M, Hoelzl MA, et al. Stat5 is indispensable for the maintenance of bcr/abl-positive leukaemia. EMBO Mol Med. Mar;2(3):98-110.

80. Ko KW, Erickson B, Lehner R. Es-x/Ces1 prevents triacylglycerol accumulation in McArdle-RH7777 hepatocytes. Biochimica et biophysica acta. 2009 Dec;1791(12):1133-43.

81. Folch J, Lees M, Sloane Stanley GH. A simple method for the isolation and purification of total lipides from animal tissues. The Journal of biological chemistry. 1957 May;226(1):497-509.

82. Tamilarasan KP, Temmel H, Das SK, Al Zoughbi W, Schauer S, Vesely PW, et al. Skeletal muscle damage and impaired regeneration due to LPL-mediated lipotoxicity. Cell death & disease.3:e354.

83. Zechner R. Rapid and simple isolation procedure for lipoprotein lipase from human milk. Biochimica et biophysica acta. 1990 May 1;1044(1):20-5.

84. Pyper SR, Viswakarma N, Yu S, Reddy JK. PPARalpha: energy combustion, hypolipidemia, inflammation and cancer. Nuclear receptor signaling.8:e002.

85. Zhang L, Yang J, Qian J, Li H, Romaguera JE, Kwak LW, et al. Role of the microenvironment in mantle cell lymphoma: IL-6 is an important survival factor for the tumor cells. Blood. Nov 1;120(18):3783-92.

86. Gupta M, Maurer MJ, Wellik LE, Law ME, Han JJ, Ozsan N, et al. Expression of Myc, but not pSTAT3, is an adverse prognostic factor for diffuse large B-cell lymphoma treated with epratuzumab/R-CHOP. Blood. Nov 22;120(22):4400-6.

87. Charbonneau B, Maurer MJ, Ansell SM, Slager SL, Fredericksen ZS, Ziesmer SC, et al. Pretreatment circulating serum cytokines associated with follicular and diffuse large B-cell lymphoma: a clinic-based case-control study. Cytokine. Dec;60(3):882-9.

88. Canbay A, Bechmann L, Gerken G. Lipid metabolism in the liver. Zeitschrift fur Gastroenterologie. 2007 Jan;45(1):35-41.

89. Reddy JK, Hashimoto T. Peroxisomal beta-oxidation and peroxisome proliferator-activated receptor alpha: an adaptive metabolic system. Annual review of nutrition. 2001;21:193-230.
90. Ai D, Chen C, Han S, Ganda A, Murphy AJ, Haeusler R, et al. Regulation of hepatic LDL receptors by mTORC1 and PCSK9 in mice. The Journal of clinical investigation. 2012 Apr 2;122(4):1262-70.
91. McCormick MA, Tsai SY, Kennedy BK. TOR and ageing: a complex pathway for a complex process. Philosophical transactions of the Royal Society of London. 2011 Jan 12;366(1561):17-27.
92. Daley GQ, Van Etten RA, Baltimore D. Blast crisis in a murine model of chronic myelogenous leukemia. Proceedings of the National Academy of Sciences of the United States of America. 1991 Dec 15;88(24):11335-8.
93. Horton JD, Shah NA, Warrington JA, Anderson NN, Park SW, Brown MS, et al. Combined analysis of oligonucleotide microarray data from transgenic and knockout mice identifies direct SREBP target genes. Proceedings of the National Academy of Sciences of the United States of America. 2003 Oct 14;100(21):12027-32.
94. Streicher R, Kotzka J, Muller-Wieland D, Siemeister G, Munck M, Avci H, et al. SREBP-1 mediates activation of the low density lipoprotein receptor promoter by insulin and insulin-like growth factor-I. The Journal of biological chemistry. 1996 Mar 22;271(12):7128-33.
95. Sekar N, Veldhuis JD. Involvement of Sp1 and SREBP-1a in transcriptional activation of the LDL receptor gene by insulin and LH in cultured porcine granulosa-luteal cells. Am J Physiol Endocrinol Metab. 2004 Jul;287(1):E128-35.
96. Luo Y, Warren L, Xia D, Jensen H, Sand T, Petras S, et al. Function and distribution of circulating human PCSK9 expressed extrahepatically in transgenic mice. Journal of lipid research. 2009 Aug;50(8):1581-8.
97. Bohm F, Kohler UA, Speicher T, Werner S. Regulation of liver regeneration by growth factors and cytokines. EMBO Mol Med. 2010 Aug;2(8):294-305.
98. Kourimate S, Le May C, Langhi C, Jarnoux AL, Ouguerram K, Zair Y, et al. Dual mechanisms for the fibrate-mediated repression of proprotein convertase subtilisin/kexin type 9. The Journal of biological chemistry. 2008 Apr 11;283(15):9666-73.
99. Feingold KR, Moser AH, Shigenaga JK, Patzek SM, Grunfeld C. Inflammation stimulates the expression of PCSK9. Biochemical and biophysical research communications. 2008 Sep 19;374(2):341-4.
100. Krauss RM. Atherogenicity of triglyceride-rich lipoproteins. The American journal of cardiology. 1998 Feb 26;81(4A):13B-7B.
101. Llaverias G, Danilo C, Mercier I, Daumer K, Capozza F, Williams TM, et al. Role of cholesterol in the development and progression of breast cancer. The American journal of pathology. Jan;178(1):402-12.
102. Simons K, Toomre D. Lipid rafts and signal transduction. Nature reviews. 2000 Oct;1(1):31-9.
103. Stoddart A, Dykstra ML, Brown BK, Song W, Pierce SK, Brodsky FM. Lipid rafts unite signaling cascades with clathrin to regulate BCR internalization. Immunity. 2002 Oct;17(4):451-62.
104. Chen L, Monti S, Juszczynski P, Ouyang J, Chapuy B, Neuberg D, et al. SYK inhibition modulates distinct PI3K/AKT- dependent survival pathways and cholesterol biosynthesis in diffuse large B cell lymphomas. Cancer cell. 2013 Jun 10;23(6):826-38.
105. Martin G, Schoonjans K, Lefebvre AM, Staels B, Auwerx J. Coordinate regulation of the expression of the fatty acid transport protein and acyl-CoA synthetase genes by PPARalpha and PPARgamma activators. The Journal of biological chemistry. 1997 Nov 7;272(45):28210-7.
106. Peters JM, Hennuyer N, Staels B, Fruchart JC, Fievet C, Gonzalez FJ, et al. Alterations in lipoprotein metabolism in peroxisome proliferator-activated receptor alpha-deficient mice. The Journal of biological

chemistry. 1997 Oct 24;272(43):27307-12.

107. Qu S, Su D, Altomonte J, Kamagate A, He J, Perdomo G, et al. PPAR{alpha} mediates the hypolipidemic action of fibrates by antagonizing FoxO1. Am J Physiol Endocrinol Metab. 2007 Feb;292(2):E421-34.

108. Zhang HH, Halbleib M, Ahmad F, Manganiello VC, Greenberg AS. Tumor necrosis factor-alpha stimulates lipolysis in differentiated human adipocytes through activation of extracellular signal-related kinase and elevation of intracellular cAMP. Diabetes. 2002 Oct;51(10):2929-35.

ACKNOWLEDGEMENT

First and foremost, I would like to express my sincerest gratitude to my supervisor Prof. Gerald Hoefler for taking me as a Ph.D candidate in the Ph.D program “Doctoral College of Metabolic and Cardiovascular Disease (DK-MCD)” and offering me the great opportunity to pursue my scientific career. I would like to thank Prof. Hoefler for mentoring me in life with your charming personality, inspiring me with your professional experiences in cancer research field, and supporting my projects by building necessary collaborations throughout the entire study during this four and half years.

I would like to thank all my colleagues in the group of Prof. Hoefler during April 2011- present. I am grateful to Dr. Pooja Jha, Dr. Wael Al-Zoughbi, Ganapathy Paramasivan and Dr. Suman Das for their experimentally support and friendship. I would like to thank Silvia Schauer, Dr. Elke Stadelmeyer and Dr. Paul Vesely for their scientific help. My special thanks to Prof. Richard Lehner from University of Alberta, for his great experimental support and advices during my research stay in Canada.

I would like to thank the Medical University of Graz and Zentrum für Medizinische Grundlagenforschung for providing an outstanding infrastructure as well as equipment and excellent personnel for training and helping the students during their scientific work.

I am grateful to all the people who provide suggestions on my work especially my thesis committee members Prof. Dagmar Kratky, Prof. Ruth Birner-Gruenberger and Prof. Rudolf Zechner. Their critical evaluation of my work has added immense value to this study.

Last but not the least, I would like to thank my family, Prof. Zaiqing Yang, Dr. An Yu, Dr. Lena Li and Wenmin Xia for their moral support, encouragement and everlasting friendship.

Funding

This work was supported by grants to G. Hoefler from the Austria Science foundation (FWF) projects W1226 DK “Metabolic and cardiovascular disease” and SFB LIPOTOX F30. Collaboration was supported by grants to R. Lehner from the Canadian Institutes of Health Research (CIHR) (MOP-69043). J. Huang was also supported by the PhD program DK “Metabolic and cardiovascular disease” (FWF projects W1226).

DECLARATION

I hereby declare that this thesis is my own original work and that I have fully acknowledged by name all of those individuals and organizations that have contributed to the research for this thesis. Due acknowledgement has been made in the text to all other material used. Throughout this thesis and in all related publications I followed the guidelines of “Good Scientific Practice”.

APPENDIX

Publication list:

Huang J, Das SK, Jha P, Al-Zoughbi W, Schauer S, Claudel T, Sexl V, Vesely P, Birner-Gruenberger R, Kratky D, Trauner M, Hoefler G. The PPARalpha agonist fenofibrate suppresses B-cell lymphoma in mice by modulating lipid metabolism. ***Biochimica et biophysica acta***. 2013 Oct;1831(10):1555-65.

Al-Zoughbi W*, **Huang J***, Paramasivan GS*, Till H, Pichler M, Guertl-Lackner B, Hoefler G. Tumor macroenvironment and metabolism. ***Seminars in oncology***. 2014 Apr;41(2):281-95. * Co-first authors.

Huang J, Li L, Lian J, Schauer S, Vesely P, Kratky D, Hoefler G*, Lehner R*. Ces3/TGH deficiency reduces tumor growth andtumor-induced hyperlipidemia. * Co-coresponding authors. (**Submitted in Oncotarget**)

Jha P,Knopf A, Koefeler H,**Huang J**,Paramasivan GS, Hoefler G, Lackner C, Claudel T, Trauner M. Deficiency of Adipose Triglyceride Lipase (ATGL) Disturbs Circadian Regulation of Hepatic Lipid Metabolism. (**Submitted in Journal of Lipid Research**)

Stiegelbauer V, **Huang J**, Bonyadirad E, Schaider H, Speicher M, Leuschner I, Hoefler G, Guertl B. *WBSCR17* and its role in tumor pathogenesis. (**Manuscript in preparation**)

Table 2.Sequences of Primer Pairs for qPCR

Gene	Genbank	Primers
Inflammation		
MCP-1	NM_011333.3	F:GGCTGGAGAGCTACAAGAGG R:ATGTCTGGACCCATTCCTTC
F4/80	NM_010130	F:TTGGCCAAGATTCTCTTCCT R:TCACTGCCTCCACTAGCATC
TNF-a	NM_013693	F:GTCTACTGAACTTCGGGGTGA R:CACCACTTGGTGGTTTGCTACGAC
Socs3	NM_007707.3	F:ATTTCGCTTCGGGACTAGC R:AACTTGCTGTGGGTGACCAT
SREBP pathway		
Insig2	NM_133748.2	F:CCCTCAATGAATGTACTGAAGGATT R:TGTGAAGTGAAGCAGACCAATGT
Fbxw7	NM_080428.3	F:AGCGGCGGAGGATTACATCT R:TGAAAGCACATAGAGTGCCAAC
Scap	NM_001001144.3	F:TGGCTACTTCACCCTCGTG R:ACACCAGGCCCACAACAG
S1p	NM_019709.4	F:TCC AGGGGA ATGACTACCTG R:CAATGTCAGGCTTCACACGA
Ldlr	NM_010700	F:AGGCTGTGGGCTCCATAGG R:TGCGGTCCAGGGTCATCT
Pcsk9	NM_153565.2	F:TTTTATGACCTCTTCCCTGGC R:ATTCGCTCCAGGTTCCATG
Srebp1	NM_011480.3	F:GAGGCGGCTCTGGAACAG R:CGGGAAGTCACTGTCTTGGT
Srebp2	NM_033218.1	F:AGACCATGGAGACCCTCACG R:GGAACTCTCCCACTTGATTGCT
Hnf1alpha	NM_009327.3	F:CGCCTCCACCCTGGTTAT R:ACTCCCCATGCTGTTGATG
Lipoprotein clearance& production		
CD36	NM_007643	F:GATCGGAACTGTGGGCTCAT R:GGTTCCTTCTTCAAGGACAACTTC
Lpl	NM_008509	F:GGACTGAGAATGGCAAGCAA R:CCACTGTGCCGTACAGAGAAA
Vldlr	NM_001161420	F:CCACAGCAGTATCAGAAGTCAGTGT R:CACCTACTGCTGCCATCACTAAGA
Ldlr	NM_010700	F:AGGCTGTGGGCTCCATAGG R:TGCGGTCCAGGGTCATCT
Apoc2	NM_001277944	F:TTACTGGACCTCTGCCAAGGA R:CCCTGAGTTTCTCATCCATGC
Apoc3	NM_001289755.1	F:CCAAGACGGTCCAGGATGC R:ACTTGCTCCAGTAGCCTTTCAGG

Apoa5	NM_080434.3	F:GACTACTTCAGCCAAAACAGTTGGA R:AAGCTGCCTTTCAGGTTCTCCT
ApoB	NM_009693.2	F:GCCCATTGTGGACAAGTTGATC R:CCAGGACTTGGAGGTCTTGGA
Mttp	NM_001163457.1	F:CAAGCTCACGTACTCCACTGAAG R:TCATCATCACCATCAGGATTCCT
PPARα pathway		
Ppar alpha	NM_001113418	F:GTGGCTGCTATAATTTGCTGTG R:GAAGGTGTCATCTGGATGG
Acox1	NM_015729	F:GGGAGTGCTACGGGTTACATG R:CCGATATCCCCAACAGTGATG
Cpt1a	NM_013495	F:TGAGTGGCGTCCTCTTTGG R:CAGCGAGTAGCGCATAGTCA
Pgc1 alpha	NM_008904	F:GACTCAGTGTCACCACCGAAA R:TGACGAGAGCGCATCCTT
Housekeeping genes		
Gapdh	NM_001289726	F:GGCCATCAAGCCAGAGCTT R:CCAAACCATCACTGACACTCAGA
cyclophilin	NM_008907	F:TCCAAAGACAGCAGAAAACTTTCG R:TCTTCTTGCTGGTCTTGCCATTCC

ELSEVIER LICENSE
TERMS AND CONDITIONS

Aug 07, 2015

This is a License Agreement between Jianfeng Huang ("You") and Elsevier ("Elsevier") provided by Copyright Clearance Center ("CCC"). The license consists of your order details, the terms and conditions provided by Elsevier, and the payment terms and conditions.

All payments must be made in full to CCC. For payment instructions, please see information listed at the bottom of this form.

Supplier	Elsevier Limited The Boulevard,Langford Lane Kidlington,Oxford,OX5 1GB,UK
Registered Company Number	1982084
Customer name	Jianfeng Huang
Customer address	Auenbruggerpl. 25 Graz, 8036
License number	3683550768395
License date	Aug 07, 2015
Licensed content publisher	Elsevier
Licensed content publication	Biochimica et Biophysica Acta (BBA) - Molecular and Cell Biology of Lipids
Licensed content title	The PPARα agonist fenofibrate suppresses B-cell lymphoma in mice by modulating lipid metabolism
Licensed content author	Jianfeng Huang,Suman Kumar Das,Pooja Jha,Wael Al Zoughbi,Silvia Schauer,Thierry Claudel,Veronika Sexl,Paul Vesely,Ruth Birner-Gruenberger,Dagmar Kratky,Michael Trauner,Gerald Hoefler
Licensed content date	October 2013
Licensed content volume number	1831
Licensed content issue number	10
Number of pages	11
Start Page	1555
End Page	1565
Type of Use	reuse in a thesis/dissertation
Portion	figures/tables/illustrations
Number of figures/tables/illustrations	5
Format	both print and electronic
Are you the author of this Elsevier article?	Yes
Will you be translating?	No
Original figure numbers	figure 1, 2, 3, 4, 5 and Figure S1

Title of your thesis/dissertation	Role of lipoprotein homeostasis in tumour growth
Expected completion date	Sep 2015
Estimated size (number of pages)	100
Elsevier VAT number	GB 494 6272 12
Permissions price	0.00 EUR
VAT/Local Sales Tax	0.00 EUR / 0.00 GBP
Total	0.00 EUR
Terms and Conditions	

INTRODUCTION

1. The publisher for this copyrighted material is Elsevier. By clicking "accept" in connection with completing this licensing transaction, you agree that the following terms and conditions apply to this transaction (along with the Billing and Payment terms and conditions established by Copyright Clearance Center, Inc. ("CCC"), at the time that you opened your Rightslink account and that are available at any time at http://myaccount.copyright.com).

GENERAL TERMS

2. Elsevier hereby grants you permission to reproduce the aforementioned material subject to the terms and conditions indicated.

3. Acknowledgement: If any part of the material to be used (for example, figures) has appeared in our publication with credit or acknowledgement to another source, permission must also be sought from that source. If such permission is not obtained then that material may not be included in your publication/copies. Suitable acknowledgement to the source must be made, either as a footnote or in a reference list at the end of your publication, as follows:

"Reprinted from Publication title, Vol /edition number, Author(s), Title of article / title of chapter, Pages No., Copyright (Year), with permission from Elsevier [OR APPLICABLE SOCIETY COPYRIGHT OWNER]." Also Lancet special credit - "Reprinted from The Lancet, Vol. number, Author(s), Title of article, Pages No., Copyright (Year), with permission from Elsevier."

4. Reproduction of this material is confined to the purpose and/or media for which permission is hereby given.

5. Altering/Modifying Material: Not Permitted. However figures and illustrations may be altered/adapted minimally to serve your work. Any other abbreviations, additions, deletions and/or any other alterations shall be made only with prior written authorization of Elsevier Ltd. (Please contact Elsevier at permissions@elsevier.com)

6. If the permission fee for the requested use of our material is waived in this instance, please be advised that your future requests for Elsevier materials may attract a fee.